MODELLING AND CONTROL OF CAPACITIVE DEIONIZATION DESALINATION SYSTEM

BY

SYED ADNAN ALI

A Thesis Presented to the
DEANSHIP OF GRADUATE STUDIES

KING FAHD UNIVERSITY OF PETROLEUM & MINERALS

DHAHRAN, SAUDI ARABIA

In Partial Fulfillment of the
Requirements for the Degree of

MASTER OF SCIENCE

In

SYSTEMS AND CONTROL ENGINEERING

MAY 2016

KING FAHD UNIVERSITY OF PETROLEUM & MINERALS

DHAHRAN- 31261, SAUDI ARABIA

DEANSHIP OF GRADUATE STUDIES

This thesis, written by **SYED ADNAN ALI** under the direction of his thesis advisor and approved by his thesis committee, has been presented and accepted by the Dean of Graduate Studies, in partial fulfillment of the requirements for the degree of **MASTER OF SCIENCE IN SYSTEMS & CONTROL ENGINEERING.**

M. Elsh.

Dr. Moustafa Elshafei
(Advisor)

17-5-2016

Dr. Hisham Al-Fares
Department Chairman

Dr. Faizan Mysorewala
(Member)

Dr. Salam A. Zummo
Dean of Graduate Studies

S. AVaqar

Dr. Sayyid Anas Vaqar
(Member)

22/8/16

Date

MA Sc. 0

Dedicated To

My Parents

ACKNOWLEDGMENTS

All praise is due to Allah alone, the Lord of the Worlds. We constantly seek His help and pray for guidance. I would like to thank Allah for providing me this opportunity to defend my MS thesis. The thesis would not have been accomplished without His help. The challenges and difficulties during the course of my MS study made me strong with a zeal to excel further in the area of my study.

I would like to thank my parents, Mr. and Mrs. Syed Sajid Ali for trusting in me and providing me with constant encouragement, prayers and support. I would also like to thank my brother, Mr. Syed Salman Ali for providing motivation and assistance in numerous ways.

I take immense pleasure in expressing my deep gratitude and appreciation to my thesis advisor Dr. Moustafa Elshafei for his assistance and professional endeavor that has helped me in completing my thesis work successfully. My task would have been difficult without his interest and co-operation and valuable suggestions throughout the tenure of my thesis. He kept track of my progress and instilled in me a passion for research. I have always admired his passion for research, wisdom and ingenuity. I remember working with him during weekends. I would like to thank him wholeheartedly for his valuable time and support.

I would also like to express my gratitude to Dr. Faiz ur Rahman for sharing with me his valuable real time desalination industry experience, that encouraged me to be actively involved in this area of active research and serve the community.

I would like to thank the faculty of Systems Engineering department, particularly Dr. Abdul Wahid A. Al Saif who gave me constant motivation and valuable advices throughout my MS and for his constant help and support. Thanks to him, I got my Schengen visa.

I also express my gratitude to my committee members, Dr. Faizan Mysorewala and Dr. Sayyid Anas Vaqar for their valuable advices and feedbacks throughout my work.

The technical staff, Mr. Shoukat Ali, Mr. Jose, Mr. Widodo owe a special mention for their support and help during lab experiments. I am also grateful to Mr. Khasim Farooqui and Mr. Mervin for their assistance. I had a great time with them during registration assistance sessions.

I would like to thank all my friends, especially Mr. Ahmed Rehan for his frequent help and support.

I would also like to thank my graduate advisor, Dr. Salih Duffua for his constant encouragement. Lastly I would like to thank King Fahd University of Petroleum and Minerals for providing me scholarship to pursue MS in a highly active research environment.

I owe a lot of thanks to everyone who supported me throughout my work.

TABLE OF CONTENTS

LIST OF TABLES

LIST OF FIGURES

LIST OF ABBREVIATIONS

AC	:	Activated Carbon
ACC	:	Activated Carbon Cloth
CC	:	Constant Current
CDI	:	Capacitive De-ionization
CV	:	Constant Voltage
ED	:	Electrodialysis
EDL	:	Electric Double Layer
EDR	:	Electrodialysis Reversal
EWP	:	Electronic Water Purifier
GC	:	Gouy-Chapman
GCS	:	Gouy-Chapman-Stern
IUPAC	:	International Union of Pure and Applied Chemistry
MCDI	:	Membrane Capacitive De-ionization
mD	:	Modified Donnan
MED	:	Multi-Effect Distillation
MSF	:	Multi-Stage Flash Distillation

RO	:	Reverse Osmosis
RR	:	Recovery Ratio
RVD	:	Reverse voltage desorption
SWCDI	:	Switched wave Capacitive De-ionization
TDS	:	Total Dissolved Solids
ZVD	:	Zero voltage desorption

ABSTRACT

Full Name : [Syed Adnan Ali]

Thesis Title : [Modelling and Control of Capacitive De-ionization Desalination System]

Major Field : [Systems and Control Engineering]

Date of Degree : [May, 2016]

Freshwater scarcity is one of the most challenging problems facing the world today. Water is necessary for human beings to maintain good health. Although water is present in abundance in the form of various sources on earth, only less than one percent of it is available for drinking purposes. To use abundantly available water resources on earth requires use of desalination technologies to remove impurities and salts from water to make it fit for drinking purposes.

Many desalination processes are available based on thermal energy, mechanical energy and electrical energy or a hybrid of these. Capacitive de-ionization (CDI) is a method of water desalination based on electrical energy that uses porous electrodes (activated carbon) to store the ions. In this thesis, we develop a model of capacitive de-ionization using its equivalent electrical circuit and a dynamical equation to describe how the effluent salt concentration varies with respect to time in a CDI cell. The model effectiveness is evaluated by comparing its results with electrosorption experiments from the literature. The typical CDI operates in two steps; ion adsorption, where we get freshwater out of CDI cell, and ion desorption that results in discharge of highly concentrated brine. A novel method of capacitive de-ionization called Switched Wave Capacitive De-ionization (SWCDI) is proposed and modelled to obtain a continuous flow of freshwater and brine

with time. Upon successful modelling of the system, an optimization of operational parameters is done to achieve desired freshwater concentration and high water recovery ratio.

Lastly, the experimental setup and results of a single CDI cell and SWCDI system is presented.

ملخص الرسالة

الاسم الكامل: سيد عدنان علي

عنوان الرسالة: نمذجة ومراقبة بالسعة نظام تحلية دي التأين

التخصص: أنظمة و هندسة التحكم

تاريخ الدرجة العلمية: مايو ٢٠١٦

إن ندرة المياه من أكبر المشاكل و التحديات التي تواجه الناس هذه الأيام. كما لا يخفى أهمية الماء في حياة الإنسان و للمحافظة على صحته. بالرغم من توفر مصادر المياه المتنوعة على ظهر الأرض إلا أن الصالح للشرب منها لا تتعدى نسبته واحد في المائة. للإستفادة من بقية مصادر المياه الغير عذبة يتطلب الأمر إستخدام تقنيات تحلية المياه لإزالة الشوائب و الأملاح لتصبح صالحة للشرب بعد ذلك. هناك أنواع من مختلفة من عمليات تحلية المياه منها ما هو معتمد على الطاقة الحرارية أو الميكانيكية أو الكهربائية أو كان هجيناً بين نوعين أو أكثر من هذه الأشكال. إزالة الأيونات السعوية (Capacitive De-ionization CDI) واحدة من طرق تحلية المياه و تعتمد على الطاقة الكهربائية مستخدمةً الإلكترودات المسامية (إلكترونات مفعلة) لحفظ الأيونات. في هذه الرسالة نقوم بتطوير نموذج لإزالة الأيونات السعوية باستخدام دائرة كهربائية مكافئة لها و معادلة ديناميكية توصف كيفية تغير تركيز الملح المتبقي في خلية إزالة الأيونات السعوية بالنسبة للزمن. يتم تقييم كفاءة النموذج بمقارنة نتائجه مع النتائج المعملية لطريقة الإمتصاص الكهربائي التي تمت في الدراسات السابقة. تتلخص طريقة ال (CDI) في خطوتين: الخطوة الأولى هي إمتصاص الأيونات حيث أننا نتحصل على الماء النقي من خلية ال (CDI)، و الخطوة الثانية هي إمتزاز الأيونات الناتجة من تفريغ المحلول الملحي ذو التركيز العالي. هنالك طريقة جديدة من طرق إزالة الأيونات السعوية تسمى (إزالة الأيونات السعوية متحولة الموجة- Switched Wave Capacitive Deionization (SWCDI)) قد إقترحت و تم إستنتاج نموذج لها للحصول على إنسياب مستمر للماء النقي و الماء المالح مع الزمن. بعد النجاح في الحصول على نموذج يتم ضبط و موائمة باراميترات (معاملات) النظام للحصول على النسبة المطلوبة من تركيز الماء النقي و كذلك أعلى نسبة إستعادة للماء.

و أخيراً يتم عرض التجارب المعملية و النتائج لهذه التجارب في حالة خلية إزالة الأيونات السعوية مفردة و في حالة إزالة الأيونات السعوية متحولة الموجة مرة أخرى.

CHAPTER 1

INTRODUCTION

1.1 Freshwater Scarcity

Freshwater scarcity is one of the most challenging problems facing the world today. Water is necessary for human beings for survival. Around 75 percent of the Earth's surface is covered by water out of which 97.5 percent is in the form of oceans and a small percentage attributes to ice mass, rivers and lakes as shown in Figure 1.1. Even though the water is present in abundance, only 1 percent of it is available for drinking purposes. Rivers, lakes and groundwater are the available freshwater sources and occupy a fraction of 0.26 % of total freshwater [1]. Over 1.5 billion people lack ready access to drinking water and approximately 2.3 billion people suffer water shortages around the globe [2]. As a result of population growth and increasing quality of lifestyle of the people, it is expected that over two-thirds of the population will be facing freshwater shortage in the near future to a small or larger extent [3]. Pollution and exploitation of freshwater sources contribute to the scarcity of freshwater around the world. Freshwater scarcity is a serious issue. It slows or stops the economic growth of a country, reduces agricultural output, deteriorates public health and quality of life.

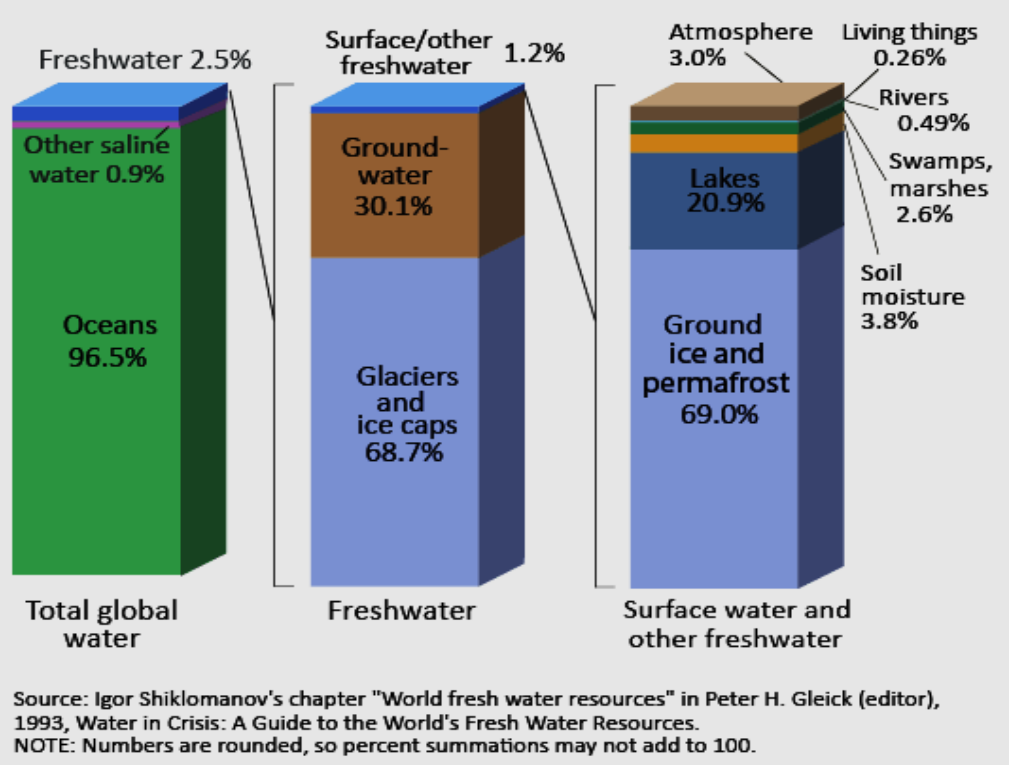

Figure 1.1 Freshwater resources in the world [4]

Although a large amount of water exists on the earth, it cannot be used for drinking and other purposes mainly because of high salinity and presence of bacteria in it. Desalination aims to remove salt and other minerals from water to make it suitable for drinking purposes.

An example of natural desalination is the water cycle. The water evaporates from the surface of the oceans, form clouds and some part precipitates to form snow while other part produces rain, the freshwater. Both the snow and rain are the purest forms of water. Gulf countries have very little rainfall per annum and thus it is the challenge of the desalination technologies to provide freshwater to satisfy the needs of the growing population as well as for industrial and agricultural purposes. These desalination technologies must be environmentally friendly causing no pollution, cost effective and energy efficient.

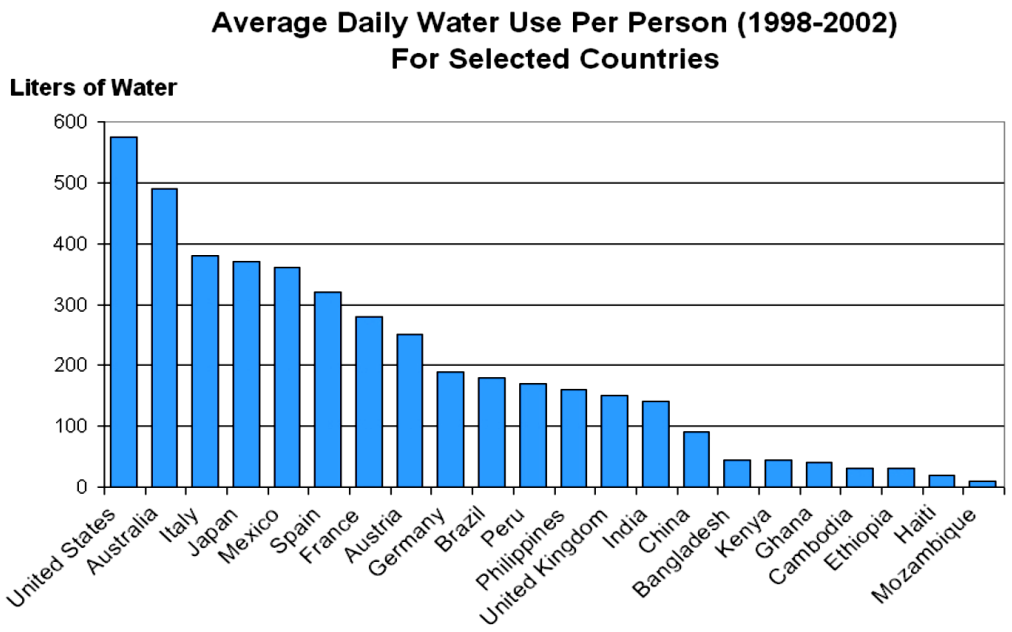

Figure 1.2 Average per capita consumption of water for selected countries [5]

Figure 1.2 shows the average daily water use per person for different countries in decreasing order. The countries differ widely in water usage. The per capita consumption is around 580 liters in the USA and around 500 liters in Australia. The average per capita consumption in the Kingdom of Saudi Arabia is equal to 265 liters/day. The average water consumption in KSA is double the average water consumption of the world [6]. This shows there is large requirement of freshwater in the Kingdom of Saudi Arabia which is met by the desalination plants.

1.2 Salinity

The salinity of water is defined based on the total dissolved solids (TDS) present in it. It is measured in parts per million (ppm) or milligrams per liter (mg/l). For dilute solutions, both the units are interchangeable, but not for concentrated solutions. TDS comprises

inorganic salts (cations- calcium, magnesium, sodium etc. and anions- carbonates, nitrates, chlorides, sulphates etc.) as well as small amount of organic matter.

Table 1 below shows the salinity levels of different types of water. As can be seen that sea water consists of maximum TDS level. TDS level of drinking water is specified by WHO as less than 500 ppm [7] though some countries still consume water up to 1500 ppm TDS [8].

Table 1.1 Classifying water based on salinity [1]

Type	**TDS (mg/liter)**
Sea water	10,000-45,000
Brackish water	1,500-10,000
Salt water	>10000
Freshwater	up to 500

Large amounts of sodium in water cause high blood pressure [9] whereas excessive fluoride in water cause a lot of dental problems [10]. The concentration of some of these ions must be lowered so as to lower the TDS of water and make it suitable for drinking, domestic and agricultural purposes. This is achieved using desalination processes.

1.3 Types of Desalination processes

Several desalination processes are used based on utilization of thermal energy, mechanical energy and electrical energy as shown in Figure 1.3.

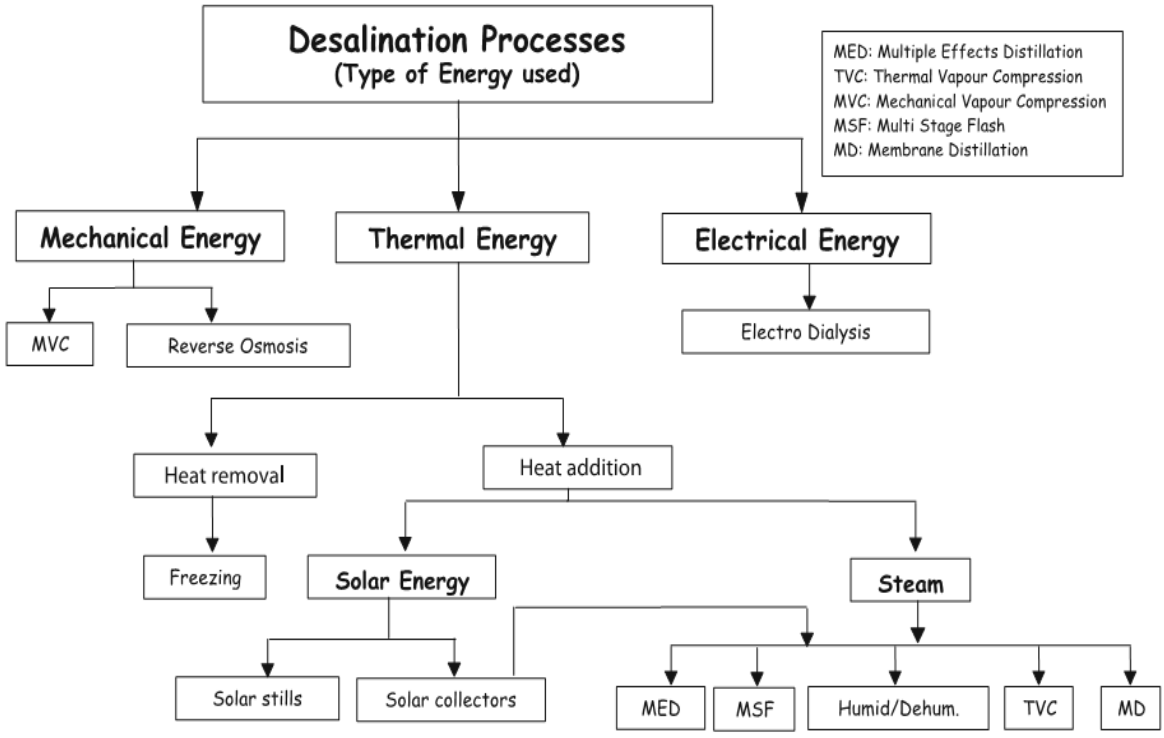

Figure 1.3 Types of desalination processes [11]

The majority of plants in Gulf region for sea water desalination are based on thermal energy. The description of some of the thermal energy plants is as follows:

1.3.1 Multi-Stage Flash (MSF) Distillation

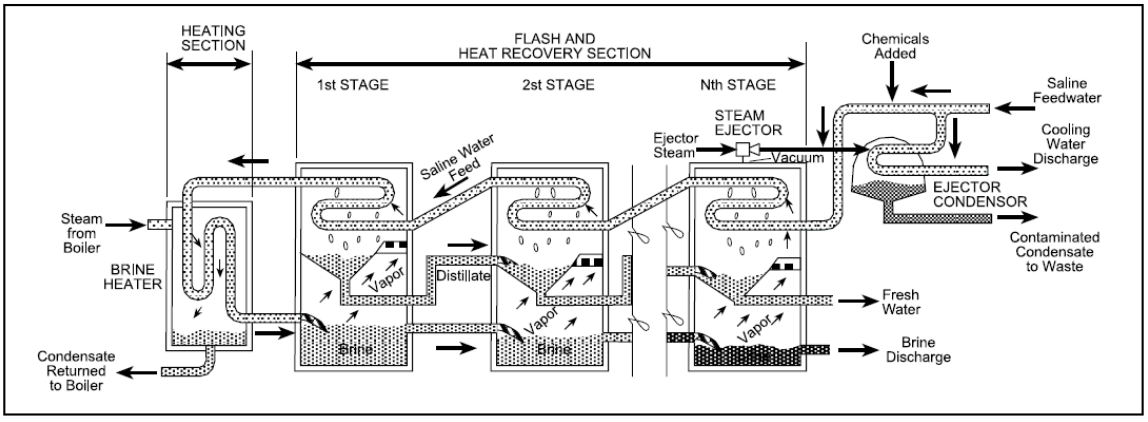

Figure 1.4 Multi-stage flash distillation diagram [12]

MSF plant consists of three main parts namely, the heat input section, the heat recovery section, and the heat reject section as shown in Figure 1.4. As the sea water passes through the tubes, it gains heat. After reaching the first stage, the remaining heat to the sea water is provided by the steam of the boiler in the brine heater. The steam flows outside the tubes whereas the seawater flows inside the tubes. As a result, heat exchange process occurs raising the temperature of sea water. The stages in MSF plants are enclosed and sealed tightly to create a vacuum. Every stage is maintained at a specific pressure. The pressure in the stages decreases from 1st stage to the last Nth stage. The sea water after gaining heat from the brine heater is still in liquid form because it is maintained at high pressure. As the water enters the orifice, the opening into the 1st stage, because of difference in pressure (lower pressure as compared to before), there is vigorous flashing. The vapors pass through demister pads to not allow any brine or impurity along with the vapor and these pure vapors condenses in contact with the tube bundles (exchange of heat raising the temperature of sea water passing from Nth stage to 1st stage). The brine stream from 1st stage passes on to the next stages lower in pressure than the previous stages and similar flashing occurs resulting in the formation of pure water. The condensed vapors from all the stages are collected as pure freshwater (approx. 0 ppm TDS) and the brine discharge is discarded.

A majority of desalination plants in Gulf region operates on this technology. MSF plants are capable of delivering pure water (0 ppm TDS theoretical). These plants have a lot of potential and many advanced plants based on MSF are in use called Dual purpose plants that perform the function of generating electricity as well as desalination. These plants are most widely used in Gulf region.

1.3.2 Multi-Effect Distillation (MED)

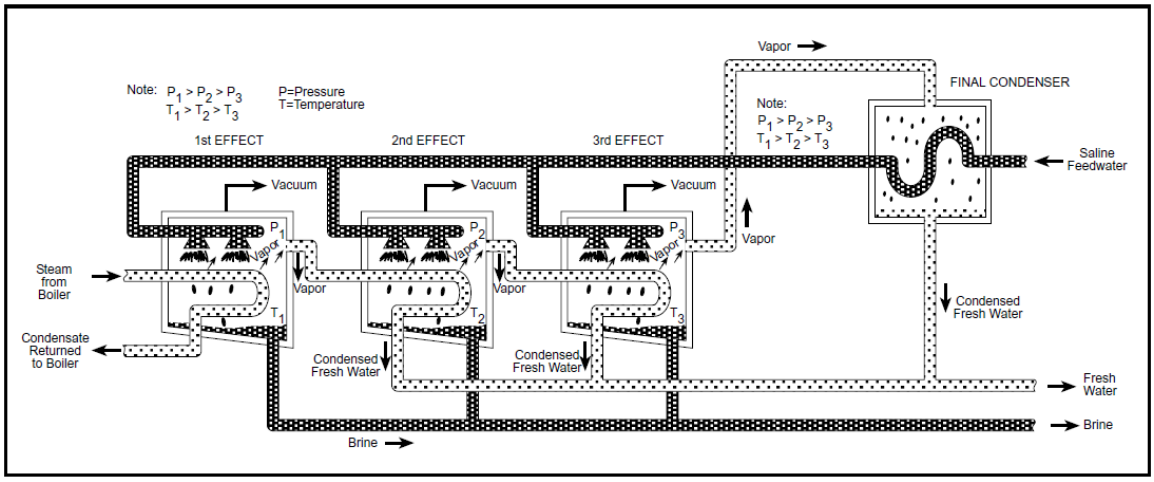

Figure 1.5 Water desalination using MED [12]

The process of MED plant utilizing horizontal tubes is illustrated in Figure 1.5. The stages here are called effects. The steam from boiler here is passed inside the tubes rather than outside as in the case of MSF plants. The sea water is sprinkled on these hot tubes as a result of which boiling occurs and hot vapors formed are passed on to the next stages or effect via the tubes. The decrease in pressure of the chambers is the principle used in this process. The hot vapors enter the next effect wherein again the saline water is sprinkled on the tubes to generate pure vapors. The hot vapors are condensed and collected as freshwater whereas the brine is collected separately and discharged into the sea. Here, we require heat only to the first stage and no subsequent heating of all the stages are required as in MSF plants. These plants are prone to more scaling problems as the water here is sprinkled on the tubes.

Water recovery which is defined as the ratio of output freshwater flow to the input feedwater flow is approximately 10 – 15 % for MSF and MED plants [13].

1.3.3 Vapor Compression

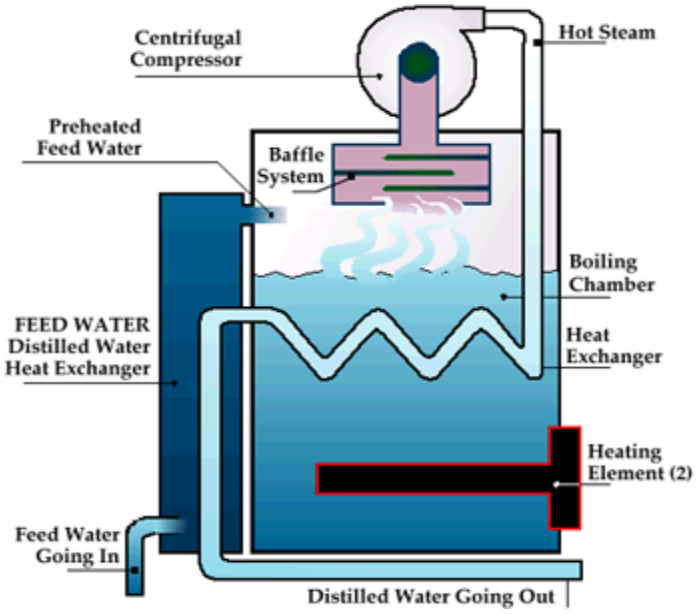

Figure 1.6 Vapor compression process [14]

Vapor-compression desalination method is based on the following principle. The process of distillation begins in the boiling chamber. When both the heating elements are switched on, the boiling process initiates. The compressor is turned on as the temperature of the water inside boiling chamber approaches boiling point. During boiling, #2 heating element is off and #1 element is cycled on and off so as to maintain the boiling at the right temperature in order to maximize efficiency. The steam produced passes through a baffle system and enters the compressor. The compressor pressurizes the steam that increases its temperature and this steam is then passed inside the tubes of heat exchanger. Exchange of heat occurs from the compressed steam that causes water to boil in the chamber to create more steam. During the process of giving the latent heat, the steam condenses and a hot distilled water slightly lower than the boiling point is obtained. During the process, either #1 or #2 elements are cycled on and off to provide the heat required to keep the system at optimum temperature and to ensure high efficiency [14].

An electric heater, e.g., an initial supply of steam is needed to start the system. Since compression energy is much less than the thermal energy in the form of latent heat of prime steam, therefore VC process is more efficient than the MED process. This desalination process has very low specific energy consumption due to which the overall costs associated is also on the lower side. The above design of Vapor compression (VC6000) utilizes 0.085 kWh energy to produce one US gallon distilled water [14].

1.3.4 Reverse Osmosis (RO)

The majority of desalination systems relying on mechanical energy are based on the principle of Reverse Osmosis.

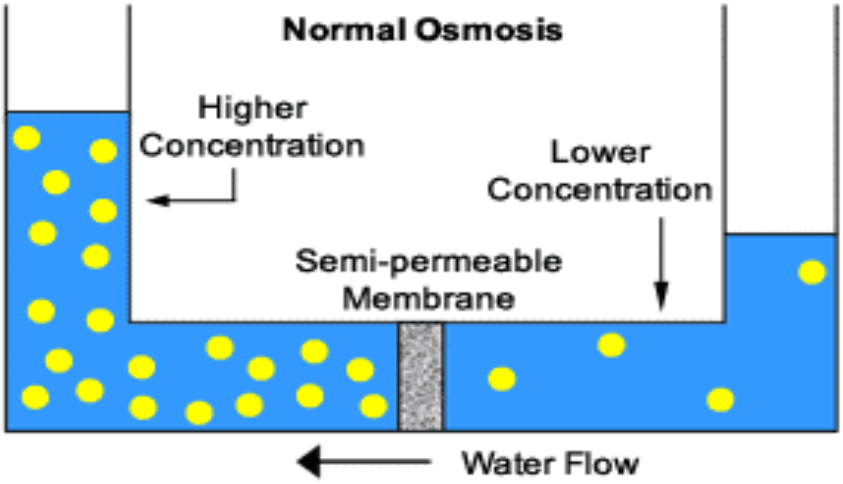

Figure 1.7 Normal Osmosis [15]

Osmosis needs to be understood first in order to understand reverse osmosis [9]. In osmosis as shown in Figure. 1.7, there is diffusion of a solvent from a region of low solute concentration to a region of high solute concentration through a semi-permeable membrane until concentrations on both sides of the membrane are equal. The semi-permeable membrane in osmosis is permeable to the solvent molecules, but not to the solute, that

results in a chemical potential difference across the membrane thus driving the diffusion. In order to stop the flow of solvent across the membrane, a pressure difference needs to be applied to the solution side which is known as the osmotic pressure.

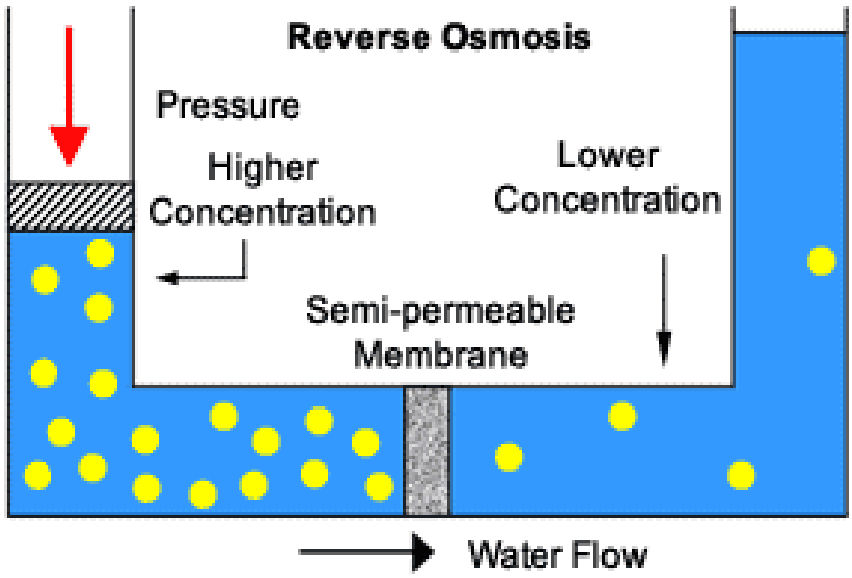

Figure 1.8 Reverse Osmosis [15]

In reverse osmosis [9] as shown in Figure. 1.8, a pressure greater than the osmotic pressure is applied to overturn the normal osmotic flow. Upon applying pressure to the saline solution, the water passes from more concentrated side to the less concentrated side through a semi-permeable membrane. The membrane is a thin microporous surface that allows water to permeate through it while blocking or rejecting impurities, bacteria, pyrogens and high percentage of inorganic solids. It also rejects polyvalent ions much easier than monovalent ions.

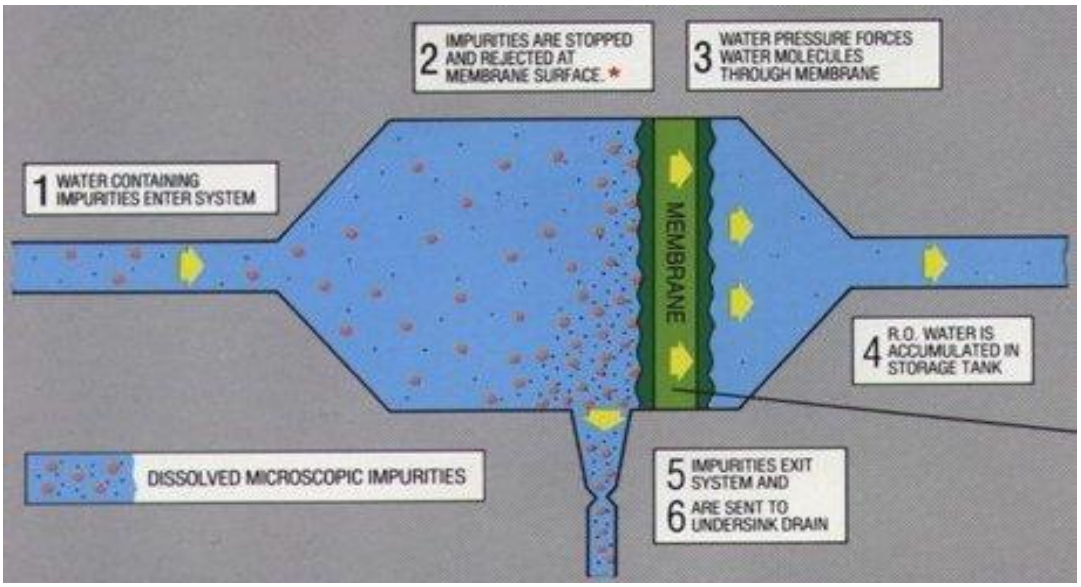

Figure 1.9 Operation of reverse osmosis depicting permeate flow and brine flow [16]

The process cannot go on indeterminately without the removal of impurities. The impurities and salt present in the saline water end up clogging the membrane that could reduce the efficiency of the process to produce freshwater. This is referred to as fouling. Fouled membranes require more pressure to force water through the membrane, thus causing more energy wastage. As a solution to the above problem, the membranes are configured so that the feed water coming to the membrane splits into two streams, one part to be purified as indicated by '4' and the other part to wash away the particles rejected by the membrane as indicated by '5' in Figure 1.9. There are two types of membranes available, spiral wound membranes and hollow fine fiber. Each has its own advantages and disadvantages.

There are two types of flow possible: conventional filtration and cross flow filtration as shown in Figure. 1.10. The process of conventional filtration is more prone to fouling as the water flow occurs perpendicular to the membrane under pressure and larger molecules tend to accumulate on the surface of the membrane. In cross flow, the flow of water occurs

tangentially to the membrane surface under pressure. The larger molecules do not accumulate on the membrane surface but instead move along with the tangential flow of water [17].

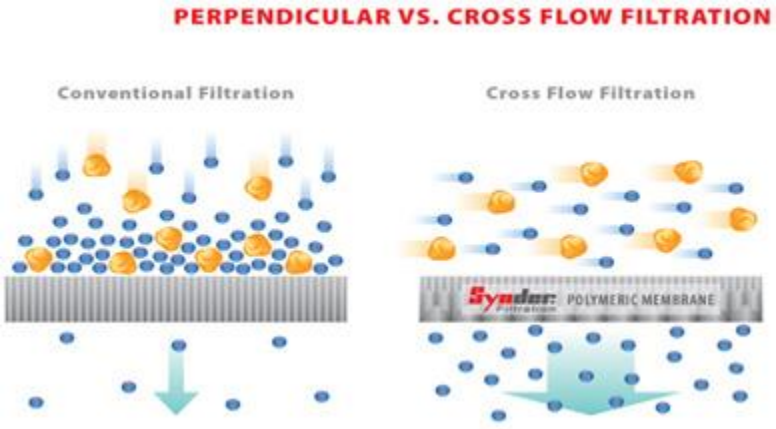

Figure 1.10 Conventional flow and Cross flow in reverse osmosis [18]

The process of Reverse Osmosis depicting cross flow is shown in Figure. 1.11.

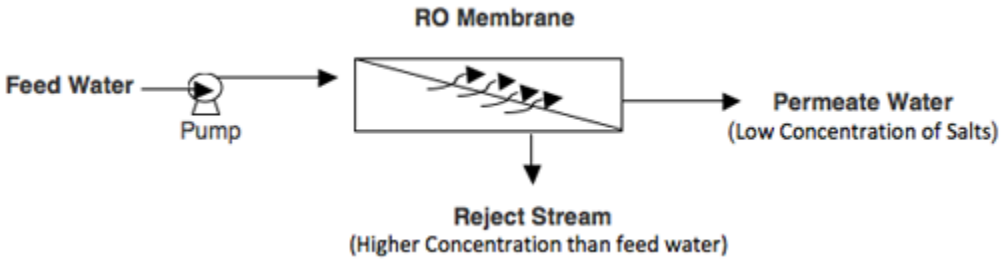

Figure 1.11 RO cross flow [19]

Figure. 1.12 below shows the filtration spectrum by Osmonics. It can be clearly seen that reverse osmosis is capable of removing materials even of ionic sizes up to as small as 0.001 micrometers. The salts and metal ions belong to the ionic range and is removed largely by the process. The particles in the higher ranges are removed via micro, ultra and nano-filtration respectively. The main cause of reverse osmosis gaining popularity is because of

its low specific energy consumption, 3-8 kWh of electric energy per $m^3$of freshwater produced from sea water.

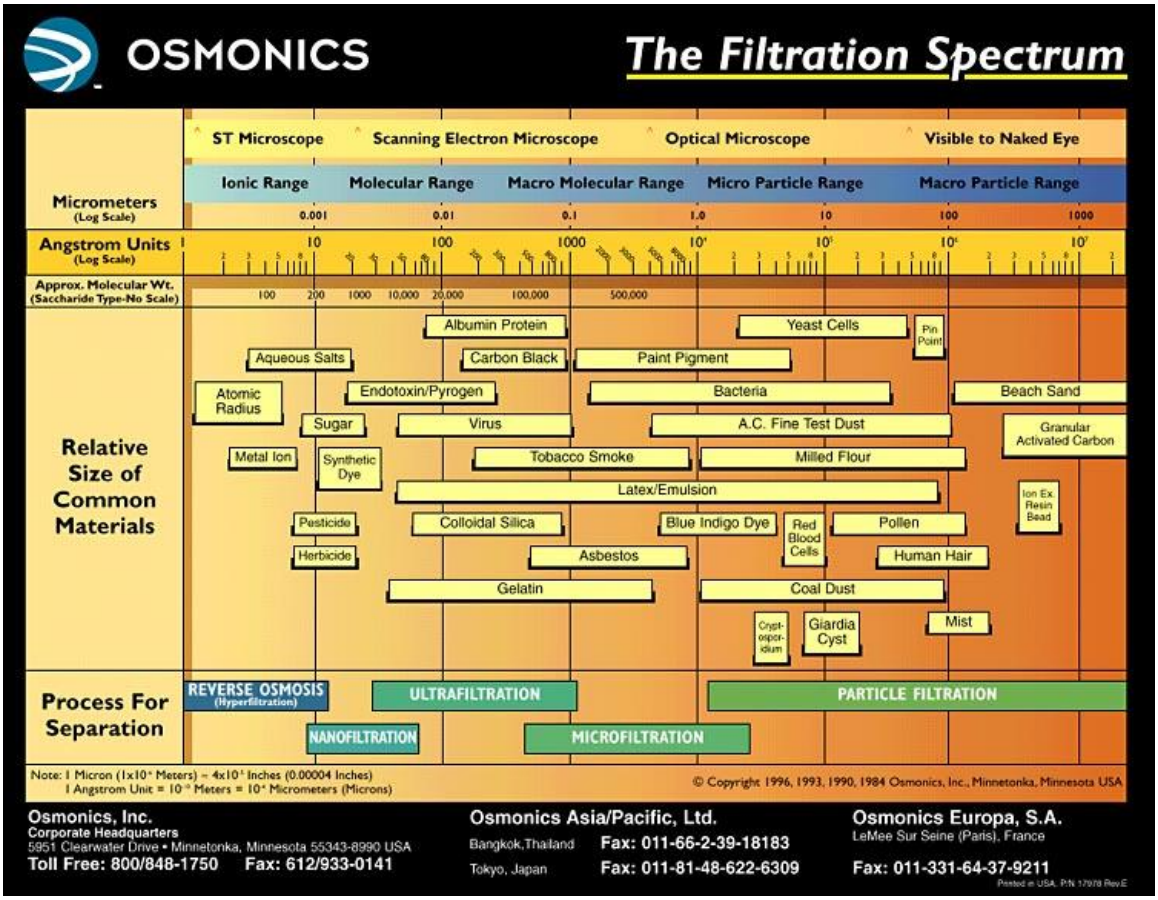

Figure 1.12 Filtration spectrum by Osmonics [20]

There is also a possibility of desalination via electrostatic means that is by supplying electrical energy. Some of the processes utilizing electrical energy for desalination are explained below.

1.3.5 Electrodialysis (ED)

Electrodialysis (ED) [12] is a membrane process driven by voltage. ED was introduced commercially in the 1960s whereas reverse osmosis was introduced commercially in the 1970s. ED is mostly used for brackish water desalination.

The basic principle underlining this technology is as follows. Most of the salts dissolved in water are in ionic form and they allow electric current to pass through them. Some ions are positively charged (cations) while others are negatively charged (anions). The electrolytic cell consists of two electrodes connected to a voltage source. The electrodes contain charge. The ions under the effect of the electric field move towards electrodes having an opposite charge. The cell consists of ion selective membranes (cation selective membranes that allow cations to pass through it blocking anions and anion selective membranes that allow only anions while blocking cations). These membranes are placed alternately in the electrolytic cell as shown in Figure 1.13 and Figure 1.14.

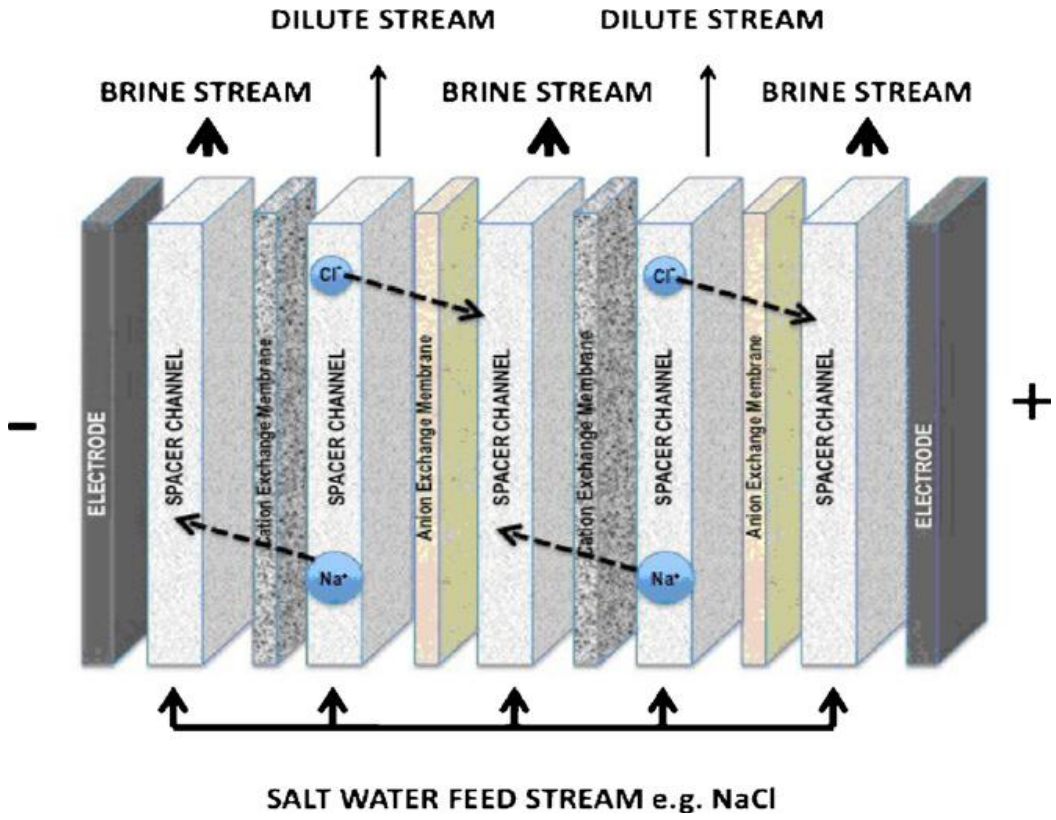

Figure 1.13 Electrodialysis process [21]

When the saline solution is fed to the cell, the ions electromigrate towards electrode of opposite polarity. Ion exchange membranes are placed such that it allows certain ion to

pass through them and restricts the flow of other type of ions. This process results in the formation of two compartments, brine compartment where the ions are present in high concentration and freshwater stream with little or no ions present. Electrodialysis cells can be arranged in stack configuration as well. The electrodes are usually made of Titanium (Ti) with Platinum (Pt) coating. During ED operation, oxygen and chlorine gases evolve at the anode and hydrogen gas at the cathode. There is a continuous supply of freshwater using this approach as we have separate compartments for both brine as well as freshwater.

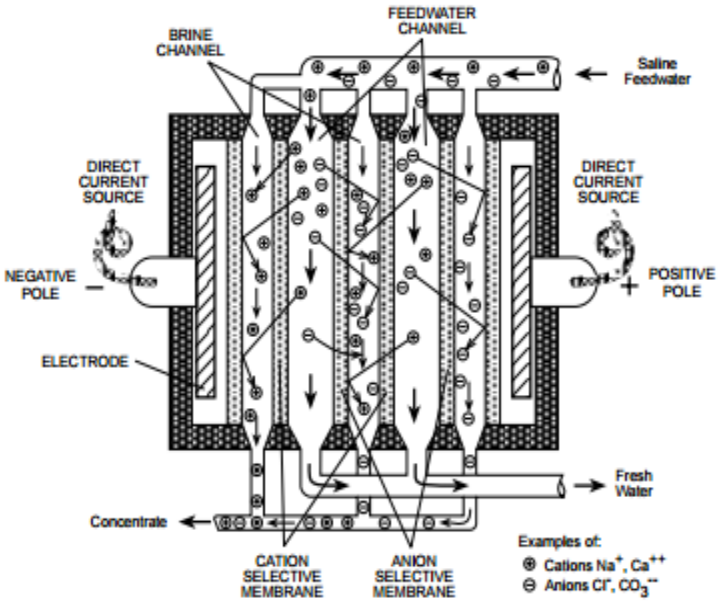

Figure 1.14 A typical ED configuration showing movement of ions [12]

Anode and Cathode Reactions

Depending upon pH of the water and potential applied, anodic and cathodic reactions occurring at each electrode are as shown below.

At cathode,

$$2e^- + 2\ H_2O \rightarrow H_2\ (g) + 2\ OH^-$$

while at the anode,

$H_2O \rightarrow 2\ H^+ + ½\ O_2\ (g) + 2e^-$

$2\ Cl^- \rightarrow Cl_2\ (g) + 2e^-$

Hydrogen gas is produced at the cathode and oxygen or chlorine is produced at the anode. These gases are consequently discharged as the electrode stream effluent from each compartment of the ED cell. Hydrogen gas evolved can be used for various energy production applications.

The pumping pressure required in an ED process is only 50-75 psi, all pumps, piping, and fittings are made of PVC. This method, however, requires periodic cleaning of membranes by circulating solutions of detergent or other cleaning agents, or by disassembling and manual cleaning.

[22] mentions that the energy required for electrodialysis can be reduced by 60-70% as the temperature increases from ambient temperature to 70 ℃. Energy consumption decreases by 1 % as temperature increases by 0.5 ℃ for temperatures above 21 ℃ [23]. However, higher temperature damages the membranes and spacers.

Some of the limitations of ED are as below:

1. Polarization Effect: In product water compartments, conductance is very low due to low TDS. The polarization effect causes the splitting of water molecules to dissociate into H^+ and OH^- ions. [24]

2. Electric power required is directly proportional to TDS of saline water. It is economical only for brackish waters of TDS ≤ 3500 ppm [25].

1.3.6 Electrodialysis Reversal (EDR)

A modified form of ED is Electrodialysis Reversal. It utilizes the same principle of electrodialysis. During the operation, the polarity of the electrodes is reversed many times, so that the ions are attracted in the opposite direction each time the polarity is reversed. At the same time, flows are also switched so that dilute compartment now becomes the concentrated compartment and vice versa. This would be beneficial in flushing and breaking scales and other deposits and also prevent membrane fouling in EDR cell. No scale control chemicals need to be injected.

1.3.7 Capacitive De-ionization (CDI)

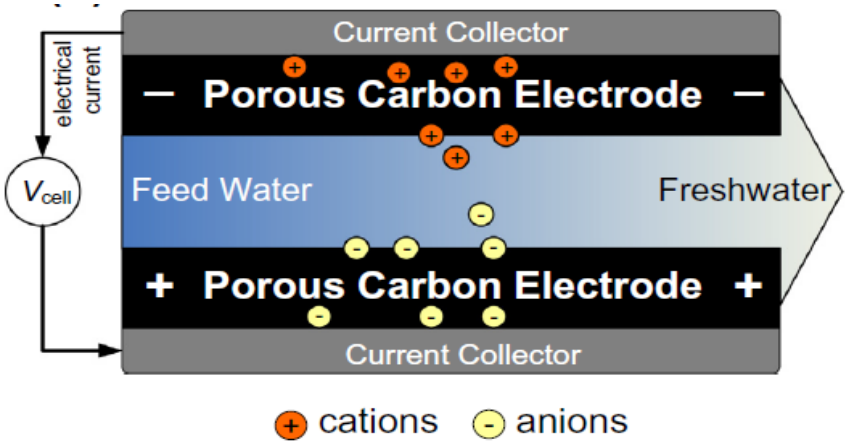

Figure 1.15 Capacitive De-ionization cell [1]

In Capacitive De-ionization (CDI) system, saline water is made to pass between a pair of electrodes connected to a voltage source. A CDI is a two-step process, the first step is ion adsorption or charging that results in a pure permeate stream where ions are adsorbed in porous charged electrodes. As the voltage is applied to the electrodes, due to the presence of an electrostatic field in between the electrodes, there is a movement of ions such that the positive ions, cations move to the cathode and anions towards the anode. Two layers of opposite polarity are formed at the electrode-solution interface which is referred to as

electrical double layer (EDL) and ions are stored in these EDL's. In the next step, voltage is reversed so that the ions get desorbed and flows out of the CDI cell as a brine stream and thus cause regeneration of electrodes. CDI differs from ED in the sense that it does not use membranes. The problems of membrane fouling are not present in CDI and since it utilizes just electrical energy for desalination, it has the potential to be energy efficient, robust technology for water desalination. The phenomenon of desalination using CDI is as illustrated in the Figure 1.15.

1.3.8 Membrane Capacitive De-ionization (MCDI)

The version of CDI with membranes is called MCDI. It is the most promising development in CDI and has a lot of scope in the future. It utilizes ion exchange membranes (ion-selective) as shown in Figure 1.16 [1].

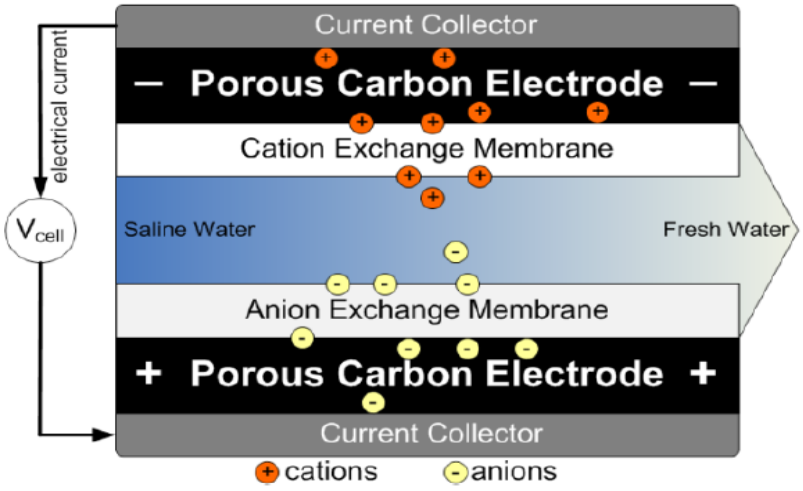

Figure 1.16 Membrane Capacitive De-ionization (MCDI) diagram [1]

Ion exchange membranes are placed in front of the electrodes, for example, a cation exchange membrane is placed in front of the cathode which allows cations to pass through but stops anions to pass through it. When an electric voltage is applied to the electrodes, due to the presence of electrostatic field in between the electrodes, the ions in the saline

water flowing in the spacer channel gets attracted to opposite polarity electrodes. Anions travel through the anion exchange membrane and gets attached to pores in the anode whereas cations pass through the cation exchange membrane and gets attached to pores in the cathode. At the same time the counter-ions are adsorbed in the respective electrodes, there is co-ion desorption as well. In CDI, these co-ions enters the spacer channel and reduces the efficiency of the process. But in MCDI, because of the ion selective membranes, these co-ions are blocked by the membrane and cannot enter the spacer channel. This results in more purified water in the spacer channel during the adsorption step. In the desorption step, as the voltage is reversed, the ions are removed from the electrode pores due to change in potential and are flushed out of the MCDI cell. The membranes in MCDI does not allow the ions released in the desorption step to get attracted to their counter electrodes and a concentrated effluent stream is obtained at the outlet of the MCDI cell. This is often referred to as flushing.

1.4 Thesis Motivation and Problem Statement

The demand for freshwater is increasing by rate of 64 billion cubic meters a year as a result of increasing world population [26]. There are various desalination technologies that are available but it is the need of the hour to develop a desalination technology that is energy efficient, cost effective, environmentally friendly and capable of meeting the ever-growing demands for water. Thermal desalination is a high-temperature process and consumes lot of energy [27], [13]. Also, membrane-based desalination, for example, reverse osmosis is a high-pressure process and has drawbacks associated with the use of membranes [13],

[28]. Capacitive De-ionization is proved to be a low pressure and low-temperature process [29]–[33]. The ions are removed from water rather than water from the ions. It just requires a small voltage of 1.2 volts for desalination. Electrode cleaning is achieved by short-circuiting the electrodes of a CDI cell. No special chemicals are required to clean the electrodes [34]. Also, during the discharging step of a CDI cell to remove the ions by short-circuiting the CDI cell, the current released can be used to charge a neighboring CDI cell or a battery. Thus, there is a possibility of energy recovery in CDI [35]–[37]. The cost of CDI desalination is low compared to RO for same capacity plants as shown in [38]. It is potentially more energy efficient for brackish water desalination [39], [29], [40]–[42], [38], [43]. The energy consumption of CDI is less compared to other desalination technologies [3], [28], [42]. It is also possible to achieve high water recovery (ratio of output flow rate to input flow rate) using CDI [44], [45].

Different models have been described in the literature to model CDI based on charge transfer between the electrodes that describe equilibrium and transport properties in CDI [29], [46], [47]. Electrostatic double layer theory describes the electrosorption of ions and storage of charge on the electrodes using the concept of the electric double layer. The double layer is described using different models in the literature [1], [48], [49]. The effectiveness of the model depends on the ability of the model to describe ions adsorbed in the double layer inside the electrodes upon application of voltage. The behaviour of the double layer is highly nonlinear. The double layer forms a capacitor at the electrode-solution interface and the solution between the electrodes contributes to solution resistance. The modelling of CDI is a challenging problem which needs to be investigated.

A typical CDI is a two-step process [29], [39], [50]. Freshwater is obtained upon applying a voltage to the electrodes in a CDI cell and highly concentrated salty water (brine) is obtained by short-circuiting the electrodes in a CDI cell. Freshwater and brine are obtained in different time slots unlike the other desalination technologies mentioned previously wherein freshwater and brine are collected at the same time. A configuration of CDI which combines the two-time slots to produce freshwater and brine at the same time needs to be investigated.

1.5 Thesis Objectives

The main objectives of this thesis are following:

1. Literature Review of Electrostatic Desalination Systems.
2. Develop a novel mathematical model of Capacitive De-ionization (CDI) Desalination system using its electrical equivalent circuit.
3. Evaluate the model by comparing the results with reported results from the literature.
4. Propose a novel capacitive de-ionization technique called, “Switched Wave Capacitive De-ionization (SWCDI)” that allows continuous operation of CDI wherein we obtain freshwater and brine at the same time and model the same using the developed mathematical model of CDI in this thesis.
5. Optimize the parameters of the modelled desalination system to meet the desired objectives.
6. Develop an experimental prototype of a single CDI cell and possibly the SWCDI.

1.6 Thesis Outcomes

Several inland communities lack access to freshwater because of semi-arid to arid climates. This climate change increases the frequency of droughts. CDI can prove to be an ideal desalination technology in an inland remote location for the supply of water for drinking and agricultural purposes as it consumes less power.

The main outcomes of the thesis are as follows:

1. Derivation of a mathematical model of capacitive de-ionization system that describes how the effluent concentration varies with respect to time in a CDI cell.
2. Studying the impact of influent feed concentration and flow rates on salt removal efficiency of CDI.
3. Development of a novel design of CDI called “Switched Wave Capacitive De-ionization (SWCDI)” and derivation of its mathematical model.
4. Optimization of parameters to achieve desired response.
5. Experimental setup of CDI and SWCDI.

1.7 Thesis Outline

In Chapter 2, a detailed literature review of Capacitive De-ionization is mentioned. It highlights the role of CDI to be a promising technology for brackish water desalination. Different operational modes of CDI are described. Various electrostatic double layer models that describe the CDI process are mentioned. The effect of different parameters on the CDI system performance is mentioned using results from the literature. Finally,

different companies providing CDI equipment commercially and for research are mentioned.

In Chapter 3, we develop a mathematical model of CDI using its electrical equivalent circuit and a dynamic equation that describes how the salt concentration varies with respect to time in a CDI cell. The model effectiveness is evaluated by comparing its results with electrosorption experimental results of AQUA EWP CDI unit. The effect of different initial feed concentration and flow rates of water on AQUA EWP CDI unit is studied using the model. Finally, an investigation on modelling of the batch mode of operation of AQUA EWP CDI unit is described.

In Chapter 4, a novel approach for continuous operation of Capacitive De-ionization system is proposed using the concept of switched electric wave which is referred to as Switched Wave Capacitive De-ionization (SWCDI). The mathematical model of a single CDI cell is modified to model SWCDI system. The parameters of the system are optimized to achieve desired freshwater concentration and recovery ratio. Also, an investigation of reflux mode operation of SWCDI is presented.

In Chapter 5, the experimental setup and results of a single CDI cell and SWCDI system is presented.

Lastly, Chapter 6 summarizes all the work involved in this research along with future work.

CHAPTER 2

LITERATURE REVIEW

2.1 Introduction to Capacitive De-ionization (CDI)

Capacitive De-ionization process has attracted interest in the recent past mostly because of its low energy consumption. The CDI cell consists of porous carbon electrodes pair that gets charged upon application of electrical potential. Upon applying a voltage to the CDI cell, the ions present in water under the effect of electrostatic field move towards their respective counter electrodes, cations moving towards the cathode and anions moving towards the anode and are stored in the electrostatic double layers formed inside the porous electrodes. This would result in freshwater flowing through the spacer channel in between the electrodes. The basis of the process is electrostatic double layer formation inside the intraparticle pores i.e., inside the carbon electrodes known as micropores. The ions are immobilized as they are adsorbed into the electrostatic double layers. These electrical double layers become charged and discharged as the cell voltage is varied and stores and releases the charge. When the micropores get saturated with adsorbed ions, the voltage is reduced to zero to release the ions from the electrode pores and thus the electrodes are regenerated. A stack of electrode pairs can be used to improve the efficiency of the process. This process removes ions from water rather than removing water from the salt and thus require less energy for desalination.

The change in ion concentration with respect to time is measured to determine desalination using CDI. Normally for CDI experiments, a single salt solution for example, sodium chloride (NaCl) is used.

As per the International Union of Pure and Applied Chemistry (IUPAC) [29], pores of size larger than 50 nm are called macropores, pores between 2 and 50 nm are called mesopores and pores smaller than 2 nm as micropores, which is different than the pore terminology in porous electrode theory.

2.2 CDI geometries

The majority of the experimental work on CDI utilizes two porous carbon electrodes that are placed parallel to each other with a small gap in between them through which the feed water flows. The porous electrodes are attached to a current collector. This small gap is referred to as the spacer channel. Different CDI geometries are used for the purpose of water desalination in the literature [29]. In one such configuration as shown in Figure 2.1-(a), the voltage is applied between the two porous electrodes and the feed water flows in the space between the electrodes. This configuration is called flow-by CDI as shown in Figure 2.1-(a).

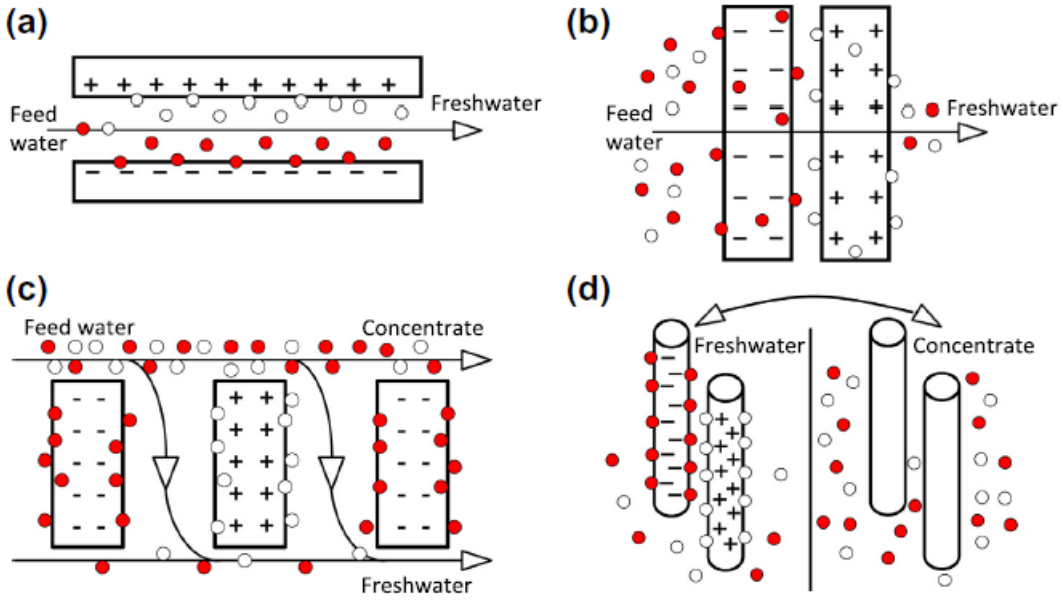

Figure 2.1 Geometries used in CDI. (a) Flow by CDI, (b) Flow through CDI, (c) electrostatic-ion pumping, (d) wire based CDI [29]

In another configuration of CDI referred to as Flow through CDI as shown in Figure 2.1-(b), the water flows perpendicularly through the pores in the electrodes. This allows for faster charging of a CDI cell as the time for ion adsorption to the pores is reduced. This architecture contributes to high capacity and low energy cost.

Another geometry used is electrostatic ion pumping as shown in Figure 2.1-(c) wherein a freshwater stream flows at one end and brine stream flows at the other end. The feed solution is fed incessantly through an opening in the center of the column. Application of voltage causes opening of valve 1 at one end of the channel allowing freshwater to come out of the valve while closing of opposite end valve 2. Applying zero voltage causes valve 1 to close and valve 2 to open to allow the brine to flow outside the system [29].

In another configuration known as wire-CDI, movable carbon electrode wires are employed for desalination as shown in Figure 2.1-(d) [51]. A CDI cell consists of wires

with anode wires being placed closely to cathode wires. These cell pairs are placed in saline water and applying a potential between cathode and anode results in ions adsorption into their oppositely charged electrodes. This results in lower salinity of water and the electrode pair is immersed in another water wherein the cell voltage is reduced to zero to cause ions release from the electrodes. Thus, in this method two streams are obtained, i.e., freshwater stream and brine stream. The problem of freshwater mixing with that of the influent feed stream upon switching the voltage is eliminated in this configuration.

2.3 Single pass operation vs Batch mode operation

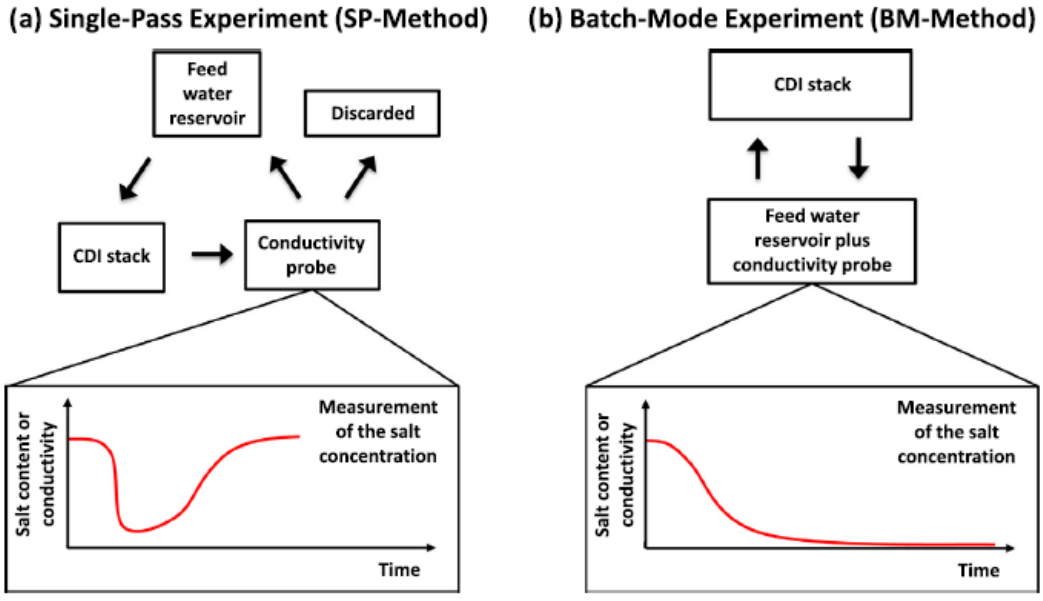

Figure 2.2 CDI experiments design (a) Single pass mode, (b) Batch mode CDI showing variation of outlet conductivity with time [29]

A typical CDI cell consists of two porous electrodes separated by a porous spacer layer. A CDI stack contains a number of CDI cells. Two types of experiments are usually performed in CDI as shown in Figure 2.2 [29]. In single pass experiment as shown in Figure 2.2-(a),

water enters the CDI cell from a feed tank and the water salinity is measured at the outlet of the CDI cell. The effluent salt concentration decreases initially as the cell voltage is applied because of ions getting adsorbed in the electrode pores. But as the electrode pores become saturated with ions, the concentration increases and reaches influent salt concentration. The amount of salt removed from the solution is calculated by integrating the salt effluent concentration with time.

In the batch mode operation of CDI as shown in Figure 2.2-(b), the conductivity of feed water is measured in the reservoir. Here, the feedwater enters the CDI cell from a feed tank and the low salt concentration water obtained at the output of the CDI cell is fed back to the tank to further removal of salts. The effluent salt concentration thereby decreases steadily and reaches a low constant value. The low constant value corresponds to the situation where all the electrodes are saturated and no more ions can be adsorbed in their pores. The electrodes are regenerated by applying zero volts between the electrodes and allowing feed solution to flow in the CDI cell. The concentration of feed rises as the ions are desorbed back into the solution and then decreases and eventually reaches influent salt concentration as all the ions are flushed from the system. The total amount of ions removed here is calculated by taking the difference in initial salinity and final salinity multiplied by the total volume of water in the system.

Charge efficiency Λ of the electric double layer is a parameter that describes the efficiency of a CDI cell. For a monovalent salt (NaCl), charge efficiency [1] is

$$\Lambda = \frac{\text{Equilibrium salt adsorption}}{\text{Electrode charge}}$$

If one salt molecule is removed from the solution for one electron transferred from one electrode to another, charge efficiency Λ would be unity. However, this is not the actual case as only 0.6-0.8 salt molecule is removed from the salt solution and charge efficiency is always less than unity [29].

2.4 Modelling of CDI process

Many attempts have been made to model the CDI process [29]. The understanding of the operation of Capacitive De-ionization and modelling based on charge transfer is discussed below.

2.4.1 Electrostatic Double layer (EDL) models

The EDL theory [29] describes charge vs voltage and salt vs voltage characteristics of CDI cell. EDL approach deals with the transfer of charge from one electrode to another, and its effect on ion concentration inside porous electrode and drop of voltage across the EDLs. The model is used to describe electrosorption and storage of charge in the micropores inside carbon electrodes.

There is formation of electrical double layers at the interface of electrode and solution. Across this interface, there is charge separation that is the electronic charge of the porous electrode is compensated locally by the charge in electrolyte filled pores. As a result of charge compensation, overall, EDL is uncharged. The theory of electrical double layer is attributed to Helmholtz [52]**.** Helmholtz model assumes all charge on the surface being compensated directly by adsorption of countercharge on the surface which implies that for

each electron transferred from one electrode to the other, one cation is moved to the cathode and one anion is moved to the anode to compensate for the respective charges considering monovalent ions. This would result in removal of one salt molecule from the spacer channel for one electron transferred from one electrode to other. This represents the ideal situation of CDI. For such a case, charge efficiency Λ would be unity. According to Helmholtz model, EDL is treated as a simple capacitor wherein a single layer of ions is adsorbed at the surface. Thus, EDL is considered a molecular dielectric and the charge is stored electrostatically. The electric potential decreases linearly with distance from the electrode surface minimizes at the Outer Helmholtz Plane as shown in Figure 2.3 (a). When the voltage is less than the electrolyte's decomposition voltage, the charge stored varies linearly with the voltage.

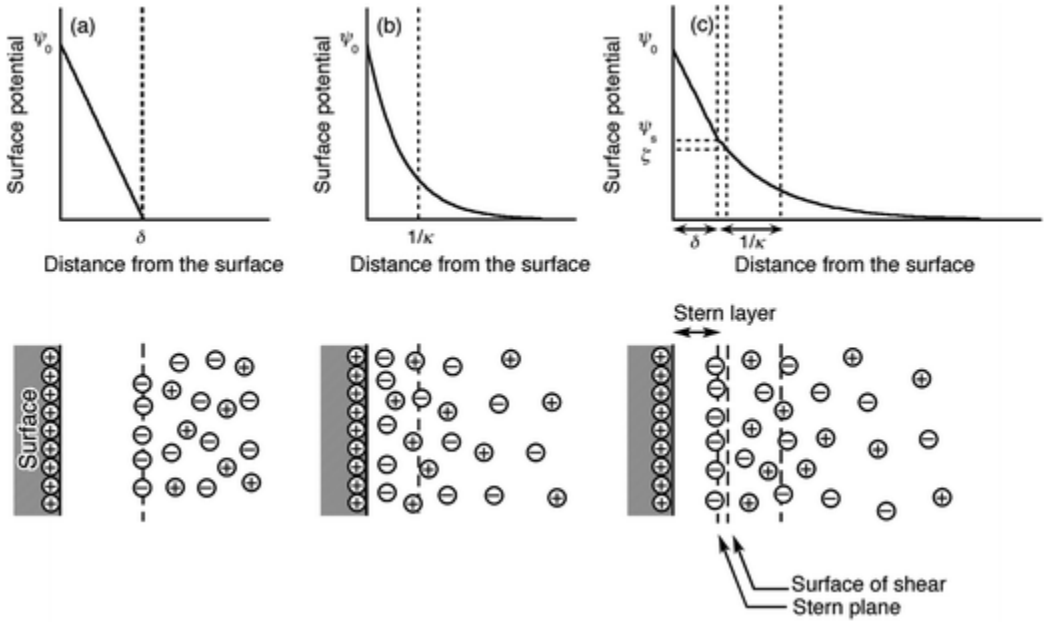

Figure 2.3 (a)Helmholtz model, (b) Gouy Chapman model, (c) Gouy-Chapman-Stern (GCS) model [53]

Helmholtz model did not consider diffusion or mixing of ions in solution, adsorption possibility onto the surface and the solvent dipole moments and the electrode interactions and insufficiently describes EDL structure in the porous electrodes.

Later on Gouy & Chapman [54], [55] made improvements in the model by introducing a diffuse model of EDL in which the electrical potential difference decreases exponentially away from the surface to the bulk electrolyte as shown in Figure 2.3-(b). They observed that the capacitance depended on the applied potential and the ionic concentration close to the surface in the diffuse layer and is not considered constant. The ions are maintained at a distance from the surface and are spread in a layer close to the surface.

Gouy-Chapman model fails for highly charged double layers. It considers ions as point charges and assumes that there are no physical limits for the ions to approach the surface. Stern suggested a model combining Helmholtz model and Gouy-Chapman model known as Gouy-Chapman-Stern (GCS) model [56]. Some ions stick to the electrode giving an inner Stern layer (as suggested by Helmholtz) while some form outer diffuse layer (as suggested by Gouy-Chapman) as also shown in Figure 2.4-(a). The Stern layer does not contain charge. As can be seen from Figure 2.3-(c), up to Outer Helmholtz Plane (OHP), the behavior of electric potential similar to that in Helmholtz and beyond that it behaves like Gouy-Chapman that is, decreases exponentially up to diffuse layer.

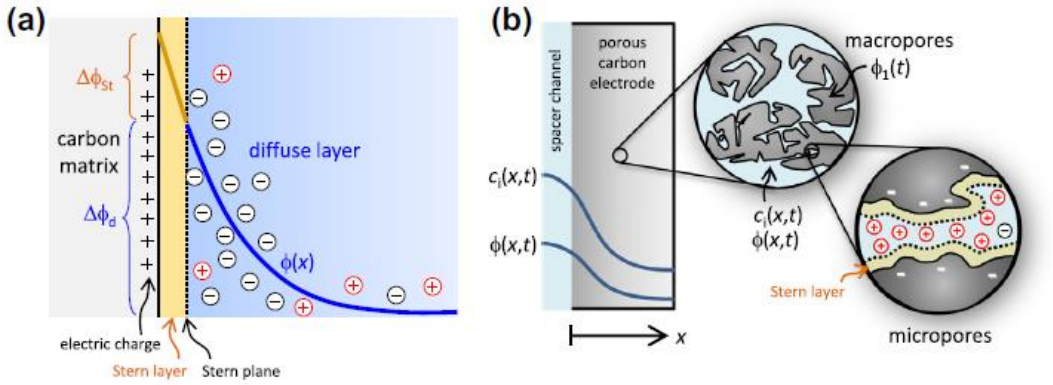

Figure 2.4 Models for Electrostatic double layers. (a) GCS model for a single planar EDL describing the EDL structure, (b) Two porosity model of the electrode [57], [58] showing macropores and micropores [29]

The width of the diffuse layer is not exact but ion concentrations decrease gradually with distance from its surface. Figure 2.4-(b) shows the macropores and micropores in the porous electrode. The macropores are the pores in contact with the solution whereas micropores are the pores in the porous carbon electrode.

The characteristic thickness of the electric double layer is given by debye length that varies with concentration in the CDI cell [29].

Inverse Debye length κ is given as [29],

$$\kappa = \sqrt{\frac{2F^2 x}{\varepsilon_r \varepsilon_0 RT}} \tag{2.1}$$

Where ε_0 is the permittivity of free space, ε_r the relative permittivity of water (78), R is the universal gas constant (8.3144621 $J\ K^{-1} moles^{-1}$), F is the Faradays constant (96500 couombs) , x is the concentration of salt in bulk solution (macropores) and T is the temperature in Kelvin (297.15 K).

Debye length is given by $\lambda_D = \frac{1}{\kappa}$.

When the average pore size in micropores of electrodes is smaller than Debye length, there is overlapping of EDL and Gouy-Chapman-Stern (GCS) model no longer describes the case of overlapping EDL's. Modified-Donnan model [46] is used to describe EDL in such cases.

2.5 Operational modes in CDI and MCDI

Two modes of operation are possible in CDI and MCDI, viz., constant voltage and constant current operation which are explained below [29].

2.5.1 Constant voltage (CV) mode of operation

During adsorption in CDI, a constant positive voltage is applied and during desorption step, a zero voltage is applied (zero voltage desorption - ZVD). However, a reversed voltage can also be applied during ion-desorption step (reverse voltage desorption - RVD). Moreover, it is also possible to increase the charge efficiency in CDI by increasing the discharge voltage during desorption step [59].

The results of effluent salt concentration with time for CDI and MCDI for CV- ZVD-mode of operation and CV-RVD mode of operation are shown in Figure 2.5. It is reported that the desalination increases when using RVD mode. In ZVD mode, the counter-ions are released from electrodes and this counter-ions expulsion occurs until the salt concentration in the macropores becomes equal to the concentration in the spacer channel or until complete discharging of micropores.

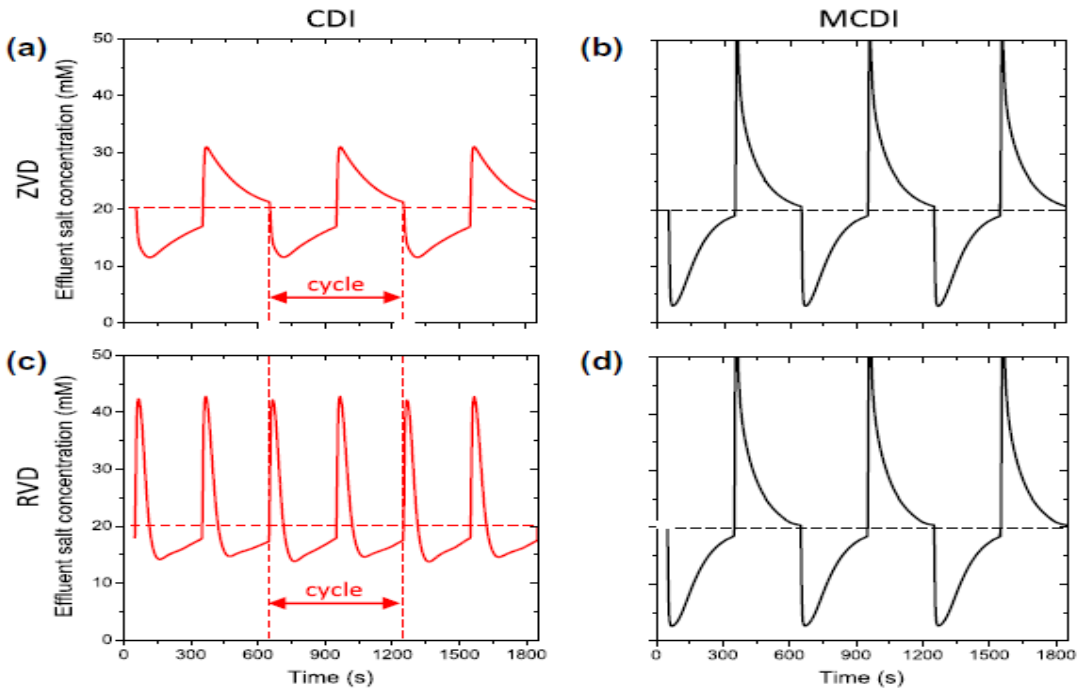

Figure 2.5 Effluent salt concentration with time for different operating modes viz., (a) CDI ZVD, (b) MCDI ZVD, (c) CDI RVD, (d) MCDI RVD [29]

However, in MCDI CV-RVD mode of operation, counter-ions desorption occurs first from all the electric double layers in the micropores of the porous carbon followed by desorption from macropores. The macropore salt concentration approaches value close to zero during salt desorption which leads to effective electrode cleaning of ions from the electrode. Also in the subsequent adsorption cycle, ions adsorption and capacity is greatly increased compared to ZVD. The reverse mode of operation is possible in MCDI because when the counter-ion reaches the spacer channel in the desorption step, even though it experiences attraction force from the opposite electrode, the membrane in front of that electrode will not allow counter-ions to penetrate the membrane and eventually ions are flushed out of the cell.

The use of reversed voltage in CDI desorption step is debated as it is expected that ions desorbed from the electrodes will be attracted to the oppositely charged electrodes because

of the absence of membranes [3], [46]**.** However, there is a possibility of ions to leave the stack via channel between the electrodes without being attracted to the electrode of opposite polarity. [29] mentions that the salt adsorption capacity per cycle is higher in CDI –CV-RVD compared to CDI-CV-ZVD. Also, there would be frequency doubling in CDI-CV-RVD owing to concentration decreasing and increasing twice over a single period as shown in Figure 1.21.

[29], [60] also report salt adsorption in the CV-RVD mode and CV-ZVD mode for CDI and MCDI where they proved experimentally that the adsorption of salt in MCDI CV-RVD > MCDI CV-ZVD > CDI CV-RVD > CDI CV-RVD. The RVD mode for both CDI and MCDI increases the salt adsorption but decreases charge efficiency [61]. Moreover, if charge efficiency is considered, MCDI is preferable over CDI, the values of Λ for MCDI is above 0.9, whereas it is below 0.8 for CDI.

2.5.2 Constant current (CC) mode of operation

In CV mode of operation, it is observed that the effluent salinity decreases during adsorption as ions are stored in the EDL's and as the cell becomes fully charged the cell concentration increases to reach the influent salt concentration. In CC-MCDI mode, it is possible to obtain a constant effluent salt concentration with time as shown in Figure 2.6 [29]. By applying fixed current between the two electrodes, the flux of ions getting stored in the EDL is also fixed, so as to obtain desired effluent concentration coming out of the CDI cell. The effluent concentration level can be tuned to a desired value by changing electrical current and/or water flow rate as explained in [57].

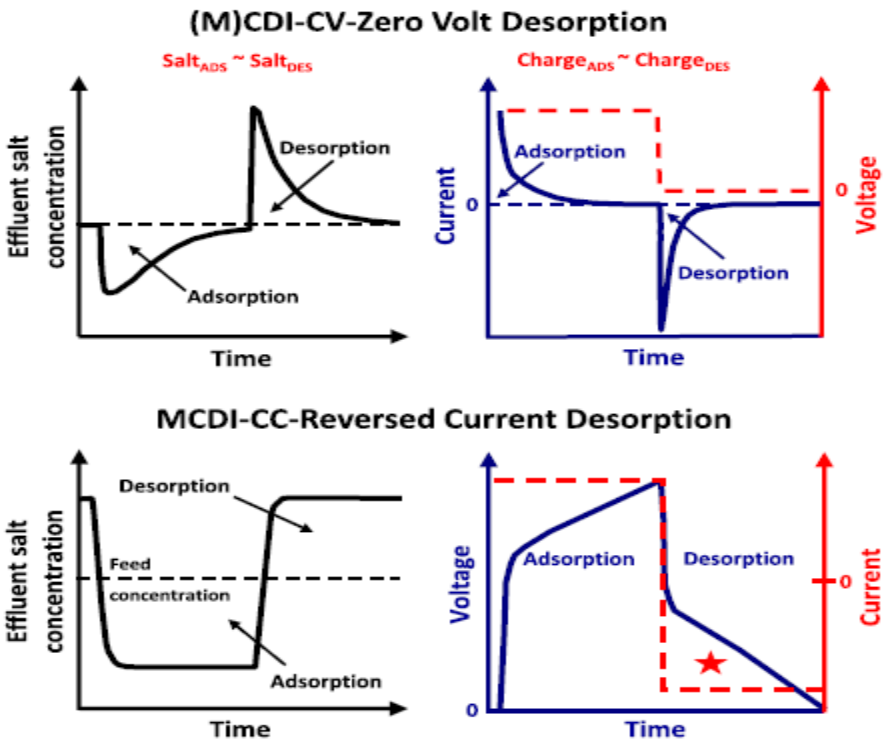

Figure 2.6 Effluent salt concentration with time for MCDI CV mode of operation and CC mode of operation [29]

In CC-MCDI operation, a constant current is applied to the electrodes until the cell voltage reaches 1.6 volts after which reversed current is applied for ion desorption until zero cell voltage is obtained. The CC mode in CDI does not help in obtaining a constant effluent concentration in adsorption step due to the absence of membranes [29].

2.6 Energy requirements in CDI

The minimum energy required for desalination increases with the concentration of the inlet feed and recovery [42]. The energy demands for some of the desalination technologies currently used are shown in Table 2.1 and compared with CDI. From Table 2.1, it is clear that CDI is competitive to RO in relation to energy requirements where CDI consumes about 0.1 to 2.03 kWh/m3 of freshwater produced whereas RO system utilizes 2-6

kWh/m^3[42]. Several works have been reported in the literature that discusses the factors influencing energy requirements in CDI and MCDI [57],[30]**.**

Table 2.1 Energy demands of different desalination technologies [42]

Desalination method	**Energy demand in kWh/m^3**
MSF	10-58
MED	6-58
RO	2-6
ED	0.4-8.7
CDI	0.1-2.03

[28] presents the comparison of MCDI and RO energy demand at different salinities of NaCl ranging from 10 mM to 80 mM (1 mM = 1 mol/m^3) in order to obtain 5 mM freshwater. The operation of the equipment for MCDI is using constant current (CC-RCD) to obtain a water recovery of 50 %. Results demonstrate that there is a crossover point at a salinity of 40 mM below which MCDI consumes less energy compared to RO. There is a hope that this crossover point will be shifted to write with the ongoing researches in the field that will prove the capability of CDI to be a competitive desalination technology for brackish water desalination.

2.7 CDI cost

A direct cost comparison of CDI vs RO was demonstrated in [62]. They compared costs for brackish water desalination plants of small capacity (3785 m^3/day), and claim that CDI gives a cost of 0.11 \$/m^3 whereas RO gives a cost of 0.35 \$/m^3.

2.8 Electrode materials used in CDI

The majority of efforts to improve the CDI technology is done by the development and synthesis of electrode materials that can improve the desalination performance. Ions are stored inside the pores of electrodes. Some pores inside carbon do not contribute to ion adsorption because it is closed from all the sides or is leaky. The electrodes are chosen on the basis of its cost, ability to tune the pores, surface area of the electrodes, low scalability. Activated carbons are the most widely used owing to its lower cost, high specific surface area (1000-3500 m^2/gram) and availability [50], [63]. Also other materials have also been used for CDI and MCDI including carbon aerogels, carbide derived carbons (CDCs), CNTs and CNFs, mesoporous carbons, graphene etc [32], [64]–[68].

2.9 Parameters affecting the CDI process

The main parameters affecting CDI process are explained below:

2.9.1 Surface properties

The presence of surface functional groups including carbonyl, phenol, carboxyl etc., impacts the desalination using CDI by enhancing surface wettability and improving the efficiency of surface utilization [69].

2.9.2 Voltage applied to CDI cell

The high voltage applied to the electrodes increases the thickness of the EDL which results in strong adsorption of ions. However, if the voltage applied to CDI cell exceeds 1.23 V, it would result in electrolysis (decomposition) of water. Electrolysis results in a change of pH in solution and oxidation of carbon electrodes (oxidation of chlorine at anodes [70]) and negatively affects the CDI process [65]. It is also reported that below 1 volts, the pH increases quickly as potential is increased due to the reduction of dissolved oxygen. It is concluded by the authors in [71] that the salt removal increases with increasing voltage in the range of 0.8-1.5 volts but increasing voltage also increases the energy consumption.

2.9.3 Flow rate

[30] showed that upon increasing flow rate from 1 to 4.5 l/min, there is approximately 28% drop in electrosorption removal efficiency. Electrosorption removal efficiency is defined as the ratio of the difference in initial and final concentration to the initial feed concentration. As the flow rate of the inlet feedwater increases, the time for which the ions

reside in the CDI cell decreases as a result of which ions do not get sufficient time to electromigrate to the electrodes that results in low electrosorption efficiency. However, increasing flow rate results in low energy consumption [72], [73]**.** Thus, the optimal flow rate must be governed by both electrosorption removal efficiency and energy consumption.

2.9.4 Feed solution concentration

As the inlet feedwater concentration increases, solution resistance decreases and adsorption velocity increases which in turn causes the capacitance and salt removal to increase [69]. The salt removal increases as more ions are adsorbed onto the electrodes but the adsorption ceases when the electrodes reach their saturation limit. [30] showed approximately 41% drop in electrosorption efficiency when the inlet feed concentration was increased from 500 ppm to 3500 ppm.

2.9.5 Treatment time

As treatment time increases, the ionic concentration decreases at first as ions adsorb onto the electrodes. However, after some time, the concentration of the effluent begins to rise as the salt adsorption limit is reached in the electrodes. The adsorption slows down until a dynamic equilibrium is reached [69].

2.9.6 Temperature

The temperature has a negative effect on salt removal in CDI process. [30] showed 11.2 % drop in electrosorption efficiency when the temperature of the solution was raised from 20 to 50 degrees Celsius. This is attributed to decrease in adsorption capacity of activated carbon electrodes with temperature. It is also possible for ions to escape from metal surface to the solution as the temperature of the feed solution is increased.

Other factors including the spacing of the electrodes, number of CDI electrode pairs used, the configuration of CDI units affects the efficiency of the CDI process. As the distance between the electrodes is small, adsorption would be stronger and less treatment time is required. High salt removal efficiency can be obtained by using more pairs of electrode in CDI.

2.10 Review of CDI

The breakthrough in the CDI technology came from the work of Farmer et al in 1995. It reported the experimental results of CDI apparatus that was developed at Lawrence Livermore National Laboratories [64], [74], [75]. Since then the process came to be known as Capacitive De-ionization (CDI).

[3] explains constant current operational mode for MCDI. MCDI consumes much less energy per mole of salt removed as compared to CDI. For MCDI, with 1-200 mM ionic strength feed solution, an energy consumption of approximately 22 kT is reported for one ion removed where k is the Boltzmann constant and T is the temperature in Kelvin. It shows that the energy consumption in MCDI does not depend on salt concentration while for CDI it is directly proportional to the inlet feed solution concentration.

[58] describes MCDI transport model that not only considers double layers formed inside micropores, but also includes the role of the macropores for ion movements to the electrode. The spacer channel is considered to be divided into stirred volumes placed in series and the transport of ions inside spacer channel and from spacer channel to the

electrodes is considered by making some assumptions. The experimental setup consists of 8 parallel CDI cells with feed concentration of water equal to 20 mM. The authors compared the adsorption/desorption cycles of MCDI both experimentally and theoretically for zero voltage desorption (0-MCDI) and for reverse voltage desorption (r-MCDI), and also compared with results for CDI. EDL-structure is described by using a modified Donnan model to describe the salt adsorption and charge in the CDI stack. The authors based on experimental results claim that the salt removal for 0-MCDI is 20% more than in CDI, and r-MCDI removes further 20% compared to 0-MCDI making r-MCDI 40% more effective than CDI. For CDI and 0-MCDI, the variation of charge with time was almost similar whereas for r-MCDI, charge increased by 20%. The authors suggested the use of validated MCDI model for further design and process optimization and attributed a little deviancy due to assuming not ideally permselective membranes (may also allow some co-ions) and also due to assuming constant chemical attraction term (attraction of ions when no voltage is applied) in Donnan theory.

[62] presented the development of prototype industrial type CDI module and evaluated its performance for brackish water desalination to compare its potential to compete with Reverse Osmosis. The main aim was to convert laboratory unit at LLNL to industrial prototype unit. The electrodes were subjected to certain quality control tests to ensure certain minimum standards based on surface area, bulk resistivity, specific capacitance etc. The energy consumption for desalination of coal bed methane (CBME) produced water was 2.25 kWh to treat 1000 gallons of produced brackish water. The energy consumption and various costs of Reverse Osmosis and CDI prototype unit were compared and it was concluded that CDI technology could replace membrane technologies in the near future.

Energy efficiency of CDI plants was more as compared to Electrodialysis Reversal (EDR) technology plants. For seawater desalination, it was emphasized that the capacitive de-ionization module production costs need to be reduced in order to compete with reverse osmosis. It is further mentioned that by utilizing energy recovery processes, industrial units can approach the laboratory energy consumption.

[76] reports an experimental approach of continuous electrodeionization through electrostatic shielding. The permselective membranes in the cell were replaced by electrostatically shielded zones. The electrostatically shielding of compartment causes the electric field to be zero inside the compartment. The authors claim using this configuration to regenerate ion exchange resins as well as for producing deionized water and desalinating brackish (0.02 M NaCl) or sea water. Co-ions are carried by counter-ions migrating in the shielded compartments. No drawbacks of concentration polarization existed in this process.

[77] presents a novel process for water desalination and electrodeionization by means of electrostatic shielding zones. These zones are used as ionic current sinks since the electric field becomes zero inside the zone when an external field is applied to the overall cell. Ions get concentrated in the sink whereas the other compartments get depleted of ions. 0.03 M NaCl solution is desalinated to obtain potable water. Even industrial effluents consisting of heavy metal ions are purified to obtain low concentration pure water. It also specifies regeneration of ion exchange resins to get high purity deionized water.

[78] modeled the CDI adsorption-desorption processes of CDI to obtain conductivity of freshwater with respect to time for a given initial feedwater concentration of saline water. The authors claim that to improve desalination performance and to obtain less concentrated

freshwater, number of CDI cells has to be increased. A stack of multiple CDI cells could be used to achieve required desalination performance.

[79] presented the transient response of the CDI cell operating in a batch mode wherein a particular volume feed water is fed back to the container incessantly until the system reaches steady state. The model for the batch system is developed by considering single pass CDI operation and the mixing phenomena that occur in the recycling tank. The model was validated using experimental results.

[80] presented experimental data of a pilot plant for outlet salt concentration and current in MCDI stack as a function of flow rate, inlet ionic strength and time. The position of anion exchange and cation exchange membranes are reversed in each of the cells because one electrode acts as a cathode of one cell while acting as the anode for other. The CDI configuration utilizes “stop-flow” operation mode that helps in concentrating all the stored salt in 25-40% volume of dilute product resulting in a small and highly concentrated brine stream. A theoretical model based on GCS theory is described for MCDI which describes the effluent ion concentration and electric current varying with time and storage of ions in the EDL both during the adsorption and desorption. The modelling of ion exchange membranes is done by considering stagnant diffusion layers placed in front of the membranes. Experimental results showed that with increase of the flow rate and ionic concentration, the effluent ionic strength increases which would also cause the current to decrease with time because at lower flow rates the average concentration in the cell is low leading to increase in resistance for ion transport which ultimately leads to low salt removal rate and less current. The agreement between the theory and experimental results is not

perfect but still satisfying. The authors suggested to improve MCDI model by introducing additional resistance located within the spacer channel and electrode.

[81] mentions the use of carbide-derived carbon (CDC) as electrodes for CDI by comparing it with commercially available activated carbons (AC) and demonstrated that CDC electrodes have a high electrosorption capacity and charge capacity (approximately 28-44% increase for salt adsorption and 23-34% increase for charge) when voltages in the levels of 1.2-1.4 V is applied to the system with a particular feedwater concentration and feedwater flow rate. The authors state that materials having high charge storage capacity can be highly suitable for CDI application. Modelling of the system is performed using mD-model.

[82] presents a method to optimize the water recovery in MCDI and the electrosorption rate by demonstrating how the variation of each parameter individually affect the CDI operation and performance such as adsorption and desorption time, feed salt concentration, current and voltage applied to the CDI cell.

[83] demonstrates the use of electret technology to desalination. The authors tried to reproduce the patent results of Douglas MacGregor who claimed the use of electrets for water desalination based on electrets being permanently polarized materials. The permanent electrostatic field attracts counter-ions to the charged surface to produce a purified effluent in between the electrets. The method was evaluated both theoretically and experimentally to investigate practical aspects of the technology. The authors reported that the design is satisfactory only when a dilute feed water is used and the system must have a

very high surface charge density to achieve desalination. The authors consider using electrets for desalination as viable and recommend further development.

The modelling of the electrostatic double layer is described using equilibrium GCS model in [47]. A description of transfer of ions from bulk solution to the electrodes via a mass transfer layer is explained. The model very well predicts the experimental datasets of current and salt concentration in the effluent water with time. A new term, differential charge efficiency is described based on GCS-model, which is the ratio of rate of salt removal relative to the electronic current. It describes the ions removed from the solution for each electron transferred from one electrode to another. During modelling, the authors assumed two electrodes to be completely non-Faradaic, that is, flow of current due to electrochemical reactions from electrodes into the solution or vice versa is zero. An approximate approach based on mass-transfer boundary layer placed in front of electrodes is used for the charge transport from bulk solution to electrodes. The charge efficiency obtained using theoretical model was slightly high (0.81) compared to experimental results (0.77). The authors suggested this drawback due to the fact that pores inside carbon must be too minute to for ions to enter and remove ions. Also because of overlapping of double layers, the pores inside carbon leads to lower salt adsorption. The author considers development of the model to encompass all the drawbacks and deviation from experimental results.

[84] calculates charge efficiency (ratio of salt adsorption and electrode charge) as a function of voltage and salt concentration experimentally, and this data is used to describe the structure of double layer inside electrode and measure the effective area for ion adsorption. First, the authors calculate charge efficiency by varying cell voltage from 0 to

1.4 Volts and ionic strength in the range of 5mM and 20mM based on the data for charge vs cell potential and salt adsorption vs cell potential. The authors used GCS double layer model to accurately describe data for charge efficiency by considering stern layer capacity, C_{st} as an adjustable parameter obtained from experimental data set of charge efficiency varying with voltage and ionic strength. An optimized value of C_{st} is used in GCS model and the same model is used to fit the full data sets for charge and salt adsorption which in turn calculate the effective surface area per gram of electrode, a_m. These two optimized values C_{st} and a_m of porous electrodes are used as input parameters in electrokinetic process model and compared with data for ion concentration of the effluent and current based on different voltages applied to the cell, different flow rates and different inlet ionic concentrations. The theoretical results matches the experimental results quite effectively. The double layer is assumed to be at equilibrium with the solution in the bulk. This paper improves the work of [47] by describing both ion removal and ion release by the same set of parameters in GCS model.

[59] showed that charge efficiency in CDI can be increased by carrying out desorption step at a voltage of $V_{disch} = 0.3$ volts instead of zero volt desorption in CV mode of operation of CDI. This caused small reduction of salt adsorption per cycle,the energy per ion removed decreased by about 14 % in case when there is no energy recovery and led to 30 % decrease in case of perfect energy recovery. For CC operational mode with 0.41 ampere current applied to CDI stack consisting of four CDI cells, the authors claim that the constant effluent concentration level reached swiftly with increased discharge voltage. The improved mD model [48] describes data set of equilibrium salt adsorption and charge

perfectly. The dynamics of ion transfer and charge storage both for CV and CC operation was illustrated by making use of porous electrode transport theory.

[85]–[87] illustrates continuous mode of desalination using CDI wherein freshwater and brine are produced at the same time. In this configuration of CDI, slurry electrodes are used that flow between the porous separator (ion selective membranes are also used as porous separator) and the electrode. The ions electromigrate to the slurry electrodes and are flushed as brine whereas freshwater is obtained from between the porous separators.

Research is done to make CDI more efficient and cheaper technology by using the concept of energy recovery [36], [35]. During the ion desorption step, a significant amount of energy is lost. This energy can be used to charge a neighbouring CDI cell or supercapacitor or battery.

[36] uses a buck-boost DC/DC converter in order to charge a neighbouring supercapacitor using ion desorption of a CDI cell. They claim to obtain a high energy recovery of 51% using buck-boost converters. The simulation and experimental results are obtained with minor deviations.

Many attempts have been made in the literature to model the CDI process based on charge transfer between electrodes utilizing Gouy-Chapman-Stern [47], [84] and Modified Donnan models [3], [60], [32], [48], [88] and improved modified Donnan models [59], [49] to describe the electrostatic double layer in the electrodes. [48] describes the transport model for membrane capacitive de-ionization where it uses modified Donnan model to describe the salt adsorption and charge in a cell. [59] uses improved modified Donnan model (i-mD) to describe data set of equilibrium salt adsorption and charge and presents

dynamics of ion transfer and charge using porous electrode transport theory. The modelling of batch mode operation of CDI is shown in [29], [89].

Electrical circuit designs have also been used to characterize a CDI cell [36], [35], [90], [91]. The most commonly used CDI equivalent circuit is the Randle's circuit [36], [35], [90], which takes into account the solution resistance, double layer capacity and leakage resistance**.** This model was used to compute energy recovery in a CDI cell utilizing different converters to recover energy in different ways. [90] compared the electrical response of CDI cells with the experimental data using Randle's equivalent circuit. The model response of CDI cell showed good agreement with experimental data, except for the prediction of solution resistance, which was overestimated.

Patents by MacGregor mention an apparatus for separating ions from liquids to produce freshwater and brine using permanently polarized materials electrets wherein the static electric fields are created in between the electrets that allow the ions of opposite charge to move towards the counter polarized materials [92], [93].

2.11 Companies providing CDI based desalination equipment

Many companies manufacture CDI equipment for research purposes as well as for commercial purposes. AQUA EWP [94] has manufactured a commercial equipment for brackish water as well as for sea water desalination and these equipments can be purchased. However other companies like PLIMMER CDI [95] also has similar principle based

equipment. The Cap DI unit is available for research by the company Voltea BV [96]. Atlantis technologies [97] have used supercapacitors for water desalination.

CHAPTER 3

MATHEMATICAL MODELLING AND ANALYSIS OF A CDI CELL

3.1 Introduction

This chapter proposes a novel mathematical modelling of capacitive de-ionization (CDI) system with activated carbon electrodes. A mathematical model of CDI is presented based on its electrical equivalent circuit and a dynamic equation that describes how the effluent salt concentration varies with respect to time in a CDI cell. The model is developed by taking into consideration the specific surface area of the electrodes, capacitance of the electrodes, double layer thickness, initial feed concentration, the flow rate of feed water, volume of the CDI cell, voltage applied to the CDI cell and solution resistance in the CDI cell. The model predicts the amount of charge captured by the CDI cell and the current in the CDI cell, both as a function of time. The effectiveness of the model is evaluated by comparing its results with the reported experimental results of AQUA EWP CDI unit [30], [31]. The model also determines the performance of the AQUA EWP CDI cell to different operational parameters i.e., the feed TDS concentration and flow rates. The model results are in good agreement with the experimental results. The batch mode operation of CDI is investigated using the derived model.

The chapter is organized as follows. First, a mathematical model of capacitive de-ionization with activated carbon electrodes is derived using an electrical equivalent circuit of CDI in Section 3.2 that takes into effect the specific surface area of the electrodes, capacitance of the electrodes, double layer thickness, initial feed concentration, flow rate of feed water, volume of the CDI cell, voltage applied and solution resistance in the CDI cell. Next, a CDI unit from AQUA EWP using activated carbon electrodes is explained in Section 3.3. The CDI model is extended to describe AQUA EWP CDI unit consisting of two CDI cells in series in Section 3.4. Finally, the model results are compared with the reported results of electrosorption [30], [31] conducted on a CDI unit from AQUA EWP in Section 3.5. The model is used to determine the efficiency of the system in treating brackish water at different feed TDS concentrations and also to evaluate the effect of flow rate on treatment efficiency. The model is further used to investigate the batch mode operation of AQUA EWP CDI unit in Section 3.6.

3.2 Modelling of Capacitive De-ionization (CDI) cell

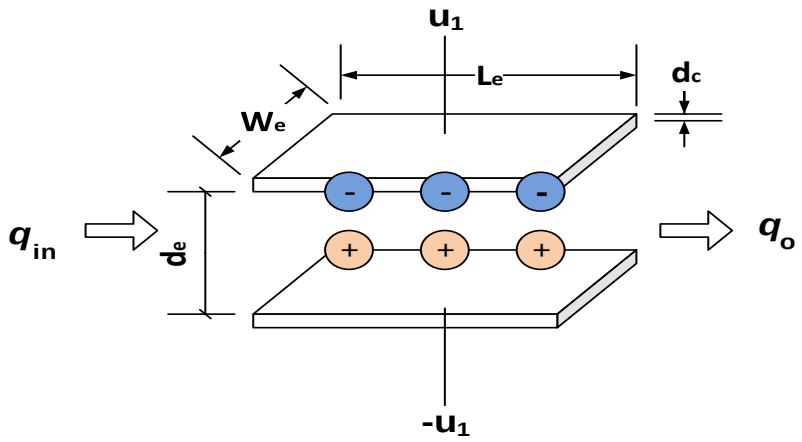

Figure 3.1 CDI cell operation during purification – anions gets adsorbed on the anode and cations to the cathode

The CDI cell as shown in Figure 3.1 is a conduit of rectangular cross section of width W_e, length L_e and height d_e. CDI cell consists of electrodes (activated carbon) of thickness d_c, and each electrode of a CDI cell is attached to a current collector. The activated carbon electrode layer is merged and fully in contact with the salty water. As shown in figure 2, the top metal collector is connected to a dc voltage signal of $+u_1$ and bottom metal collector to a dc voltage signal of $-u_1$ during purification that causes the anions to move towards anode and cations to move towards cathode. During regeneration, the CDI cell is powered off with zero voltage or a voltage of opposite polarity is applied to the current collectors. The purification and the regeneration step completes the CDI cycle. The water flows at a flow rate of q_{in} to the CDI cell and the flow rate at the exit q_o can be controlled using a valve.

The capacitance associated with each electrode is given by

$$C_e = \frac{k_c \varepsilon_0 (L_e W_e)}{t_{cs}} \tag{3.2}$$

where k_c depends on the effective area ratio of the activated carbon and its wet permittivity, t_{cs} is the thickness of the double layer which is of the order of nanometers. The electrical double layer thickness is often approximated as Debye length using Gouy Chapman model [29].

$k_c = k_s \rho_c t_c$; where k_s is the specific surface area of the Activated carbon which is typically around 800-2500 $m^2/gram$, ρ_c is the density of AC, t_c is the thickness of Activated carbon electrode.

The equivalent circuit of a CDI cell with two electrodes is shown in Figure 3.2.

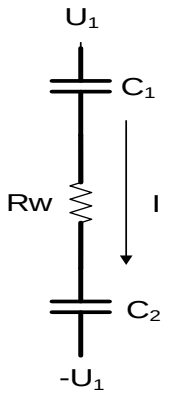

Figure 3.2 Equivalent electric circuit of a CDI cell

The top activated carbon electrode capacity is represented by capacitor C_1 which is positively charged and bottom electrode capacity is represented by capacitor C_2 which is negatively charged. The capacitance associated with the two electrodes is equal to maintain charge balance in solution i.e., C_1=C_2.

R_w is the electrical resistance of the salty water between the two opposite electrodes and I is the current flowing in the CDI cell through R_w resistance.

The resistance of water is given by the formula

$$R_w = \frac{\rho_e d_e}{A_c} \tag{3.3}$$

where A_c is the physical area of the activated carbon in m^2

d_e is the distance between the activated carbon electrodes

ρ_e is the resistivity of the water.

The resistivity of water depends on temperature and concentration and for saline water is given by the approximation [98], [99],

$$\rho_e \cong \frac{5}{x(1 + \alpha_T(T - 25))} \tag{3.4}$$

Where x is the concentration of salt in kg/m^3 (or grams/l); and $\alpha_T = 0.022/℃$

3.2.1 Modelling equations of a CDI cell

Let V_c be the voltage across the capacitor, and I be the current flowing throw R_w resistance and q be the flow rate of feed water to the CDI cell.

Let the initial feed concentration to the CDI cell be denoted by x_f and V be the volume of the CDI cell.

From the equivalent electrical circuit of CDI cell as shown in Figure 3.2, we write the following salt balance equation,

$$V\frac{dx}{dt} = q(x_f - x) - KI \tag{3.5}$$

where $K = M_{ws}/F$, where M_{ws} is the molecular weight of NaCl and F is Faradays number (F=96500 Coulombs).

The current is related to the voltage across the capacitor, V_c by the formula,

$$I = C_e\frac{dV_c}{dt} = \frac{2V_{in} - 2V_c}{R_{wc}} \tag{3.6}$$

The equations (3.4) and (3.5) can be written as,

$$\frac{dx}{dt} = \frac{q}{V}(x_f - x) - \frac{K}{V}\frac{(2V_{in} - 2V_c)}{R_{wc}} \tag{3.7}$$

$$\frac{dV_c}{dt} = \frac{2V_{in} - 2V_c}{C_e R_{wc}} \tag{3.8}$$

Equations (3.7) and (3.8) are the state equation of a CDI cell that describes the relationship between CDI cell salt concentration and voltage across the capacitor with respect to time.

3.3 Description of the AQUA EWP CDI experimental setup

The block diagram of capacitive de-ionization system for desalination is as shown in Figure 3.3.

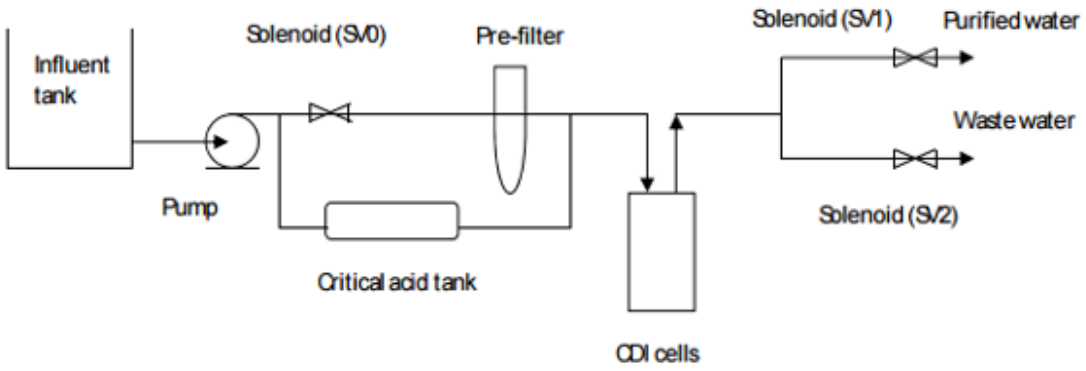

Figure 3.3 Capacitive de-ionization system schematic diagram [31]

The feed solution used in the experiment [30], [31] is Sodium chloride (NaCl) of desired concentration. The salty water (NaCl) is first collected in an inlet tank. A pump takes the salty water from the inlet tank and passes through a sand filter for pre-treatment and water flows at a flow rate of q to the CDI cells. Two CDI cells were used in the experiment. A potential of 1.5 V DC is applied per CDI cell so that electrolysis does not occur. There are 3 valves in the system viz., influent solenoid valve SV0, outlet solenoid valves SV1 and SV2. The CDI operational cycle is of 2.5 mins and occurs in two main steps: the purification mode step (90 seconds) - wherein the inlet valve SV0 and the outlet valve SV1 are opened and a voltage of 1.5 VDC is applied to CDI cells to purify the feed solution and the regeneration mode that occurs in two steps – in the first 30 seconds, the outlet valve SV1 and the inlet valve SV0 are closed and the power supply is off that results in discharging the ionic charge on the electrodes, followed by another 30 s when the outlet valve (SV2) and the inlet valve (SV0) are opened and the voltage is applied to CDI cells

with a opposite polarity of 1.5 VDC that results in removal of ions from the electrodes along with flushing of highly concentrated brine [31]. The operation of the system is as illustrated below in the Table 3.1.

Table 3.1 Operation of AQUA EWP CDI unit

Operational cycle (**Time -** 2.5 minutes = 150 seconds)	**Description**	**Time (sec)**	**Feed pump and SV0**	**SV1**	**SV2**
1. Purification	Application of 1.5 volts	90	ON	ON	OFF
2. Regeneration – 2 steps	1. Discharging the ionic charge on the electrodes, no flushing done 2. Flush mode with opposite polarity (negative voltage -1.5 volts)	1. 30 2. 30	1. OFF 2. ON	OFF	1. OFF 2. ON

The recovery ratio of this process is 75 % as it includes 90 seconds of product flow during purification versus 120 seconds of total flow. The AQUA EWP CDI unit consisted of activated carbon electrodes with a single CDI cell containing 1354 grams of activated carbon. The specific area of activated carbon electrodes used was 800 m^2/gram. Each cell assembly contained 200 sheets of activated carbon (100 cathodes and 100 anodes) with dimensions of 158 mm × 174 mm × 0.3 mm. These electrodes were connected to the two sides of the DC power supply.

3.4 Modelling of AQUA EWP CDI unit

The experiments in the paper [30], [31] consisted of two CDI cells in their setup as shown in Figure 3.4. In this configuration, the feed water with a concentration of x_f and a flow rate of q flows through the CDI cell 1. During purification mode of 90 seconds, the water is purified in the CDI cell 1 and attains the concentration x_1 at the exit of cell. The water is passed on to CDI cell 2 for further purification and attains a concentration x_2 at the outlet of CDI cell 2. During regeneration mode, the ions are flushed back into the feed water and the concentration at the outlet of CDI cells 1 and 2 increases with time. The application of voltage to both the CDI cells is simultaneous.

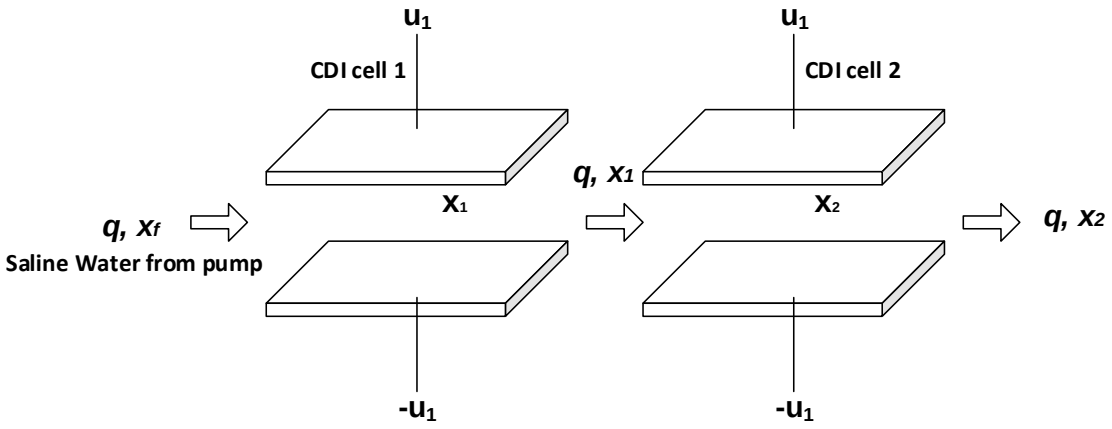

Figure 3.4 Diagram illustrating two CDI cells in series

The state equations for CDI cells in Figure 3.4 can be derived using equations (3.6) and (3.7) as follows that describes the concentration varying in the CDI cells and the voltage across capacitances with respect to time. The subscripts 1, 2 denote parameters of CDI cell 1 and CDI cell 2 respectively.

$$\frac{dx_1}{dt} = \frac{q}{V}(x_f - x_1) - \frac{K}{V}\frac{(2V_{in} - 2V_{c_1})}{R_{wc_1}} \tag{3.9}$$

$$\frac{dV_{c_1}}{dt} = \frac{2V_{in} - 2V_{c_1}}{C_e R_{wc_1}} \tag{3.10}$$

$$\frac{dx_2}{dt} = \frac{q}{V}(x_1 - x_2) - \frac{K}{V}\frac{(2V_{in} - 2V_{c_2})}{R_{wc_2}} \tag{3.11}$$

$$\frac{dV_{c_2}}{dt} = \frac{2V_{in} - 2V_{c_2}}{C_{e_2} R_{wc_2}} \tag{3.12}$$

3.5 Simulation Results

The theoretical model is simulated with the parameters of AQUA EWP CDI unit mentioned in the paper [30], [31].

3.5.1 Simulating the experimental AQUA EWP CDI system using the model

The CDI system model is simulated with the following specifications as mentioned in Table 3.2.

Table 3.2 Parameters used in AQUA EWP CDI simulation model

Number of CDI cells	2
Feed water concentration	1 g/l (1000 mg/liter (ppm))
Dimension of electrodes ($W_e * L_e * d_c$)	0.158 m × 0.174 m × 0.0003 m
Separation between electrodes, d_e	0.002 m
Feed water flow rate q_f	2 liters/min
Specific area of electrodes, k_s	800 $m^2/gram$
Mass of activated carbon in a CDI cell, $m_{c1} = A_{c_1} t_c \rho_c$	1352.6 grams

The other parameters of the system used in the model can be computed using the data in Table 3.2.

The characteristic thickness of the electric double layer is given by debye length that varies with concentration in the CDI cell.

Inverse Debye length κ is given as [29] as given in Equation (2.1),

$$\kappa_{1,2} = \sqrt{\frac{2F^2 x_{1,2}}{\varepsilon_r \varepsilon_0 RT}} \tag{3.13}$$

where x_1 and x_2 are the effluent concentration varying with respect to time in CDI cell 1 and cell 2.

Debye length is given by $\lambda_{D_{1,2}} = \frac{1}{\kappa_{1,2}}$.

The effective capacitance of AC is given as,

$$C_{e_{1,2}} = \frac{\varepsilon_0 K_c A_{c_{1,2}}}{t_{c_{1,2}}} \tag{3.14}$$

Where t_{c_1} and t_{c_2} are the thickness of double layer in CDI cell 1 and CDI cell 2.

The simulations are performed in MATLAB. A potential of 1.5 Volts DC is applied to the CDI cells during purification for 90 seconds followed by zero volts for 30 seconds and -1.5 volts DC for 30 seconds to totally remove the adsorbed ions during purification step.

The plot of effluent concentration varying with respect to time is obtained using the model and is shown in Figure 3.5. The salt concentration decreases from 1 grams/liter (g/l) to a minimum of 0.108 g/l at the end of purification phase of 90 seconds, whereas the

concentration reaches a maximum of 3.570 g/l during regeneration phase whereas the experimental results in [30] for one of the cycles showed a minimum concentration of 90 ppm at the end of purification phase and a maximum TDS concentration of 3.400 g/l during regeneration phase.

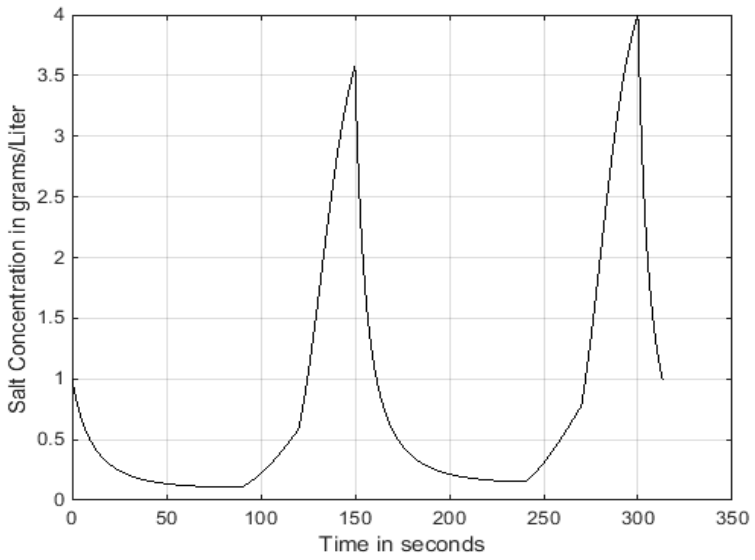

Figure 3.5 CDI operational cycle using model- purification and regeneration – showing effluent concentration with time

The capacitor voltage profile for CDI cell 2 is shown in Figure 3.6. The voltage increases during charging of the CDI cell upon application of a positive voltage and decreases during the regeneration step.

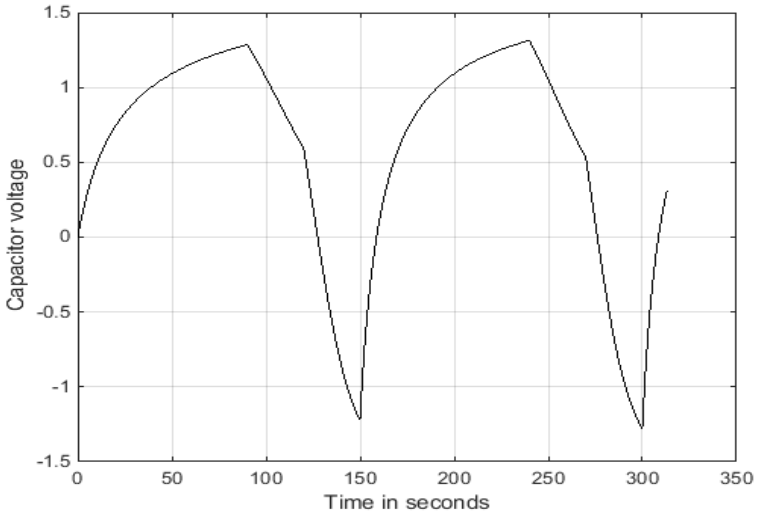

Figure 3.6 Capacitor voltage profile with time

The charge captured by the CDI cell 2 with respect to time is shown in Figure 3.7. During charging, as the ions are adsorbed onto the electrodes we see that the charge increases with time while during regeneration or discharging of the CDI cell, the charge decreases to a negative value.

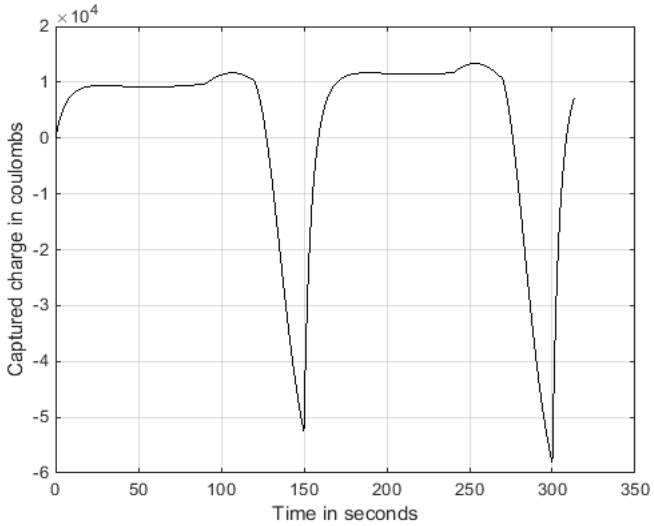

Figure 3.7 Captured charge in coulombs in the CDI cell 2

The current profile in CDI cell 2 as a function of time is shown in Figure 3.8. It decreases during charging of a CDI cell. As the concentration reaches the lowest value, the current decreases to zero.

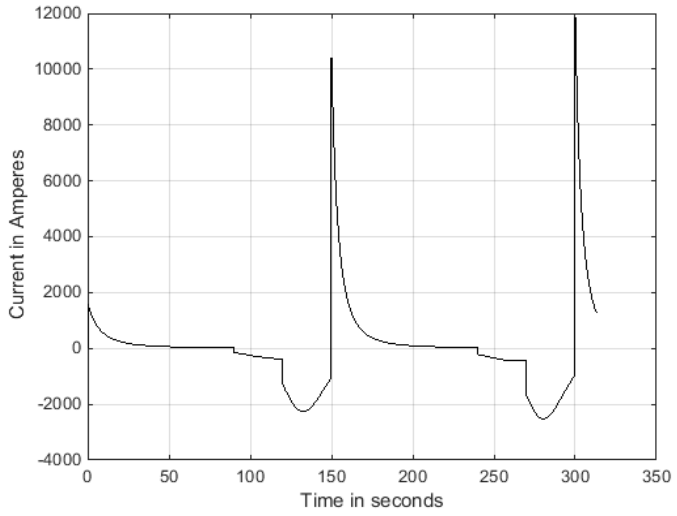

Figure 3.8 Current in CDI cell 2 varying as a function of time (in amperes)

3.5.2 Investigating removal efficiencies and other operational parameters

TDS removal efficiency is defined as the ratio of the difference of feedwater concentration, x_{in} and the freshwater concentration, x_p (or the lowest effluent concentration) to the feedwater concentration.

TDS removal efficiency = $\frac{x_{in}-x_p}{x_{in}} \times 100\ \%$

Investigation I. TDS removal efficiencies were calculated using the model in Section 3.2 for different concentrations of feed water with a flow rate of 2 liters/minute and temperature of 24 ℃ and the results are compared with the experimental results of the paper [31]. The

TDS removal efficiency is calculated for different concentrations ranging from 0.5 – 2.5 g/l and the results are compared with experimental values as shown in Table 3.3.

Table 3.3 Comparison of TDS removal efficiency between model and experiment [31] **for different TDS concentrations.**

Concentration g/l	**TDS removal efficiency (Model) (%)**	**TDS removal efficiency** [31] **(Experiment) (%)**
0.5	94.02	95.26 ± 1.02
1	89.10	87.67 ± 0.55
1.5	83.85	79.54 ± 1.26
2	79	71.43 ± 1.74
2.5	74.35	62.39 ± 0.79

As the feed concentration increases, the TDS of the water coming out during purification phase increases. Also, the rate of salt removal increases and reaches a constant value as the electrodes reach their saturation capacity, i.e., no more ions can be adsorbed on to the electrodes. The thickness of double layer decreases with increase in concentration. In Table 3.3, we see that the electrosorption removal efficiency using the model is very well described for concentration ranging from 0.5-2 g/l. However, as the concentration increases, the model predicts decreasing trend in efficiency but does not predict the results accurately. The inconsistency could be attributed to some ions residing in the electrode pores during regeneration and not being flushed out so that in the next purification phase the salt removal is less and the electrodes reach saturation much faster. The electrode capacity obtained using the model is just an approximation. The actual response of porous electrodes is nonlinear and needs to be further investigated and incorporated in the model.

Investigation II. TDS removal efficiencies were calculated using the model in Section 3.2 for different flow rates of feed water with a fixed TDS concentration of 1 g/l and temperature of 24 ℃ and the results are compared with the experimental results of the paper [31]. The comparison of results obtained using theoretical model and experiment is mentioned in Table 3.5.

Table 3.4 Comparison of effluent TDS concentration of the purified stream between model and experiment [31] **for different flow rates.**

Flow rates	**TDS removal efficiency (Model) (%)**	**TDS removal efficiency** [31] **(Experiment) (%)**
1	92.14	95.08 ± 0.51
1.5	90.61	91.11 ± 0.59
2	89.10	87.68 ± 0.55
2.5	87.55	84.28 ± 0.51
3	85.98	81.41 ± 0.52
3.5	84.40	78.20 ± 0.63

TDS removal efficiency is computed using the model for feed water concentration of 1 g/l but with different flow rates ranging from 1-3.5 liters/ min at a temperature of 24 ℃. As the flow rate increases, the water stays in the cell for smaller duration and as a result less time is available for ions to move to the activated carbon electrodes. Thus, we see there is a declining trend in TDS removal efficiency with the flow rate which is very well described using the model.

3.6 Investigation of CDI batch mode of operation using model

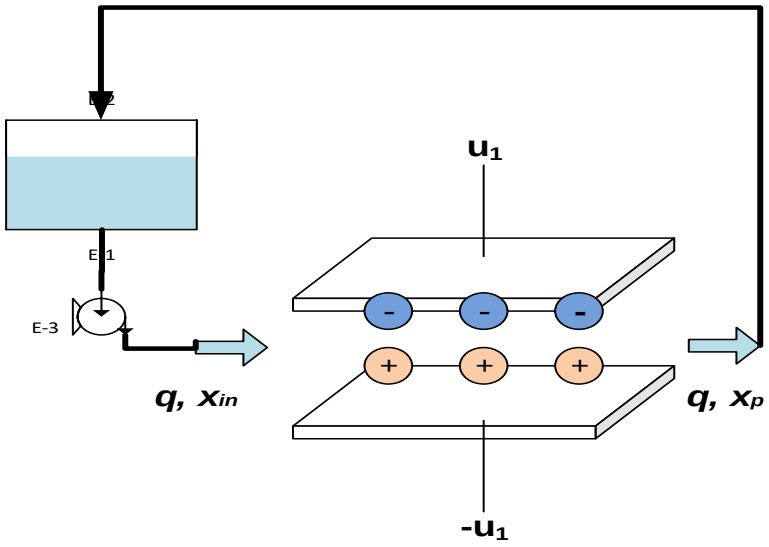

Figure 3.9 CDI Batch mode of operation

In the batch mode of operation, the freshwater obtained at the outlet is recycled back to the inlet tank [29], [89]. The water from the tank now flows back again into the CDI cell. The batch mode of operation allows further purification of the produced water. As the electrodes get saturated with ions, the voltage is removed so that the ions are released into the solution and the water is discarded away.

3.6.1 CDI model – batch mode

Let V_{in} be the volume of water in the inlet tank, x_{in} be the concentration of the inlet tank. The flow rate in and out of the CDI cell is same. Let q be the flow rate of water to and out of the CDI cell and V_{tank} be the volume of the inlet tank.

The salt balance equation of the inlet tank is written as,

$$V_{tank}\frac{dx_{in}}{dt} = qx_p - qx_{in} \tag{3.15}$$

The state equations describing effluent salt concentration and voltage across capacitor for CDI batch mode of operation can be written as,

$$\frac{dx_p}{dt} = \frac{q}{V}\left(x_{in} - x_p\right) - \frac{K}{V}\frac{(2V_{in} - 2V_c)}{R_{wc}} \tag{3.16}$$

$$\frac{dV_c}{dt} = \frac{2V_{in} - 2V_c}{C_e R_{wc}} \tag{3.17}$$

Equation (3.15), (3.16) and (3.17) form the state equations for batch mode CDI operation.

3.6.2 Results – CDI batch mode of operation

The simulation for batch mode operation of AQUA EWP CDI unit is performed. The inlet water tank is filled with 10 liters of water of concentration 1 g/l. The water flows through the CDI cell at a flow rate of 2 liters/min. The voltage is applied to the CDI cell until a constant effluent concentration is reached in the inlet tank. The water is recirculated back to the tank until a constant effluent salt concentration is reached. As seen in Figure 3.10, it is observed that the water concentration in the tank decreases from 1 g/l and reaches a steady concentration of 0.323 g/l at the end of 1000 seconds. This implies it takes about 1000 seconds for the electrodes to reach saturation.

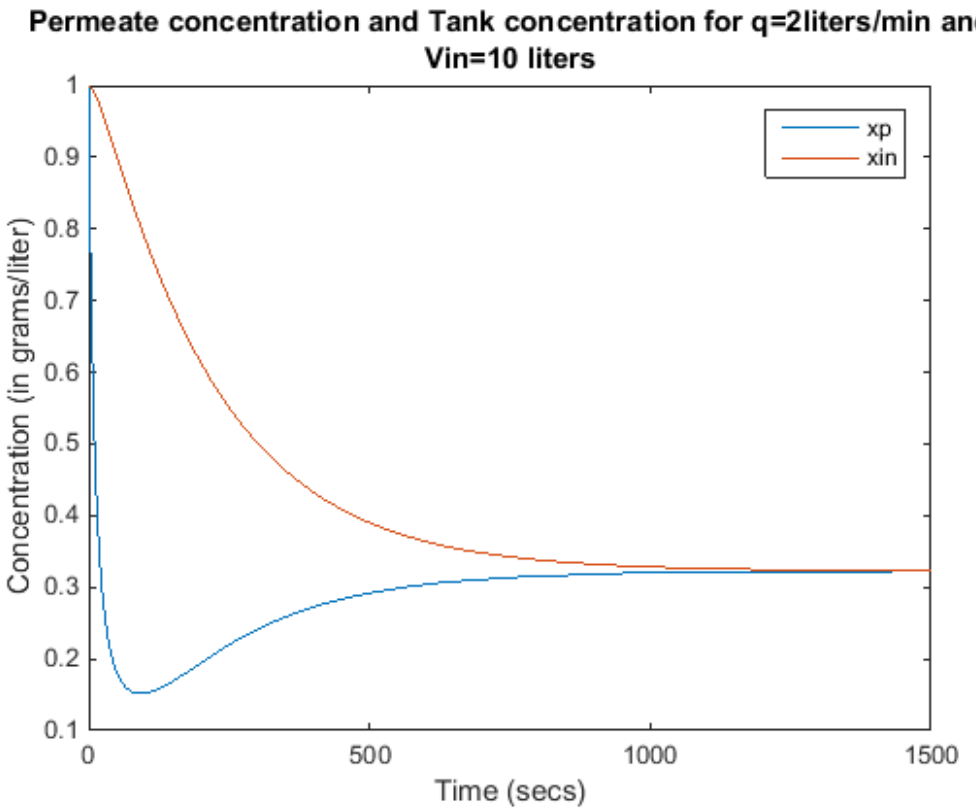

Figure 3.10 Effluent concentration at the output of CDI cell and in the inlet tank

From Figure 3.11, it is observed that as the flow rate of water increases, the steady-state effluent concentration is less compared to the case of low flow rate. This implies that flow rate is directly proportional to CDI desalination capability.

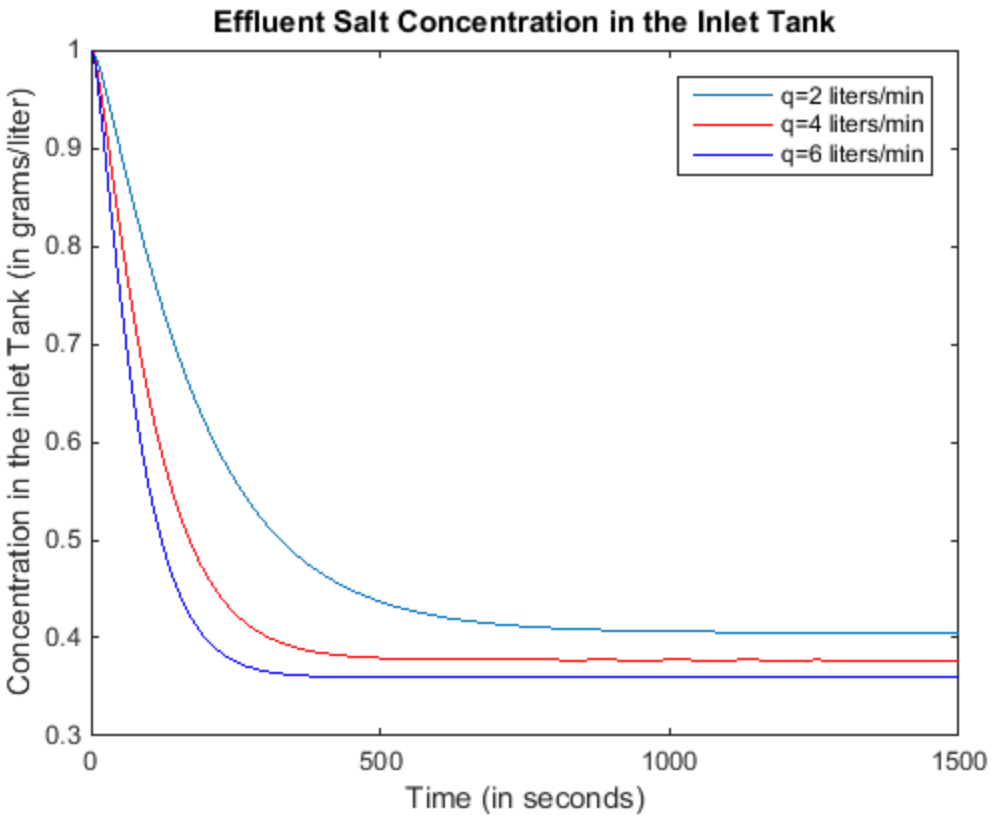

Figure 3.11 Effluent concentration in the inlet tank at different flow rates q

Moreover, it is also observed from Figure 3.11 that the time taken to reach the lowest concentration in the steady state is small if the flow rate is high. At a flow rate of 4 liters/minute, the steady state concentration of 0.307 g/l is reached after 500 seconds whereas, at a flow rate of 6 liters/min, a steady state concentration of 0.297 g/l is reached after 450 seconds. This behavior of batch mode operation to flow rate is attributed to the mixing activity in the inlet tank as the water is recycled suggesting that lower flow rate would reduce the flow of the water back into the inlet tank which would stop continuous removal of ions by CDI cell. As the flow rate increases, a point is reached where the lowest effluent concentration in the tank no longer decreases. Thus, an optimized flow must be used for efficient batch mode CDI operation [89].

3.7 Conclusion

A mathematical model of capacitive de-ionization system with activated carbon electrodes is described for water desalination. The model is extended to two CDI cells to model AQUA EWP CDI unit. The model is used to reproduce the operational cycle of AQUA EWP CDI cell that shows the effluent concentration varying with time. The model results are in good agreement with the reported results of AQUA EWP CDI unit. The model also predicts the amount of charge captured by the CDI cell and the current in the CDI cell, both as a function of time. The influence of parameters such as flow rate and influent TDS concentration on the TDS removal efficiency of a CDI system is very well described by the model. The model predicts decreasing trend in TDS removal efficiency with increase in feed concentration and flow rate. However, at higher concentrations of the feed, a deviation from experimental values is observed. The electrode capacity obtained using the model is just an approximation. However, the actual electrode capacity depends on various parameters and the relation describing it is highly nonlinear that needs to be further investigated. The influence of other parameters on the system performance can be studied by minor additions to the model.

The batch mode of operation of CDI is investigated using the same model and it has been found that the flow rate has a positive effect on CDI performance. As the flow rate increases, the lowest effluent salt concentration decreases for the same influent concentration. This is attributed to the mixing activity in the recycling tank that decreases the concentration in the tank. Higher flow rate causes more water to circulate back in the tank and thus the concentration decreases fast. Moreover, the time required to reach steady

state decreases with increase in flow rate. As the flow rate is increased, a point is reached when the lowest effluent salt concentration remains same no matter how much the flow rate is increased. Therefore, an optimized flow is required for efficient batch mode CDI operation.

This model can serve as a benchmark to study the performance of CDI system under different configurations, different operating conditions, understanding the effect of different parameters on system performance and also optimization of the system parameters to achieve maximum efficiency.

CHAPTER 4

SWITCHED WAVE CAPACITIVE DE-IONIZATION

4.1 Introduction

A typical CDI process as described in Chapter 3 consists of 2 steps viz., ion adsorption wherein freshwater is obtained and ion desorption wherein a highly concentrated brine is obtained. This chapter proposes a novel approach of continuous mode of operation of Capacitive De-ionization called Switched wave capacitive de-ionization (SWCDI) wherein freshwater and brine are collected at the same time. The mathematical model developed in Chapter 3 is extended to describe SWCDI operation using the concept of switched electric wave. Three CDI cells in series are considered wherein a moving electric field in the first cell separates the salt ions by adsorption of cations to the cathode and anions to the anode further forcing the cations and anions to move to a second CDI cell and finally to the third one. The flow out of the first cell has a substantially less total dissolved salt (TDS) than the inlet flow to the cell. The accumulated charged water in the regions of third CDI cell is recombined and discharged as brine. The brine flow rate is adjusted to achieve an economical water recovery ratio. The parameters involved in the system are optimized using a genetic algorithm to achieve desired freshwater concentration and high water recovery ratio.

This chapter is organized as follows. Section 4.2 describes the instrumentation involved in the switched wave capacitive de-ionization (SWCDI) for continuous operation of CDI

along with overall mass balance and salt balance equations of the system. The description of Switched wave Capacitive De-ionization system is presented in Section 4.3. Next, a mathematical model of switched wave capacitive de-ionization (SWCDI) system is derived using an electrical equivalent circuit of CDI in Section 4.4. Simulation results for SWCDI system is presented in Section 4.5. In Section 4.6, reflux mode of operation of SWCDI system is investigated and its results are discussed.

4.2 Description of SWCDI system

The block diagram of proposed switched wave capacitive de-ionization system is as shown in Figure 4.1.

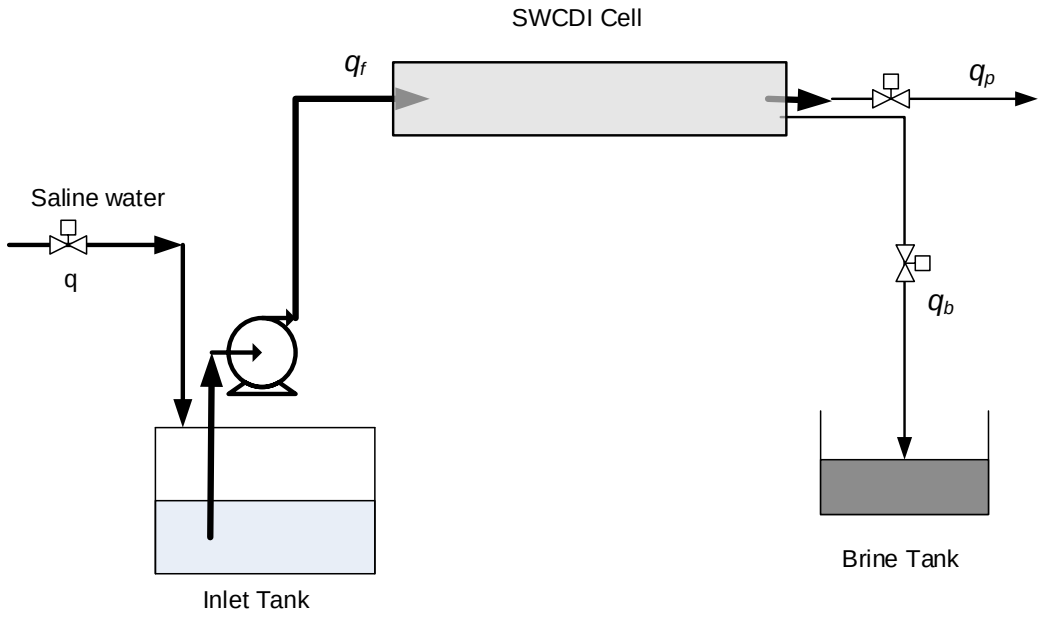

Figure 4.1 Block diagram of switched wave capacitive de-ionization system

The salty water is first collected in an inlet tank, where the inlet flow q is controlled by a standard level control instrumentation. A pump takes the salty water from the inlet tank at a flow rate of q_f to the assembly of CDI cells. The CDI cells consist of a main conduit, preferably of a rectangular shape, made from an electrically insulated material as plastic or glass. The feed raw water q_f is supplied through the pump to the Switched Wave Capacitive De-Ionization (SWCDI) Cell. Across two sides of the main conduit, for example the upper and lower sides, the electrodes are connected to an electronic voltage waveform generator. The inlet water q_f passes into the CDI cells assembly wherein the salt ions are separated under the applied electric field and attracted towards respective electrodes. The travelling wave allows the ions to move from one electrode to another and finally the ions are transported to the final CDI cell, where the cation and anion ions reunite again in the outlet chamber, where the water becomes neutralized, with high concentration and leaves the conduit through the brine output pipe. The brine discharge rate q_b can be adjusted to produce the desired water recovery ratio. The low salt water flow flows through a separate pipe from the output of first CDI cell with a flow rate q_p.

At steady state, the overall mass balance equation of the entire system is given by

$$q_f = q_b + q_p \tag{4.1}$$

Where

q_f is the salty water inlet volume feed rate (m^3/sec)

q_p is the permeate (distillate) volume flow rate

q_b is the brine volume flow rate.

The salt balance equation is given as,

$$x_f q_f = x_p q_p + x_b q_b \tag{4.2}$$

Where

x_f is the feed water concentration in $g/liter$

x_p is the permeate salt concentration in $g/liter$.

x_b is the brine salt concentration in $g/liter$.

The recovery ratio is given by $RR = \frac{q_p}{q_f}$.

which implies that salt balance equation can be written as,

$$x_f = x_b(1 - RR) + x_p RR \tag{4.3}$$

4.3 Switched Wave Capacitive De-ionization (SWCDI) cell

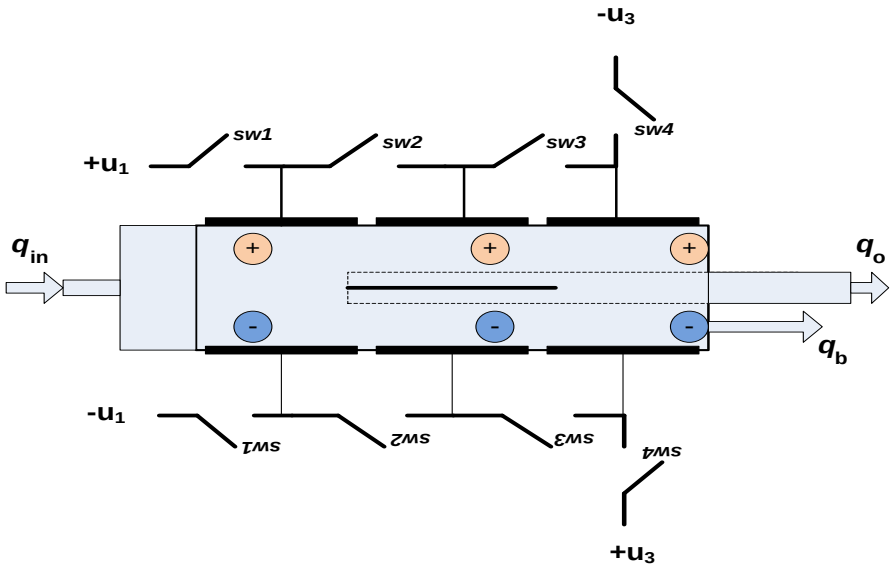

Note: The lower part is simply a mirror image of the upper part

Figure 4.2 Assembly of CDI cells arrangement in a SWCDI cell

The SWCDI cell is a conduit of rectangular cross section of width W_e, length L_e and height d_e. As shown in Figure 4.2, a SWCDI conduit carries a series of electrodes on two opposite sides. Each electrode of a CDI cell consists of a conducting charge collector and an activated carbon (AC) layer sheet of thickened t_c. The activated carbon layer merged and fully in contact with the salty water. The top metal electrode in the first CDI cell is connected to electrical signal u_1^+, while the lower metal electrode is connected to electrical signal u_1^-. The switching action determines the charging and discharging of the neighboring cells.

The capacitance associated with each electrode is given by $C_e = \frac{k_c \varepsilon_0 (L_e W_e)}{t_{cs}}$, where k_c depends on the effective area ratio of the activated carbon and its wet permittivity, t_{cs} is the thickness of the Stern layer which is of the order of 1 nanometer.

$k_c = k_s \rho_c t_c$; where k_s is the specific surface of the AC. k_s is typically 1000-2500 m^2/g.

The Table 4.1 below demonstrates the working principle of SWCDI cell.

Table 4.1 Switching time and operation in SWCDI cell

Timeslot (seconds)	**Sw1**	**Sw2**	**Sw3**	**Sw4**
T_{s_1}	On	Off	On	Off
T_{s_2}	Off	On	Off	On
T_{s_3}	On	Off	On	Off
T_{s_4}	Off	On	Off	On

The principle of operation of SWCDI cell is as follows as shown in Table 4.1.

1. Initially, the CDI cell 1 is charged, that results in ion adsorption onto the electrodes.
2. The charge on CDI cell 1 is transferred to CDI cell 2, that results in ion desorption in CDI cell 1. The desorbed ions are adsorbed onto the CDI cell 2.
3. The charge on CDI cell 2 is transferred to CDI cell 3, that results in ion desorption from CDI cell 2. The desorbed ions are adsorbed onto CDI cell 3.
4. CDI cell 3 is discharged by a negative voltage u_3 that results in flushing of all the ions with a brine flow.

The steps are performed in parallel, steps 1,3 in one-time slot (T_{s_1}) and steps 2,4 in the next time slot. (T_{s_2}). These steps are repeated until a steady state of the system is reached.

The equivalent circuit of the six electrodes during T_{s_1} and T_{s_2} is shown in Figure 4.3.

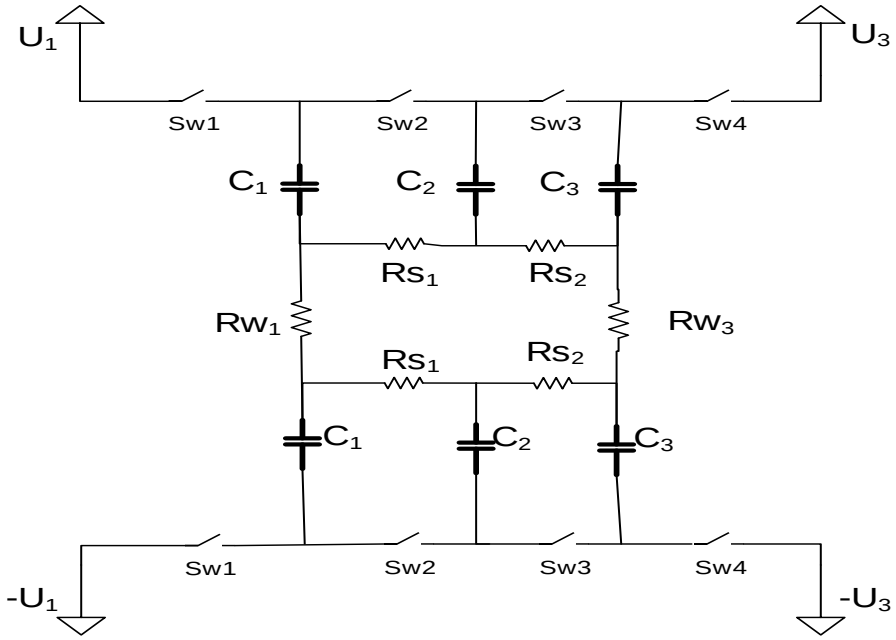

Figure 4.3 Equivalent electrical circuit of 3 CDI cells in series

R_w is the electrical resistance of the salty water between the two opposite electrodes, while R_s is the electrical resistance between two adjacent electrodes.

The resistance of water R_w and resistivity is given by the equation (3.3) and (3.4).

The series resistance R_s governs the movement of ions from one CDI cell electrode to the adjacent electrode. The series resistance R_s is given by the approximation,

$$R_s = \frac{\rho_e d_t}{W_e t_c k_p} \tag{4.4}$$

Where k_p is the shaping factor,

ρ_e is water resistivity,

d_t is the distance between adjacent electrode,

W_e is width of the electrode, and

t_c is the thickness of Activated carbon layer.

During normal operations, x_f and RR are constants and q_f is adjusted to achieve the desired freshwater salt concentration (say 500 ppm).

Using equation (4.1), $q_p = q_f * RR$, and $q_b = q_f * (1 - RR)$.

4.4 Modelling of SWCDI cell

Let V_{c_i} be the voltage across the ith capacitor, and I_{s_i} be the current throw the R_{s_i} resistance and I_{w_i} be the current going throw R_{w_i} resistance (i=1,2,3).

The values of V_{c_i}, I_{w_i} and I_{s_i} are calculated for two different timeslots T_{s_1} and T_{s_2} as follows.

During T_{s_1}:

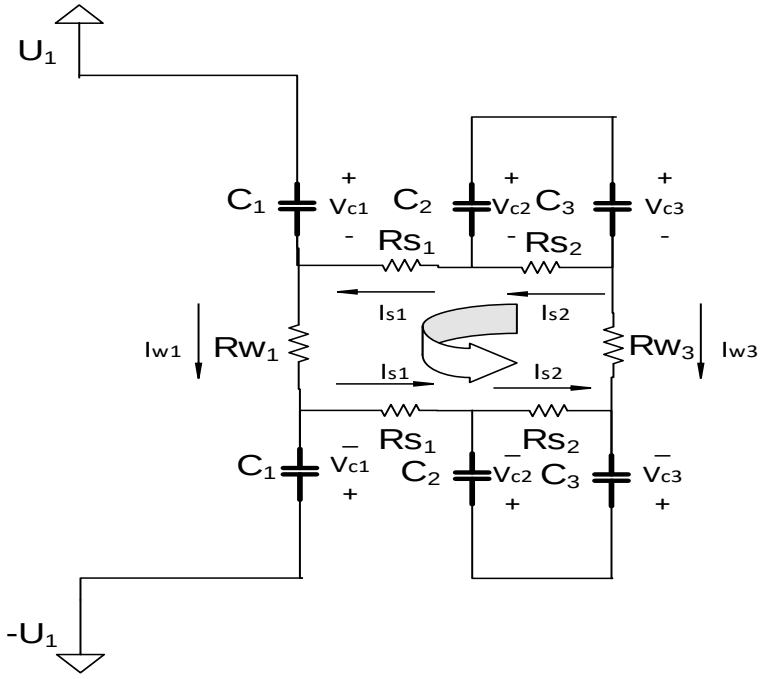

Figure 4.4 Equivalent electrical circuit during T_{s_1}

From the equivalent electrical circuit of CDI cell in Figure 4.3, we write the following equations,

$$I_{w_1} = \frac{2}{R_{w_1}}(u_1 - V_{c_1}) \tag{4.5}$$

Applying KVL,

$$I_{s_2} = \frac{1}{R_{s_2}}(V_{c_2} - V_{c_3}) \tag{4.6}$$

$$I_{c_3=} - I_{c_2} \tag{4.7}$$

Applying KVL to inner loop,

$$-I_{w_3}R_{w_3} + 2I_{s_1}R_{s_1} + 2I_{s_2}R_{s_2} + I_{w_1}R_{w_1} = 0 \tag{4.8}$$

$$I_{c_1} = C_1\frac{dV_{c_1}}{dt} = I_{w_1} - I_{s_1} \tag{4.9}$$

$$I_{c_2} = C_2\frac{dV_{c_2}}{dt} = I_{s_1} - I_{s_2} \tag{4.10}$$

$$I_{c_3} = C_3\frac{dV_{c_3}}{dt} = I_{s_2} + I_{w_3} \tag{4.11}$$

From Equations (4.7), (4.10) and (4.11),

$$I_{w_3} = -I_{s_1} \tag{4.12}$$

From Equations (4.8), (4.12),

$$I_{w3} = \frac{1}{R_{w_3} + 2R_{s_1}}\left(2R_{s_2}I_{s_2} + I_{w_1}R_{w_1}\right) \tag{4.13}$$

Equations (4.5), (4.6), (4.12), (4.13) provides the values of $I_{w_1}, I_{s_2}, I_{s_1} and\ I_{w_3}$ while Equations (4.9), (4.10) and (4.11) provide state equations for capacitor voltages.

During T_{s_2}:

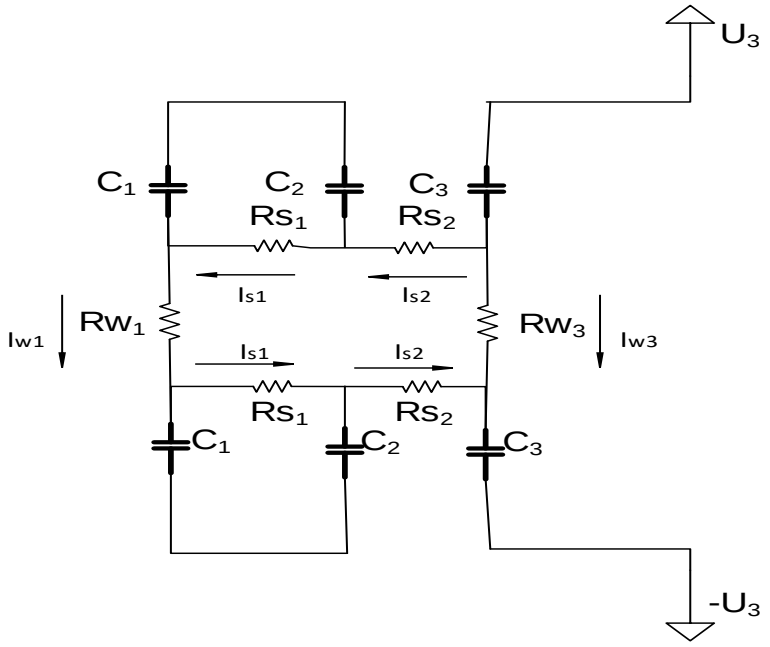

Figure 4.5 Equivalent electrical circuit during T_{s_2}

$$I_{s_1} = \frac{1}{R_{s_1}}(V_{c_1} - V_{c_2}) \tag{4.14}$$

$$I_{c_1=} - I_{c_2} \tag{4.15}$$

$$I_{w_3} = \frac{1}{2R_{w_3}}\left(u_3 - V_{c_3}\right) \tag{4.16}$$

From Equations (4.9), (4.10), (4.11) and (4.15),

$$I_{s_2} = I_{w_1} \tag{4.17}$$

From Equation (4.8),

$$I_{w_1} = \frac{1}{R_{w_1} + 2R_{s_2}}\left(-2R_{s_1}I_{s_1} + I_{w_3}R_{w_3}\right) \tag{4.18}$$

Equations (4.14), (4.16), (4.17) and (4.18) give $I_{s_1}, I_{w_3}, I_{s_2}, I_{w_1}$ respectively while Equations (4.11), (4.12) and (4.13) provide state equations for capacitor voltages.

The concentration, x_1 and x_3 in the first and last chamber of the SWCDI cell is calculated using the differential equation,

$$\frac{dx_1}{dt} = sn_1 \frac{K}{V_1} I_{w_1} + \frac{q_f x_f}{V_1} - \frac{q_p x_1}{V_1} \tag{4.19}$$

$$\frac{dx_3}{dt} = s_{n_3} \frac{K}{V_3} I_{w_3} + \frac{q_b}{V_3} (x_f - x_3) \tag{4.20}$$

Where $= M_{ws}/F$; and M_{ws} is the molecular weight of salt, and F is Faraday's constant.

$s_{n_i} = \pm 1$ depending on V_{c_i} and $\frac{dV_{ci}}{dt}$ as illustrated in the table.

Table 4.2 Sign of s_{n_i} for V_i and $\dot{V}_i$

$V_i > 0, \dot{V}_i > 0$	$s_{n_i} = -1$
$V_i > 0, \dot{V}_i > 0$	$s_{n_i} = +1$
$V_i < 0, \dot{V}_i < 0$	$s_{n_i} = -1$
$V_i < 0, \dot{V}_i > 0$	$s_{n_i} = +1$

The above equations describe the relationship between currents and voltages for each stage, as well as the concentration of the three regions.

$$x_p = x_1; x_b = x_3 \tag{4.21}$$

where x_p is the freshwater concentration coming out of the SWCDI cell and x_b denotes the brine concentration coming out of SWCDI cell

4.5 Optimization algorithm to achieve desired response

The flow rate has significant effect on CDI process as mentioned in Chapter 3. Lower the flow rate, higher the salt removal efficiency as the ions get sufficient time to move to respective electrodes inside the CDI cell.

The distance between the electrodes is another significant parameter affecting CDI performance. As the voltage is applied between the electrodes, an electrostatic field is generated that causes the ions to move towards oppositely charged electrodes. This electrostatic field decreases as the spacing is increased corresponding to low salt removal. The spacing between the electrodes must be small but it must be made sure that the activated carbon on the top and bottom electrodes are not in contact with each other which would otherwise result in short-circuiting of the CDI cell.

The separation between adjacent electrodes is also critical for movement of ions from one CDI cell electrode to the next. Smaller the distance, higher is the rate of transfer of ions under the effect of switched configuration. All these parameters are therefore optimized for efficient SWCDI operation.

The desired objective is to obtain freshwater with low concentration of salts (500 ppm or 0.5 grams/liter) and to increase the water recovery ratio (RR). The initial feed concentration is 1 g/l. To achieve the required objectives, a genetic optimization algorithm is run to minimize the following objective function

$$J = (x_1 - x_d)^2 + \left(\frac{50}{q_f}\right) + \left(\frac{1}{RR}\right) \tag{4.22}$$

Where x_1 is the freshwater concentration varying with time according to Equation (4.14), x_d is the desired freshwater concentration, RR is the water recovery ratio.

An optimization algorithm is run in MATLAB to obtain the following optimized set of parameters for the SWCDI cell: Switching times $T_{s_1}\ and\ T_{s_2}$, negative voltage u_3, feed flow rate q_f, spacing between electrodes of a CDI cell d_e, spacing between adjacent electrodes in SWCDI cell d_t and water recovery ratio RR. The other parameters of the SWCDI system are kept constant during the optimization as shown in Table 4.2.

4.6 Simulation Results

The feed solution considered is sodium chloride $NaCl$ of 1 g/l concentration. The three zone SWCDI system is simulated with the following parameters in Table 4.3.

Table 4.3 Parameters of SWCDI cell

Feed water concentration	1 g/l
Length of each electrode, L_e	0.3 m
Width of each electrode, W_e	0.3 m
Specific surface area of AC, k_s	2000 $m^2/gram$
Thickness of the Activated carbon film	0.5 mm
Applied voltage, u_1	1.2 volts
Molecular weight NaCl, M_{ws}	58.44 grams

During optimization, the parameters in Table 4.3 are kept constant and the parameters in Table 4.4 are varied by an optimization routine to minimize the cost function J in equation (4.17). The optimized set of parameters of SWCDI system is as shown in Table 4.4.

Table 4.4 Optimized parameters of SWCDI system

Separation between adjacent electrodes, d_t	0.001 m or 1 mm
Separation between electrodes, d_e	0.008 m or 8 mm
Switching times, T_{s_1} and T_{s_2}	344 seconds
Feed water flow rate, q_f	4.5 ml/min
Water recovery ratio, RR	0.73
Voltage to CDI cell 3, u_3	-0.3 volts

The saline water concentration change in the first CDI cell and the last CDI cell of SWCDI system is shown in Figure 4.4. A decrease in salt concentration in the first CDI cell is observed with time whereas there is an increase in salt concentration in third CDI cell owing to movement of ions from first to third CDI cell. The ions accumulated in the third CDI cell is discharged with a flow rate of q_b as highly concentrated brine whereas the low concentration water out of the first CDI cell is collected as freshwater.

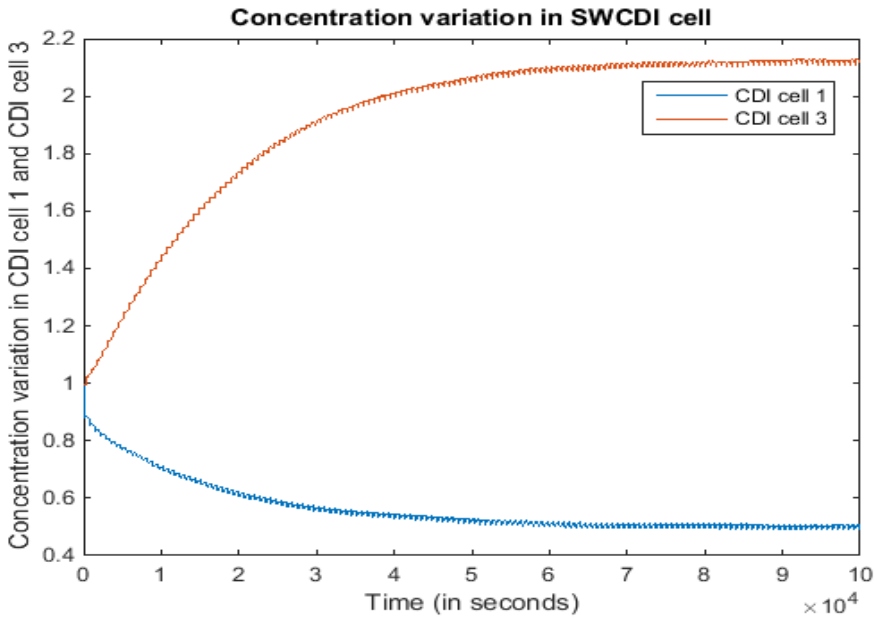

Figure 4.6 Concentration variation in SWCDI cell

The voltage across capacitor (V_{c_1}, V_{c_2} *and* V_{c_3}) varies in CDI cell 1,2 and 3 as shown in Figure 4.5. The voltage across capacitor increases during charging of a CDI cell and decreases when the cell is discharged.

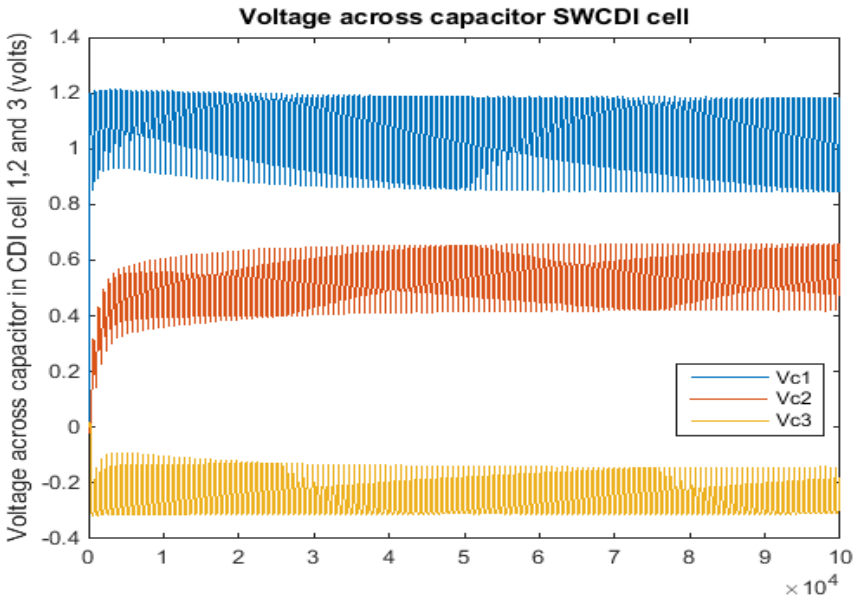

Figure 4.7 Voltage across capacitor in SWCDI cell

4.6.1 Discussion

All the parameters in Table 4.3 are optimized to achieve desired response of the SWCDI cell. Simulations are performed using the optimized set of parameters. As shown in Figure 4.4, the concentration in the first CDI cell decreases from 1 g/l to 0.5 g/l whereas the brine concentration in the last CDI cell increases from 1 g/l to 2.2 g/l.

4.7 Investigation of reflux mode of operation of SWCDI

The reflux mode of operation of SWCDI cell is investigated in this study wherein a fraction of low salt water is recycled back to the inlet tank for controlling the amount of salt in produced freshwater.

4.7.1 Description of reflux SWCDI

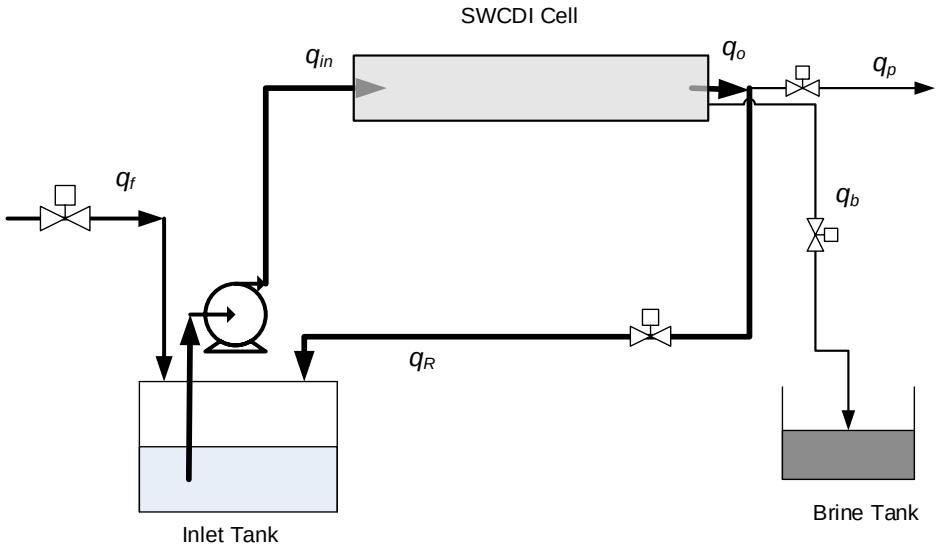

Figure 4.8 Diagram of SWCDI system with reflux

The SWCDI cell with reflux flow is shown in Figure 4.6. The description is same as in Section 4.2 except that the low salt water output q_o here is split into two flows, a permeate flow q_p, and reflux flow q_R. The reflux flow is governed by a pump or a control valve. The reflex q_R is recombined with the inlet salty water for controlling the amount of salt in the produced freshwater q_p.

In order to model the system, additional modelling of the inlet tank is required.

4.7.2 Inlet tank model

The mass balance equation for the inlet tank is given by,

$$\frac{dV_{in}}{dt} = q_f + q_R - q_{in} \tag{4.23}$$

Where

V_{in} is the volume of water in the inlet tank, q_R is the reflex volume flow rate, and the change in the streams densities is neglected.

The reflux ratio is defined by the parameter,

$$\alpha_R = \frac{q_R}{q_f} \tag{4.24}$$

At steady state, the mass balance equation is written as

$$q_f + q_R = q_{in} \tag{4.25}$$

$$\text{or } \; q_{in} = (1 + \alpha_R) q_f \tag{4.26}$$

The salt balance equation of the inlet tank is given as,

$$\frac{d(V_{in} x_{in})}{dt} = q_f x_f + q_R x_p - q_{in} x_{in} \tag{4.27}$$

If the inlet tank volume is regulated by a separate loop control, then V_{in} can be considered constant. Thus, equation can be written as,

$$V_{in} \frac{dx_{in}}{dt} = q_f x_f + q_R x_p - q_{in} x_{in} \tag{4.28}$$

At steady state,

$$q_{in}x_{in} = q_f x_f + q_R x_p \tag{4.29}$$

$$\text{Or } x_{in} = \frac{x_f + \alpha_R x_p}{1 + \alpha} \tag{4.30}$$

4.7.3 Modelling of reflux SWCDI

The modelling equations are same as in Section from Equation (4.7) – (4.13). The concentration in the first and last chamber, x_1 and x_3 is calculated using the differential equation,

$$\frac{dx_1}{dt} = s_{n_1}\frac{K}{V_1}I_{w1} + \frac{q_{in}x_{in}}{V_1} - \frac{q_p x_1}{V_1} - \frac{q_R x_1}{V_1} \tag{4.31}$$

$$\frac{dx_3}{dt} = s_{n_3}\frac{K}{V_3}I_{w3} + \frac{q_b}{V_3}(x_f - x_3) \tag{4.32}$$

$$x_{in} = \frac{x_f + \alpha x_p}{1 + \alpha}; x_p = x_1; x_b = x_3 \tag{4.33}$$

4.7.4 Results – Effect of reflux ratio on permeate concentration

We investigate the effect of reflux flow rate (or reflux ratio - Alpha) on the system performance. The recovery ratio is set to 80 % and feed water flow rate q_f to 0.15 liters/min. The other parameters used in the simulation are given in Table 4.5.

Table 4.5 Parameters used in simulation of reflux SWCDI system

Feed rate	0.15 liters/minute
Feed concentration, x_f	4 grams/liter
Volume of the inlet tank, V_{in}	20 liters
Discharging voltage, u_3	-0.8 volts
Switching time, $T_{s_{1,2}}$	60 seconds
Total cycle time, T_p	$T_{s_1} + T_{s_2}$
Length of each electrode, L_e	0.4 m
Width of each electrode, W_e	1 m

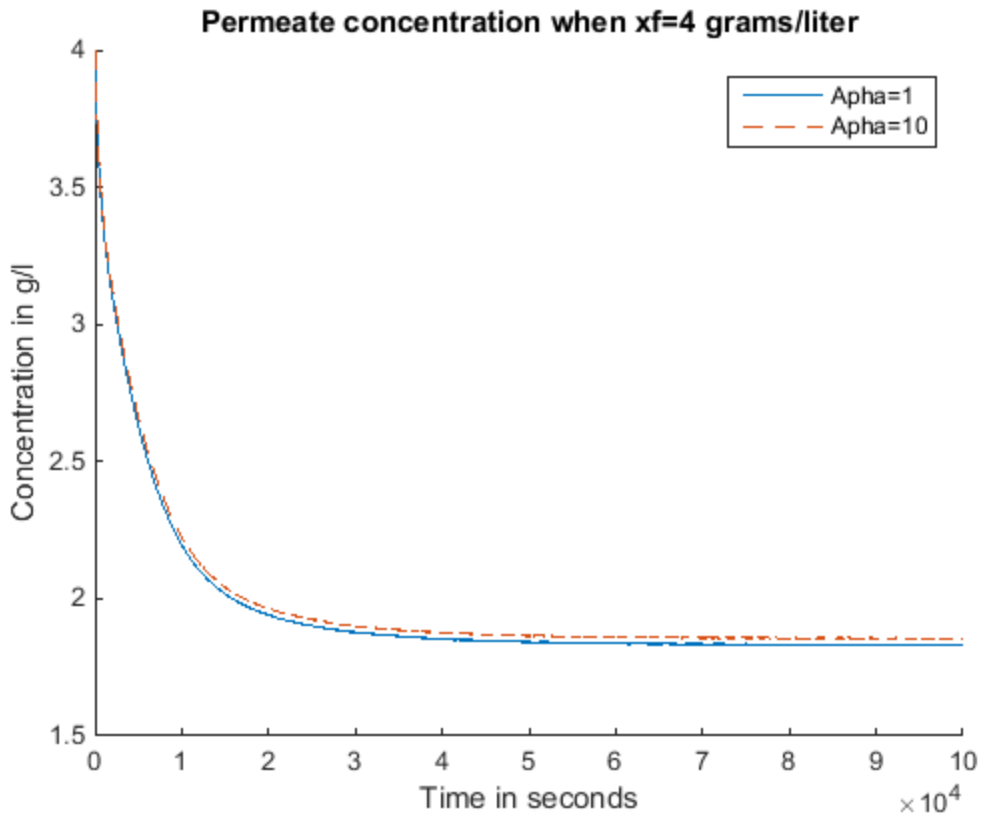

Figure 4.9 Variation of permeate concentration with time for $\alpha_R = 1$ and $\alpha_R = 10$

Using reflux ratio of $\alpha_R = 1$ as shown in Figure 4.9, we obtain a minimum permeate concentration of 1.832 grams/liter and the concentration of solution in the inlet tank is 2.916 grams/liter, but as α_R is increased to 10**,** the permeate concentration increases marginally to 1.857 grams/liter and the concentration in the inlet tank decreases to 2.05 grams/liter.

As shown in Figure 4.10, due to mixing in the inlet tank, the concentration reduces from 4 g/l to around 2.1 g/l during SWCDI operation.

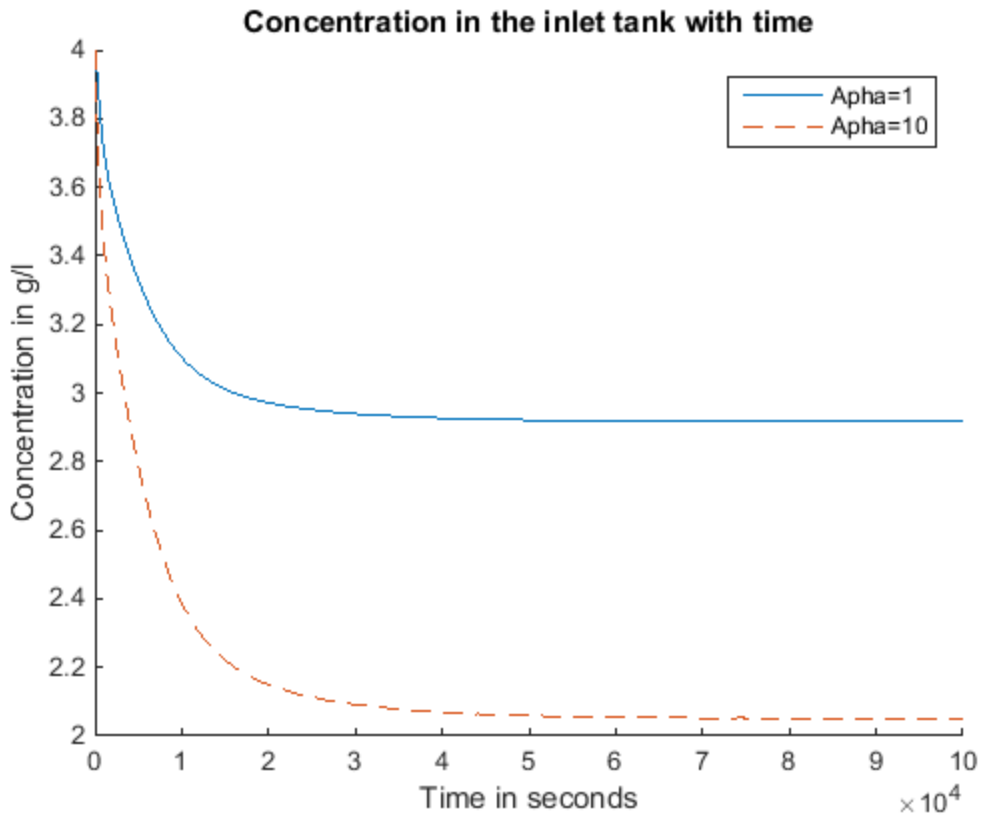

Figure 4.10 Concentration in the inlet tank

The results are illustrated in Table 4.6 that compares the permeate concentration, tank concentration and brine concentration for values of $\alpha_R = 4$ and $\alpha_R = 10$.

Table 4.6 Permeate, Inlet and brine concentration for different reflux ratio

$\alpha_R = 4$	$\alpha_R = 10$
x_p =0.7733 g/l x_{in} =1.4193 g/l x_b = 24.8903 g/l	x_p =0.77340 x_{in} = 1.0680 x_b = 24.6559

From Table 4.6, it is noticed that as α increases, x_p increases but x_{in}decreases**.** This implies that as alpha increases, SWCDI desalination performance decreases. This could be

attributed to the fact that higher flow rate deteriorates the desalting capability of CDI cell as less time is available for ions to adsorb on the electrodes.

It is also observed that if the volume of tank V_{in} is increased, the concentration in the inlet tank, x_{in}decreases less rapidly with time. It takes a long time to reach a state where the concentration variation with respect to time is negligible. Because of large volume of the tank, the concentration reduction is less rapid due to mixing of feed water and reflux water.

4.8 Conclusion

A switched travelling wave capacitive de-ionization system is described for water desalination wherein inlet brackish water is subjected to an electrostatic field which causes the positive and negative ions to move to respective electrodes and the switching action further causes these ions to move from one electrode to other until the ions reach the last electrode. The positive and negative ions are combined and discharged as brine whereas a fraction of low salt water is collected and stored in a tank. There is decrease in concentration in first CDI cell and increase in concentration in the last CDI cell owing to movement of ions from first CDI cell to last CDI cell. The parameters of SWCDI cell are optimized to achieve desired concentration and higher water recovery using an optimization algorithm. The brine flow rate is also adjusted to obtain high recovery ratio.

The effect of reflux on SWCDI operation is studied and it is observed that reflux has no critical role in desalination capability as it increases the flow rate to the SWCDI cell. Higher flow rate causes poor desalination capability resulting in very few ions being removed from the feedwater.

CHAPTER 5

CDI EXPERIMENTS

5.1 Introduction

A Capacitive De-ionization cell is built using the following components:

1. Acrylic sheet to support the system
2. Aluminium sheets that serve as current collectors
3. Zorflex Knitted FM-10K Activated Carbon cloth
4. Loctite Water proof silicone to seal off the edges
5. Nuts and screws
6. Power supply to supply a voltage of 1.2 volts to the CDI cell
7. Valves and pipes
8. Water tank

The CDI cell is built using acrylic glass that houses the aluminium sheets and activated carbon cloth. The activated carbon cloth is glued onto the aluminium sheet. A spacing of 5 mm between the two activated carbon cloth is achieved using side acrylic plates.

A voltage of 1.2 volts dc is applied to the CDI cell as shown in Figure 5.1 that causes the anions in water to move towards anode and cations to move towards the cathode. The ions are adsorbed on the activated carbon electrodes during adsorption that results in freshwater production with less TDS compared to the feed. A salinity sensor is used to measure the concentration of the solution. As the electrode pores get saturated with ions, the effluent

concentration begins to rise and the voltage is removed from the CDI cell so that the ions get desorbed from the electrodes. This step is known as desorption. A typical CDI process comprises of two-steps viz., adsorption (when the voltage is applied) and desorption (when the voltage is removed).

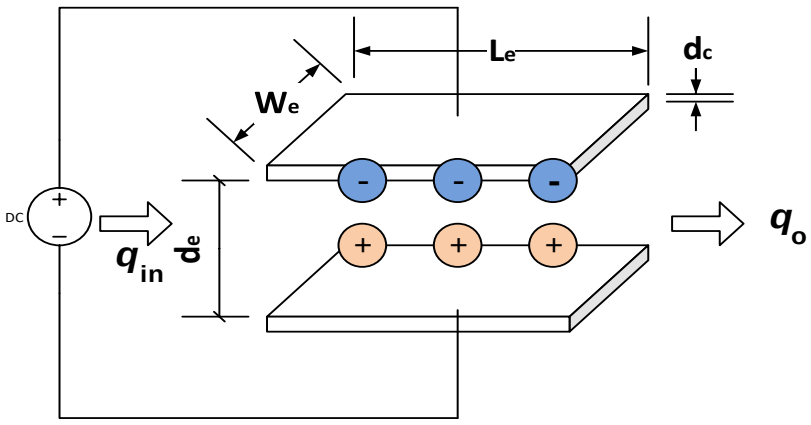

Figure 5.1 Diagram illustrating CDI operation

5.2 Zorflex Knitted FM-50K Activated Carbon cloth (ACC)

FM-50K ACC [100] is manufactured by the company Calgon carbon. It has an extremely large surface area of 2000 $m^2/gram$. Surface density for FM50K though is nominally 130 g/m^2. Higher specific surface area implies, more ions can be adsorbed on the activated carbon cloth which means more purification.

Zorflex Knitted Activated carbon cloth FM-50k is resistant to bacteria, fungus and molds, fibrous, flexible, non-toxic and light weight. Figure 5.2 shows FM-50K ACC attached to an aluminium sheet that serves as electrode for CDI experiments.

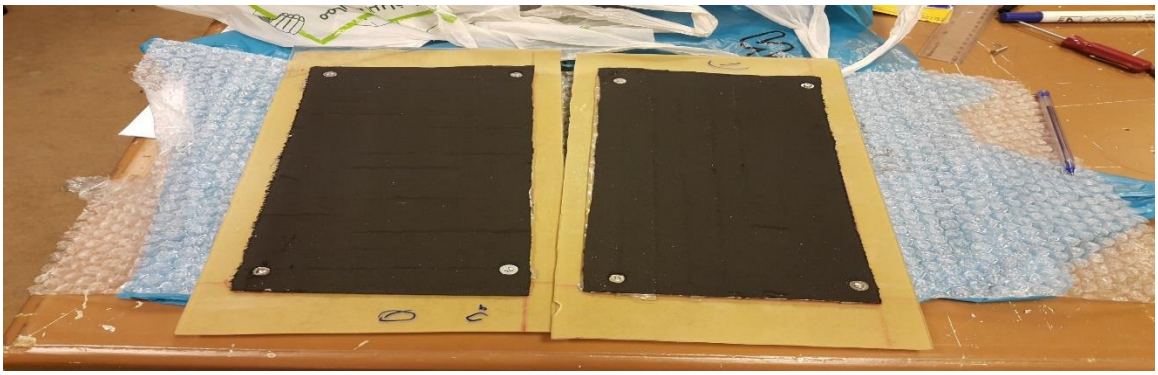

Figure 5.2 FM-50K Activated carbon cloth attached to the aluminium sheet

The efficiency and adsorption capacity of knitted activated carbon is less affected by pre-adsorbed moisture than granular activated carbon. The main applications of this cloth is for water purification, air purification and as electrodes, wound dressing, protective clothing as socks and gloves.

5.3 Experimental setup of a CDI cell

The experimental prototype is built using an acrylic sheet of 2.8 mm thickness. As shown in Figure 5.3, a single CDI cell consists of acrylic of dimension 30 cm x 15 cm x 0.5 cm (length x width x height).The aluminium plate is glued onto the acrylic sheet on the opposite sides. Activated Carbon cloth is attached to the aluminium sheets using double sided tape. The metallic nuts and screws hold the aluminium and activated carbon cloth and provide means to apply a voltage to the CDI cell. The nuts and screws are so attached to maintain isotropic conductivity vertically i.e., along the aluminium sheet and activated carbon cloth such that voltage applied to aluminium sheet charges and discharges the activated carbon cloth respectively. Two holes are drilled one on the top sheet and other at the bottom sheet to allow water to enter and exit the CDI cell as shown in Figure 5.2. A

spacing of 0.5 cm between the activated carbon electrodes is achieved using side acrylic sheets.

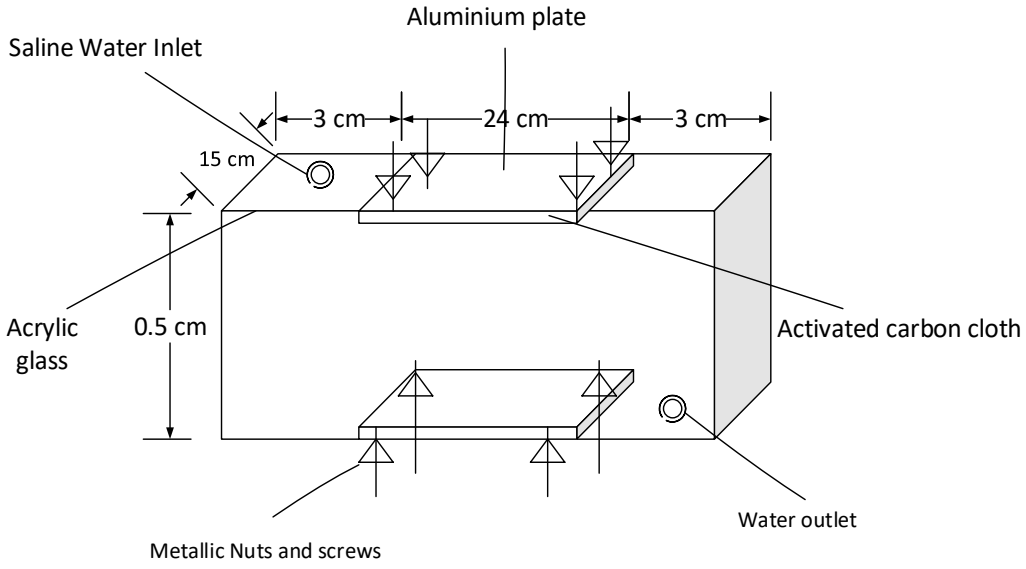

Figure 5.3 Illustration of experimental setup of a CDI cell

5.3.1 Description of the experimental setup

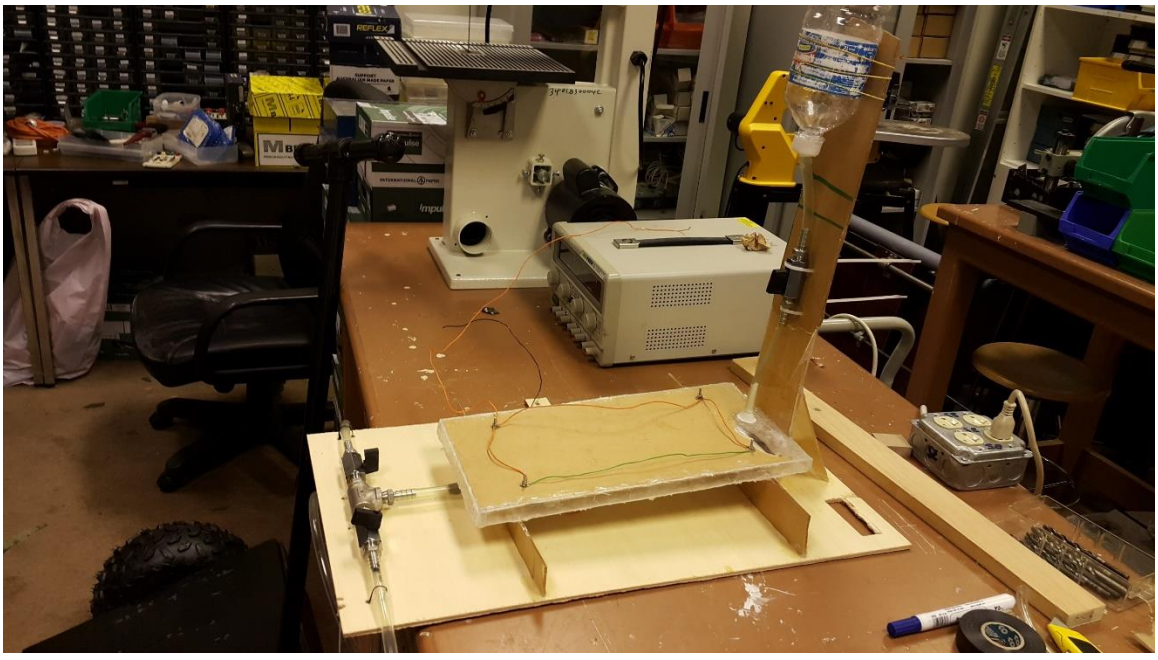

Figure 5.4 CDI Experimental setup

A prototype of CDI is built as shown in Figure 5.4. A DC regulated power supply is used to apply a fixed voltage of 1.2 volts during the adsorption step.

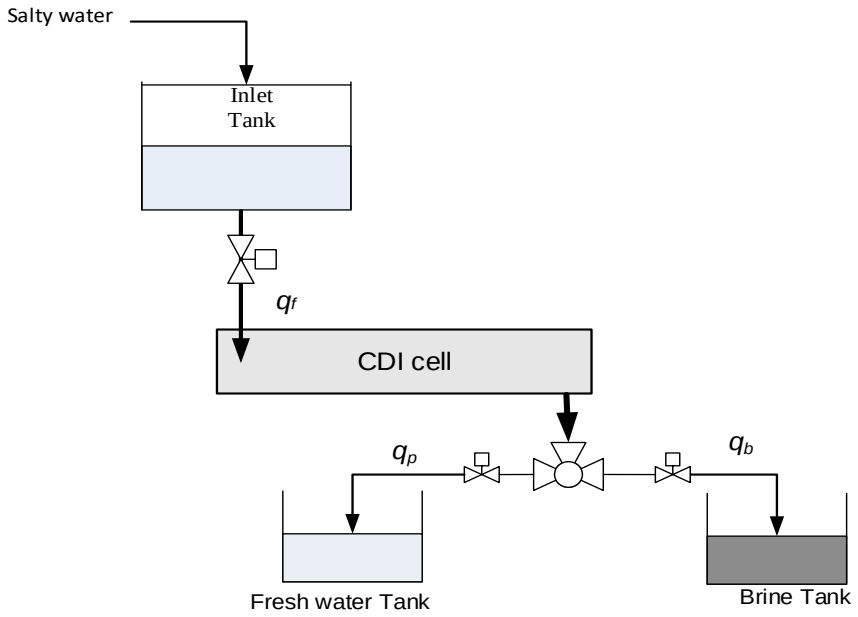

Figure 5.5 Instrumentation of CDI experimental prototype

The piping and instrumentation diagram for a single CDI cell is as shown in Figure 5.5. The saline water is stored in the inlet tank. The flow of saline water into the CDI cell is controlled using a valve. As the water flows into the CDI cell, a voltage of 1.2 volts dc is applied that polarizes the Activated carbon cloth which causes the ions in the water to move towards oppositely polarized electrodes (anions towards anode and cations towards cathode). During purification, the valve at the outlet is closed so as not to allow any water to flow outside the cell. As sufficient ions are removed from the water, the outlet purification valve is opened to exit freshwater out of the CDI cell.

The ions that are still present in the electrode pores are removed by filling the CDI cell with water again and short-circuiting the two electrodes that cause the ions to desorb from

the electrodes and flow back into the water. This results in highly concentrated stream (brine) that is discharged using brine discharge valve into the brine tank.

5.3.2 Results and Observation

The saline water with an initial concentration of 5500 ppm (5.5 g/l) is fed to the CDI cell. The water is purified during adsorption step and reaches a concentration of 4500 ppm (4.5 g/l) upon application of 1.2 volts to the system. During desorption, the CDI cell is again filled with water and the voltage is removed that causes ions to flush back in water. This water is discharged as brine. We noticed a brine concentration of 5500 ppm (5.5 g/l) for same concentration of feed water. Water recovery can be adjusted by varying the flow rates accordingly. Low flow rates enhance the performance of CDI.

The water discharged as freshwater can be further purified by feeding it back to the inlet tank. This would imply the batch mode of operation of CDI.

During adsorption, the current to the CDI cell is measured to be 32 mA and decreases to 25 mA in 30 mins. The power consumption is calculated only during ion adsorption step in CDI as no voltage is applied during ion desorption step. The power consumption is calculated to be 0.0384 watts.

Precautions:

Care must be taken while handling Activated Carbon cloth as it removes oxygen from the air. It must be made sure that the activated carbon cloth on the opposite sides must not be in contact with each other which would result in shorting of a CDI cell.

5.4 Experimental setup – SWCDI

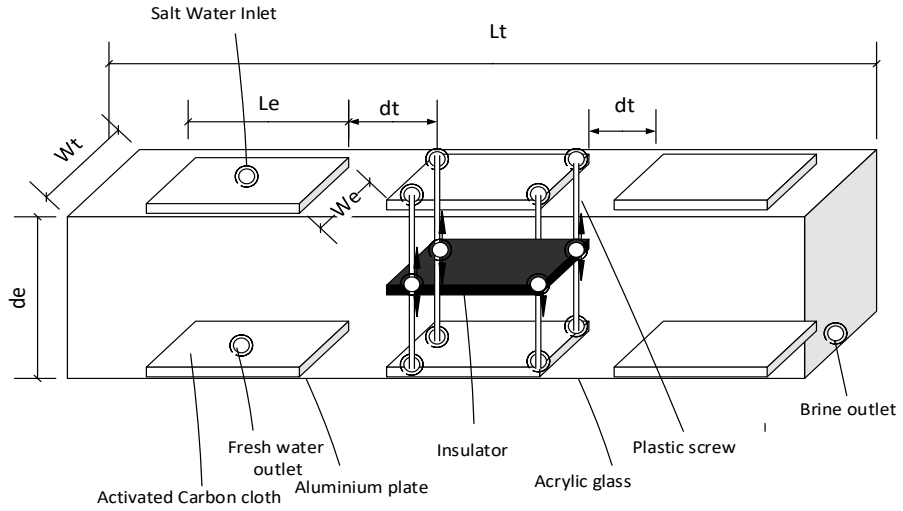

Figure 5.6 SWCDI experimental setup

The switched wave capacitive de-ionization requires 3 CDI cells in series as explained in Chapter 4. A diagram illustrating experimental SWCDI system with all its parts is shown in Figure 5.6. The experimental prototype of SWCDI consists of acrylic sheets of dimension 1.2 m x 0.5 m x 0.003 m ($L_t * W_t * d_t$). The aluminium and activated carbon cloth is cut in the dimension 0.3 m x 0.3 m ($L_e * W_e$). The dimensions of the SWCDI system is mentioned in Table 5.1.

Table 5.1 Dimension of SWCDI system

Length of acrylic sheet, L_t	1.2 m
Width of acrylic sheet, W_t	0.5 m
Thickness of acrylic sheet, d_t	0.003 m
Length of ACC, L_e	0.3 m

Width of ACC, W_e	0.3 m
Thickness of ACC, t_e	0.5 mm

Figure 5.7 depicts aluminium sheets attached to acrylic sheet that serve as the current collector in SWCDI system.

Figure 5.7 Aluminium sheets attached to the Acrylic sheet

Activated carbon cloth (FM-50k) is attached to aluminium using 3M-9713 double sided electrical conductive tape [101] as shown in Figure 5.8. The spacing of d_t = 0.002 m is maintained between adjacent activated carbon cloths as shown in Figure 5.8. The spacing between the top and bottom electrodes is maintained to be 6 mm. An insulator material is fitted in between the activated carbon electrodes in the second CDI cell using plastic nuts and screws that cancels the effect of electrostatic field in the second CDI cell as shown in Figure 5.9. As the water flows through the inlet, the ions are adsorbed in the first CDI cell. The ions move through water from first CDI cell to the last CDI cell under switching operation of SWCDI system as explained in Section 4. As a result, the freshwater is collected from first CDI cell and brine is collected from last CDI cell. The experimental prototype is as illustrated in Figure 5.7-5.9.

Figure 5.8 Activated carbon attached to the aluminium sheets using 3M-9713 Electrical conducting tape

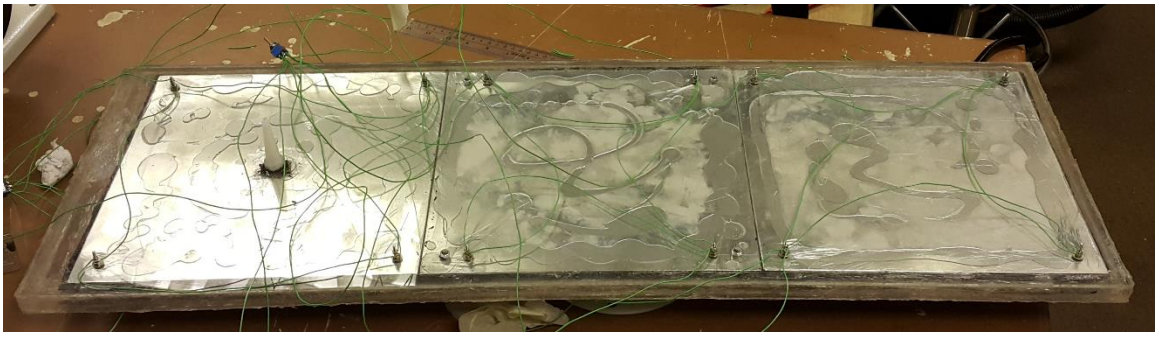

Figure 5.9 SWCDI system with connections to switches

5.4.1 Observations and Recommendation

The activated carbon particles often end up in the 2 mm space between the adjacent electrodes that forms an electrical contact between the adjacent electrodes. This can be avoided by using an insulator material between adjacent electrodes. The ions moving from first CDI cell to next is dependent on the series resistance $R_{S_{1,2}}$. Lower the resistance, more

will be the ion transport from one CDI cell to the next. The resistance can be reduced by employing different geometries of activated carbon electrodes.

Another concern is the time constant of the system which is given by $\tau = RC$. The capacitance is very high because of the specific surface area of activated carbon electrodes. To have a small time constant for the system, the resistance must be small which would imply more transport of ions from one CDI cell to the next in small duration.

The voltage to the first CDI cell is 'V' volts. Upon switching action, the next adjacent CDI cell is charged with a voltage 'V/2' volts. A more general switching scheme can be used. A possible recommendation would be to use an overlapping waveform i.e., before one CDI cell gets discharged, the neighboring cell is charged so as to allow ions in the water top move to the neighboring cell with the water flow rather than being flushed back completely into the water.

All these factors are essential for proper functioning of SWCDI system and requires further investigation.

CHAPTER 6

CONCLUSIONS AND FUTURE WORK

6.1 Conclusions

This thesis presents modelling and control of capacitive de-ionization system. A mathematical model is presented using an electrical equivalent circuit of CDI along with a dynamic equation that describes how the effluent concentration varies with respect to time in a CDI cell. The modelling is done considering various parameters associated with a CDI process viz., the specific surface area of activated carbon electrodes, dimensions of the electrodes, spacing between the electrodes, solution resistance between the electrodes, initial feed concentration, flow rate, temperature. The effectiveness of the model to describe CDI process is evaluated by comparing its results with reported experimental results of AQUA EWP CDI unit. Simulations were carried out to compute TDS removal efficiency for different initial feed concentrations of water and flow rates. The model results showed good agreement with the experimental results. The model predicts decreasing salt removal efficiency with increase in feedwater salt concentration as electrodes reach their saturation capacity i.e., they are fully filled with ions. At higher concentrations, the model does not predict the results accurately, that is attributed to nonlinear characteristics of porous electrodes that must be incorporated in the model. It is also observed that salt removal efficiency decreases with increase in flow rate, that is attributed to low residence time for ions at high flow rates. The batch mode of AQUA EWP

CDI unit is investigated using the mathematical model developed for a CDI cell. It is observed that the effect of flow rate on the batch mode CDI operation is different from the single flow mode. Here, the salt removal efficiency increases with increase in flow rate due to the mixing that occurs in the inlet tank and as more water is circulated back to the tank.

The thesis also proposes a novel operational mode that allows continuous mode operation of CDI cell using the concept of switched electric wave, wherein we obtain continuous supply of freshwater and brine with time. The model for a single CDI cell is extended to model Switched Wave Capacitive De-ionization Cell (SWCDI). The simulation results demonstrate decrease in concentration in the first CDI cell and increase in concentration in the last CDI cell of SWCDI with respect to time. The system parameters are optimized using an objective function to achieve desired response i.e., desired freshwater concentration of 500 ppm and high water recovery ratio.

A reflux mode of SWCDI is also investigated, wherein it is observed that reflux has no critical effect on CDI desalination performance, as with the increase in reflux rate, the flow to the SWCDI cell is also increased due to balance equations. This would result in low desalination performance of SWCDI cell, as flow rate weakens the desalination capability of the CDI cell.

Lastly, a prototype of a CDI cell is developed wherein it is observed that the salt concentration decreases under the effect of applied potential to the electrodes. A prototype of SWCDI system is also developed to demonstrate its ability to produce freshwater and brine simultaneously and the critical factors for efficient functioning of the SWCDI system are studied.

6.2 Future Work

The following are the recommendations for further research in this work:

1. Incorporate the nonlinear model describing electrical double layer in the developed mathematical model.
2. Use of overlapping voltage waveforms in SWCDI system.
3. Investigate different schemes of CDI using the developed model and study dependence of parameters on the system performance.
4. Integrate the model with energy converter that recovers the energy released during desorption in a CDI cell and uses it to charge a neighboring CDI cell or a battery.
5. Solar powered CDI devices can be manufactured that can be deployed to a location on demand that would save power consumption of CDI cell.
6. Extend the model to describe Solar based CDI.
7. Extend the model to describe the hybrid mode of CDI with other desalination systems.

References

[1] R. Zhao, *Theory and operation of capacitive deionization systems*. 2013.

[2] "Water Crisis | Water Ambassadors Canada." [Online]. Available: http://www.waterambassadorscanada.org/water_crisis.html. [Accessed: 04-Apr-2015].

[3] R. Zhao, P. M. P. Biesheuvel, A. van der Wal, and A. Van der Wal, "Energy consumption and constant current operation in membrane capacitive deionization," *Energy & Environmental Science*, vol. 5, no. 11, p. 9520, 2012.

[4] P. Gleick, "Water in Crisis: A Guide to the World's Freshwater ResourcesOxford University Press," *New York*, 1993.

[5] "Lesson 1: The Water Crisis, Teacher Materials." [Online]. Available: http://nanosense.sri.com/activities/finefilters/watercrisis/FF_Lesson1Teacher.pdf. [Accessed: 11-May-2016].

[6] "KSA water consumption rate twice the world average | Arab News." [Online]. Available: http://www.arabnews.com/news/532571. [Accessed: 14-Apr-2016].

[7] J. Fawell, U. Lund, and B. Mintz, "Total dissolved solids in drinking-water. Background document for development of WHO guidelines for drinking-water quality," *World Health Organization, Geneva*, 2003.

[8] N. Works, "Brackish groundwater: a viable community water supply option?," *The National Water Commission, Australian …*, 2011.

[9] A. E. Khan, A. Ireson, S. Kovats, S. K. Mojumder, A. Khusru, A. Rahman, and P. Vineis, "Drinking Water Salinity and Maternal Health in Coastal Bangladesh: Implications of Climate Change," *Environmental Health Perspectives*, vol. 119, no. 9, pp. 1328–1332, Apr. 2011.

[10] W. H. O. (WHO), "Guidelines for drinking-water quality 4th edition," *Geneva, Switzerland*, 2011.

[11] A. Cipollina, G. Micale, and L. Rizzuti, *Seawater desalination: conventional and renewable energy processes*. 2009.

[12] O. Buros and I. D. Association, *The ABCs of desalting*. 2000.

[13] M. Abdel-Jawad, "Energy sources for coupling with desalination plants in the GCC countries," *Consultancy report prepared for ESCWA,(September …*, 2001.

[14] "Water Systems Aqua technology." [Online]. Available: http://www.aquatechnology.net/vaporcompressiondistillers.html. [Accessed: 05-Apr-2015].

[15] “Reverse Osmosis units.” [Online]. Available: http://www.rotogo.co.uk/reverse-osmosis.php. [Accessed: 05-Apr-2015].

[16] “Aqua Sky USA INC.” [Online]. Available: http://www.aquaskyusa.com/under_sink_systems. [Accessed: 05-Apr-2015].

[17] J. Kucera, *Reverse Osmosis: Design, Processes, and Applications for Engineers*. John Wiley & Sons, 2011.

[18] “Pressure-Driven Membrane Filtration Processes.” [Online]. Available: http://synderfiltration.com/learning-center/articles/introduction-to-membranes/pressure-driven-membrane-filtration-processes/. [Accessed: 11-May-2016].

[19] “PURETEC Industrial Water - Article: What is Reverse Osmosis?” [Online]. Available: http://puretecwater.com/what-is-reverse-osmosis.html. [Accessed: 11-May-2016].

[20] G. Osmonics, “The Filtration Spectrum,” *GE Osmonics, Minnesota USA*, 1996.

[21] M. A. Anderson, A. A. L. Cudero, and J. Palma, “Capacitive deionization as an electrochemical means of saving energy and delivering clean water. Comparison to present desalination practices: Will it compete?,” *Electrochimica Acta*, vol. 55, no. 12, pp. 3845–3856, Apr. 2010.

[22] S. A. W. R. C. electrodialysis AWWA Research Foundation, Lyonnaise des eaux-Dumez (Firm), *Water treatment membrane processes*. New York: McGraw-Hill, New York ©1996., 1996.

[23] A. Bernardes, M. Rodrigues, and J. Ferreira, “Electrodialysis and Water Reuse,” *Novel Approaches, Springer*, 2013.

[24] A. Doyen, C. Roblet, L. Beaulieu, L. Saucier, Y. Pouliot, and L. Bazinet, “Impact of water splitting phenomenon during electrodialysis with ultrafiltration membranes on peptide selectivity and migration,” *Journal of Membrane Science*, vol. 428, pp. 349–356, Feb. 2013.

[25] J. (Eds. . Bundschuh, J., & Hoinkis, *Renewable Energy Applications for Freshwater Production*. CRC Press, 2012.

[26] U. Water, “The United Nations World Water Development Report 3–Water in a Changing World,” 2009.

[27] F. Rahman and Z. Amjad, “14 Scale Formation and Control in Thermal Desalination Systems, in Z. Amjad (Ed.),” in *The Science and Technology of Industrial Water Treatment, CRC Press, New York*, 2010, pp. 271–296.

[28] R. Zhao, S. Porada, P. Biesheuvel, and A. Van der Wal, “Energy consumption in membrane capacitive deionization for different water recoveries and flow rates, and comparison with reverse osmosis,” *Desalination*, 2013.

[29] S. Porada, R. Zhao, A. van der Wal, V. Presser, and P. M. Biesheuvel, “Review on the science and technology of water desalination by capacitive deionization,” *Progress in Materials Science*, vol. 58, no. 8, pp. 1388–1442, Oct. 2013.

[30] M. Mossad and L. Zou, “A study of the capacitive deionisation performance under various operational conditions,” *Journal of hazardous materials*, vol. 213–214, pp. 491–7, Apr. 2012.

[31] M. Mossad and L. Zou, “Effects of operational conditions on the electrosorption efficiencies of Capacitive deionization,” *Chemeca 2011: Engineering a Better World: Sydney Hilton Hotel, NSW, Australia, 18-21 September 2011*, p. 1648, 2011.

[32] S. Porada, L. Weinstein, R. Dash, A. van der Wal, M. Bryjak, Y. Gogotsi, and P. M. Biesheuvel, “Water desalination using capacitive deionization with microporous carbon electrodes.,” *ACS applied materials & interfaces*, vol. 4, no. 3, pp. 1194–9, Mar. 2012.

[33] R. Zhao, S. Porada, P. M. Biesheuvel, and A. van der Wal, “Energy consumption in membrane capacitive deionization for different water recoveries and flow rates, and comparison with reverse osmosis,” *Desalination*, vol. 330, pp. 35–41, Dec. 2013.

[34] Y. Oren, “Capacitive deionization (CDI) for desalination and water treatment — past, present and future (a review),” *Desalination*, vol. 228, no. 1–3, pp. 10–29, Aug. 2008.

[35] A. M. Pernía, J. G. Norniella, J. A. Martín-Ramos, J. Díaz, and J. A. Martínez, “Up–Down Converter for Energy Recovery in a CDI Desalination System,” *IEEE Transactions on Power Electronics*, vol. 27, no. 7, pp. 3257–3265, Jul. 2012.

[36] M. Alkuran and M. Orabi, “Utilization of a buck boost converter and the method of segmented capacitors in a CDI water purification system,” in *2008 12th International Middle-East Power System Conference*, 2008, pp. 470–474.

[37] A. M. Pernia, F. J. Alvarez-Gonzalez, M. A. J. Prieto, P. J. Villegas, and F. Nuno, “New Control Strategy of an Up–Down Converter for Energy Recovery in a CDI Desalination System,” *IEEE Transactions on Power Electronics*, vol. 29, no. 7, pp. 3573–3581, Jul. 2014.

[38] T. J. Welgemoed and C. F. Schutte, “Capacitive Deionization Technology^{TM}: An alternative desalination solution,” *Desalination*, vol. 183, no. 1–3, pp. 327–340, Nov. 2005.

[39] M. E. Suss, S. Porada, X. Sun, P. M. Biesheuvel, J. Yoon, and V. Presser, “Water desalination via capacitive deionization: what is it and what can we expect from it?,” *Energy Environ. Sci.*, vol. 8, no. 8, pp. 2296–2319, Jul. 2015.

[40] K. Laxmana, M. Myinta, and M. Al Abric, “Efficient Desalination of Brackish

Ground Water via a Novel Capacitive Deionization Cell Using Nanoporous Activated Carbon Cloth Electrodes," *The Journal of Engineering Research (TJER), Vol. 12, No. 2 (2015) 22-31*.

[41] F. Ahmad, S. J. Khan, Y. Jamal, H. Kamran, A. Ahsan, M. Ahmad, and A. Khan, "Desalination of brackish water using capacitive deionization (CDI) technology," *Desalination and Water Treatment*, vol. 57, no. 17, pp. 7659–7666, Apr. 2015.

[42] F. A. AlMarzooqi, A. A. Al Ghaferi, I. Saadat, and N. Hilal, "Application of Capacitive Deionisation in water desalination: A review," *Desalination*, vol. 342, pp. 3–15, Jun. 2014.

[43] G.-H. Huang, T.-C. Chen, S.-F. Hsu, Y.-H. Huang, and S.-H. Chuang, "Capacitive deionization (CDI) for removal of phosphate from aqueous solution," *Desalination and Water Treatment*, vol. 52, no. 4–6, pp. 759–765, Nov. 2013.

[44] L. Weinstein and R. Dash, "Capacitive Deionization: Challenges and Opportunities," *Desalin. Water Reuse*, vol. 23, pp. 34–37, 2013.

[45] R. Atlas and E. Aqua, "Purification of brackish water using hybrid CDI-EDI technology," *presentation to International Desalination Conference, Aruba.*, 2007.

[46] P. M. Biesheuvel, R. Zhao, S. Porada, and A. van der Wal, "Theory of membrane capacitive deionization including the effect of the electrode pore space.," *Journal of colloid and interface science*, vol. 360, no. 1, pp. 239–48, Aug. 2011.

[47] P. M. P. Biesheuvel, B. van Limpt, and A. van der Wal, "Dynamic adsorption/desorption process model for capacitive deionization," *The Journal of Physical Chemistry C*, vol. 113, no. 14, pp. 5636–5640, Apr. 2009.

[48] P. M. Biesheuvel, S. Porada, M. Levi, and M. Z. Bazant, "Attractive forces in microporous carbon electrodes for capacitive deionization," *Journal of Solid State Electrochemistry*, vol. 18, no. 5, pp. 1365–1376, May 2014.

[49] J. E. Dykstra, R. Zhao, P. M. Biesheuvel, and A. van der Wal, "Resistance identification and rational process design in Capacitive Deionization.," *Water research*, vol. 88, pp. 358–70, Jan. 2016.

[50] K. Laxman, M. T. Z. Myint, M. Al Abri, P. Sathe, S. Dobretsov, and J. Dutta, "Desalination and disinfection of inland brackish ground water in a capacitive deionization cell using nanoporous activated carbon cloth electrodes," *Desalination*, vol. 362, pp. 126–132, Apr. 2015.

[51] S. Porada, B. B. Sales, H. V. M. Hamelers, and P. M. Biesheuvel, "Water Desalination with Wires," *The Journal of Physical Chemistry Letters*, vol. 3, no. 12, pp. 1613–1618, Jun. 2012.

[52] H. Helmholtz, "Ueber einige Gesetze der Vertheilung elektrischer Ströme in körperlichen Leitern mit Anwendung auf die thierisch-elektrischen Versuche," *Annalen der Physik und Chemie*, vol. 165, no. 6, pp. 211–233, 1853.

[53] J. Araki, “Electrostatic or steric? – preparations and characterizations of well-dispersed systems containing rod-like nanowhiskers of crystalline polysaccharides,” *Soft Matter*, vol. 9, no. 16, p. 4125, 2013.

[54] M. Gouy, “Sur la constitution de la charge électrique à la surface d’un électrolyte,” *Journal de Physique Théorique et Appliquée*, vol. 9, no. 1, pp. 457–468, 1910.

[55] D. L. Chapman, “LI. A contribution to the theory of electrocapillarity,” *Philosophical Magazine Series 6*, vol. 25, no. 148, pp. 475–481, Apr. 1913.

[56] O. Stern, “Zur theorie der elektrolytischen doppelschicht,” *Zeitschrift für Elektrochemie und angewandte physikalische Chemie*, vol. 30(21–22), pp. 508–516., 1924.

[57] R. Zhao, P. M. Biesheuvel, and a. van der Wal, “Energy consumption and constant current operation in membrane capacitive deionization,” *Energy & Environmental Science*, vol. 5, no. Mcdi, p. 9520, 2012.

[58] P. M. Biesheuvel, R. Zhao, S. Porada, and a. van der Wal, “Theory of membrane capacitive deionization including the effect of the electrode pore space,” *Journal of Colloid and Interface Science*, vol. 360, pp. 239–248, 2011.

[59] T. Kim, J. E. Dykstra, S. Porada, A. van der Wal, J. Yoon, and P. M. Biesheuvel, “Enhanced charge efficiency and reduced energy use in capacitive deionization by increasing the discharge voltage.,” *Journal of colloid and interface science*, vol. 446, pp. 317–26, May 2015.

[60] R. Zhao, O. Satpradit, H. H. M. Rijnaarts, P. M. Biesheuvel, and a. van der Wal, “Optimization of salt adsorption rate in membrane capacitive deionization,” *Water Research*, vol. 47, no. 5, pp. 1941–1952, Apr. 2013.

[61] T. Humplik, J. Lee, S. C. O’Hern, B. A. Fellman, M. A. Baig, S. F. Hassan, M. A. Atieh, F. Rahman, T. Laoui, R. Karnik, and E. N. Wang, “Nanostructured materials for water desalination,” *Nanotechnology*, vol. 22, no. 29, p. 292001, Jul. 2011.

[62] T. J. Welgemoed and C. F. Schutte, “Capacitive Deionization Technology^{TM}: An alternative desalination solution,” *Desalination*, vol. 183, no. 1–3, pp. 327–340, Nov. 2005.

[63] K. Laxman, M. T. Z. Myint, H. Bourdoucen, and J. Dutta, “Enhancement in ion adsorption rate and desalination efficiency in a capacitive deionization cell through improved electric field distribution using electrodes composed of activated carbon cloth coated with zinc oxide nanorods.,” *ACS applied materials & interfaces*, vol. 6, no. 13, pp. 10113–20, Jul. 2014.

[64] J. Farmer, D. Fix, and G. Mack, “Capacitive deionization of NaCl and NaNO3 solutions with carbon aerogel electrodes,” *Journal of the Electrochemical Society*, vol. 143, no. 1, p. 159, Jan. 1996.

[65] L. Pan, X. Wang, Y. Gao, Y. Zhang, Y. Chen, and Z. Sun, “Electrosorption of anions with carbon nanotube and nanofibre composite film electrodes,” *Desalination*, vol. 244, no. 1–3, pp. 139–143, Aug. 2009.

[66] L. Zou, L. Li, H. Song, and G. Morris, “Using mesoporous carbon electrodes for brackish water desalination.,” *Water research*, vol. 42, no. 8–9, pp. 2340–8, Apr. 2008.

[67] A. Aghigh, V. Alizadeh, H. Y. Wong, M. S. Islam, N. Amin, and M. Zaman, “Recent advances in utilization of graphene for filtration and desalination of water: A review,” *Desalination*, vol. 365, pp. 389–397, Jun. 2015.

[68] C. Nie, Y. Zhan, L. Pan, H. Li, and Z. Sun, “Electrosorption of different cations and anions with membrane capacitive deionization based on carbon nanotube/nanofiber electrodes and ion-exchange membranes,” *Desalination and Water Treatment*, vol. 30, no. 1–3, pp. 266–271, Aug. 2012.

[69] W. Huang, Y. Zhang, S. Bao, and S. Song, “Desalination by capacitive deionization with carbon-based materials as electrode: a review,” *Surface Review and Letters*, 2013.

[70] J. Lee, W. Bae, and J. Choi, “Electrode reactions and adsorption/desorption performance related to the applied potential in a capacitive deionization process,” *Desalination*, 2010.

[71] J.-H. Lee and J.-H. Choi, “The production of ultrapure water by membrane capacitive deionization (MCDI) technology,” *Journal of Membrane Science*, vol. 409–410, pp. 251–256, Aug. 2012.

[72] A. (2014). El Shahat, “Empirical Capacitive Deionization ANN Nonparametric Modeling for Desalination Purpose.,” *Journal of Engineering Research and Technology*, vol. 1, no. 2, pp. 58–65, 2014.

[73] M. Mossad, W. Zhang, and L. Zou, “Using capacitive deionisation for inland brackish groundwater desalination in a remote location,” *Desalination*, vol. 308, pp. 154–160, Jan. 2013.

[74] J. C. Farmer, D. V. Fix, G. V. Mack, R. W. Pekala, and J. F. Poco, “Capacitive deionization of NH4ClO4 solutions with carbon aerogel electrodes,” *Journal of Applied Electrochemistry*, vol. 26, no. 10, pp. 1007–1018, 1996.

[75] J. Farmer, “Method and apparatus for capacitive deionization, electrochemical purification, and regeneration of electrodes,” *US Patent 5,425,858*, 1995.

[76] K. Dermentzis, “Continuous electrodeionization through electrostatic shielding,” *Electrochimica Acta*, 2008.

[77] K. Dermentzis and D. Papadopoulou, “A new process for desalination and electrodeionization of water by means of electrostatic shielding zones-ionic current sinks,” *Journal of Engineering Science and Technology Review*, no. 2(1), pp. 33–

42., 2009.

[78] J. H. Ryu, T. J. Kim, T. Y. Lee, and I. B. Lee, “A study on modeling and simulation of capacitive deionization process for wastewater treatment,” *Journal of the Taiwan Institute of Chemical Engineers*, vol. 41, no. 4, pp. 506–511, 2010.

[79] Y. a C. Jande and W. S. Kim, “Modeling the capacitive deionization batch mode operation for desalination,” *Journal of Industrial and Engineering Chemistry*, vol. 20, no. 5, pp. 3356–3360, 2014.

[80] P. M. Biesheuvel and a. van der Wal, “Membrane capacitive deionization,” *Journal of Membrane Science*, vol. 346, pp. 256–262, 2010.

[81] S. Porada, L. Weinstein, R. Dash, a. Van Der Wal, M. Bryjak, Y. Gogotsi, and P. M. Biesheuvel, “Water desalination using capacitive deionization with microporous carbon electrodes,” *ACS Applied Materials and Interfaces*, vol. 4, pp. 1194–1199, 2012.

[82] R. Zhao, O. Satpradit, H. H. M. Rijnaarts, P. M. Biesheuvel, and A. van der Wal, “Optimization of salt adsorption rate in membrane capacitive deionization.,” *Water research*, vol. 47, no. 5, pp. 1941–52, Apr. 2013.

[83] H. Ni, R. C. Amme, and Y. Jin, “Desalination by electret technology,” *Desalination*, vol. 174, pp. 237–245, 2005.

[84] R. Zhao, P. M. Biesheuvel, H. Miedema, H. Bruning, and A. van der Wal, “Charge Efficiency: A Functional Tool to Probe the Double-Layer Structure Inside of Porous Electrodes and Application in the Modeling of Capacitive Deionization,” *The Journal of Physical Chemistry Letters*, vol. 1, no. 1, pp. 205–210, Jan. 2010.

[85] S. Jeon, H. Park, J. Yeo, S. Yang, C. H. Cho, M. H. Han, and D. K. Kim, “Desalination via a new membrane capacitive deionization process utilizing flow-electrodes,” *Energy & Environmental Science*, vol. 6, no. 5, p. 1471, 2013.

[86] Y. Gendel, A. K. E. Rommerskirchen, O. David, and M. Wessling, “Batch mode and continuous desalination of water using flowing carbon deionization (FCDI) technology,” *Electrochemistry Communications*, vol. 46, pp. 152–156, Sep. 2014.

[87] A. Rommerskirchen, Y. Gendel, and M. Wessling, “Single module flow-electrode capacitive deionization for continuous water desalination,” *Electrochemistry Communications*, vol. 60, pp. 34–37, Nov. 2015.

[88] S. Porada, L. Borchardt, M. Oschatz, M. Bryjak, J. S. Atchison, K. J. Keesman, S. Kaskel, P. M. Biesheuvel, and V. Presser, “Direct prediction of the desalination performance of porous carbon electrodes for capacitive deionization,” *Energy & Environmental Science*, vol. 6, no. 12, p. 3700, Nov. 2013.

[89] Y. A. C. Jande and W. S. Kim, “Modeling the capacitive deionization batch mode operation for desalination,” *Journal of Industrial and Engineering Chemistry*, vol. 20, no. 5, pp. 3356–3360, Sep. 2014.

[90] A. Omosebi, X. Gao, J. Landon, and K. Liu, “Membrane Assisted Capacitive Deionization with Binder-Free Carbon Xerogel Electrodes,” *ECS Transactions*, vol. 61, no. 21, pp. 9–17, Oct. 2014.

[91] K. Laxman, L. Al Gharibi, and J. Dutta, “Capacitive deionization with asymmetric electrodes: Electrode capacitance vs electrode surface area,” *Electrochimica Acta*, vol. 176, pp. 420–425, Sep. 2015.

[92] D. MacGregor and M. Smith, “Method and apparatus for separating ions from liquids to produce separate diluted and concentrated effluents,” *US Patent 4,948,514*, 1990.

[93] D. MacGregor, “Method for separating ions from liquids,” *US Patent 5,061,376*, 1991.

[94] “Aqua EWP.” [Online]. Available: http://aquaewp.com/. [Accessed: 11-May-2015].

[95] “Plimmer – CDI.” [Online]. Available: http://www.idropan.com/en/portfolio-view/plimmer-cdi/. [Accessed: 11-May-2015].

[96] “Voltea - Unlocking the world’s water potential.” [Online]. Available: http://www.voltea.com/#1. [Accessed: 11-May-2015].

[97] “Atlantis Technologies.” [Online]. Available: http://www.atlantis-water.com/about-us. [Accessed: 11-May-2015].

[98] M. Hayashi, “Temperature-Electrical Conductivity Relation of Water for Environmental Monitoring and Geophysical Data Inversion,” *Environmental Monitoring and Assessment*, vol. 96, no. 1–3, pp. 119–128, Aug. 2004.

[99] P. N. Sen and P. A. Goode, “Influence of temperature on electrical conductivity on shaly sands,” *GEOPHYSICS*, vol. 57, no. 1, pp. 89–96, Jan. 1992.

[100] “ZORFLEX ACC Activated Knitted Carbon Cloth datasheet.” [Online]. Available: http://www.calgoncarbon.com/wp-content/uploads/product-literature/Zorflex_Knitted.pdf. [Accessed: 13-Apr-2016].

[101] “3M XYZ-Axis Electrically Conductive Tape 9713 datasheet.” [Online]. Available: http://multimedia.3m.com/mws/media/66127O/3mtm-xyz-axis-electrically-conductive-tape-9713.pdf. [Accessed: 16-May-2016].

Vitae

Name	: Syed Adnan Ali
Nationality	: Indian
Date of Birth	: 9/8/1992
Email	: syedadnanali26@gmail.com
Address	: 16-9-438/1, Old Malakpet, Telangana, Hyderabad, 500036
Academic Background	: B.E. in Electronics and Communication Engineering, 2013, Osmania University, Hyderabad, India.
Conferences Attended	: Moustafa Elshafei, Syed Adnan Ali, "**Modelling and Control of Travelling wave Capacitive Deionization Desalination System",** CDI&E 2015, International Conference on Capacitive Deionization and Electrosorption, Saarbrücken, Germany, October 26-29, 2015. Moustafa Elshafei, Syed Adnan Ali, "**Modeling of capacitive de-ionization with activated carbon electrodes",** 2nd International Conference on Desalination and Environment (ICODE), Doha, Qatar, January 23-26, 2016.
Journal publications	: **Modeling of capacitive de-ionization with activated carbon electrodes (under review),** by Desalination and Water Treatment Journal.